Reeja Johnson “Structural, corrosion inhibition and biological investigations of schiff bases containing sulphur and their metal chelates.” Thesis. Research and postgraduate department of chemistry, St. Thomas’ college (autonomous), University of Calicut, 2021.

PART III

CORROSION INHIBITION STUDIES

CHAPTER 10
INTRODUCTION AND REVIEW

From the day of metal invention, corrosion is a costly crisis in material science. Corrosion is the ongoing degradation/deterioration of the property of metal/material due to environmental circumstance and or by chemical reactions ensuing new and undesirable stuff from the original. The word "corrode" originates from "corrodere", a Latin word which indicates "nibble into pieces". Most of the time, corrosion refers to metals, but other materials such as polymers and glass are also undergone corrosion. This reaction can be electrochemical, as in the case of metals and alloys due to their high conductivity. It can also be a chemical deterioration as in the case of non-conducting materials such as ceramics, plastics and concrete. Protection of different metals and their alloys from corrosion in acidic media is the most demanding work in contemporary period. Corrosion shortens the life and demolishes the lustre and beauty of the materials, especially metals. Electron acceptors in the environment assist oxidation of metals ($M \rightarrow M^{+} + e^{-}$) and thereby corrosion. Metals have a strong affinity to go back to its native (low energy oxide) state because the free energy of pure metal is higher than its metal oxide. The process of this conversion to its native oxide state is described as corrosion. The simple pictorial representation of the corrosion process and the components involved are shown in Fig. 3.1.

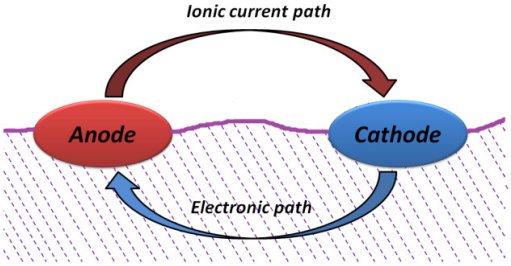

Fig. 3.1: Demonstration of components of corrosion

Corrosion leads to the replacement or repair of the structures, may lead to potential hazards and even becomes a threat to natural resources. Consequences of accidents of the corroded structures direct to damages of resources, safety concerns, loss of life etc. Drinking water is polluted by failed pipelines. Engine corrosion distress ships, aircraft and automobiles. Corrosion to machinery parts negatively influence the production of petrochemicals, mining, defense, food processing and agricultural production. Corrosion also hampers with safety, cause disruptions in industrial operations and poses danger to environment. Corroded bridges may collapse leading to death, public outcry, traffic delays and other crisis. When prosthetic implants like valves, pacemakers, plates and hip joints corrode, serious health problems will occur. Corrosion cause dangerous & expensive damage to highways, bridges, automobiles, home appliances, sewer systems, electrical utilities, ships, aircraft, petroleum refining, food processing, gas transmission, water pipelines etc. Corrosion impacts in different areas are shown in Fig. 3.2.

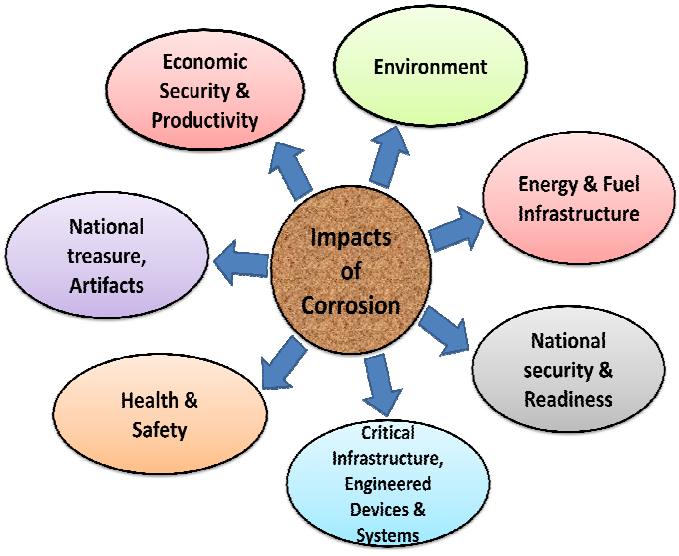

Fig. 3.2: Corrosion impacts in various areas

Economic factor is the major concern for the present studies on corrosion. Corrosion cost in the U.S. was estimated as $276 billion per year which was 3.1% of the

GDP in U.S. as of 1998. The direct cost of corrosion for India estimated during 2011-2012 was 26.1 billion U.S. $ [1].

Pickling is the process of exclusion of any contaminants from the metal surface at a high-temperature range. For the elimination of inorganic impurities like contaminants and any adjacent metal like chromium layer from the stainless steel surface, pickle liquor (acids like hydrochloric acid, nitric acid and sulphuric acid) is used [2]. When steel is exposed to high temperatures in industries, a discolouring oxide scale is developed on its surface and to remove this useless scale from the workpiece (metal) and reinstate the elevated performance of anti-corrosion, it is dished into a case of pickle liquor.

During pickling, addition of inhibitors is advantageous and safe since it protects the surface of metal from the corrosive attack. If inhibitors are not being used, a considerable quantity of metal loss will occur by the corrosive effect of acid on metals. In pickling baths, during corrosion, hydrogen gas is evolved and diffused throughout and makes the metal brittle via hydrogen embrittlement. The addition of inhibitors develops a barrier layer of film on the clean metal surface and decrease metal-acid interaction and thus inhibits surplus release of hydrogen. Consequently, metal becomes less vulnerable to hydrogen embrittlement by the addition of inhibitors in pickling baths [3].

Fig. 3.3: Application of carbon steel/mild steel in various areas

Low carbon steel or mild steel is the cheapest steel type which contains 0.05-0.25% of carbon. These are used in diverse vicinities such as cookware, automobiles, petrochemical industry, oil and gas industry, electrical appliances, agricultural implants, boilers, heat exchangers, marine applications, medical prosthetic implants etc; (Fig. 3.3). It readily undergoes rusting while exposed to environments containing acidic humidity.

Even corrosion looks highly complex, it can be elucidated by three plain electrochemical steps (Fig. 3.4)

a) Loss of metal occurs from the low potential part by oxidation and it acts as anode. In this current illustration, iron gets oxidized from Fe^0 to Fe^{2+}state.

b) Oxygen dissolved in aqueous medium migrate to cathode and completes the electric circuit.

c) Electrons released by Fe reduce oxygen to water at the cathode which is another region of the same metal.

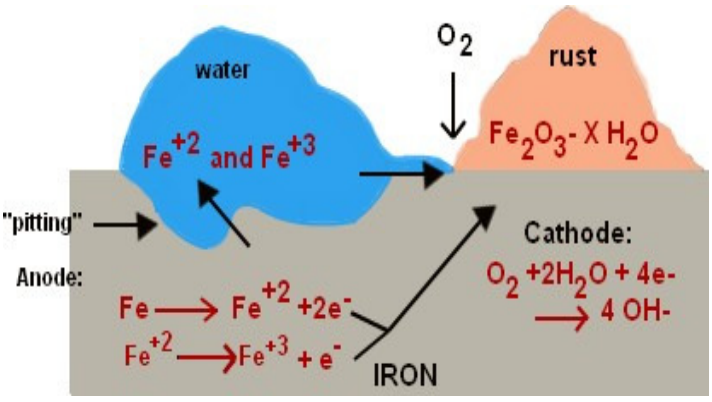

Fig. 3.4: Reactions occurring throughout the corrosion of steel

At anode: $Fe \longrightarrow Fe^{2+} + 2e^-$ (1)

At cathode: $O_2 + 8H^+ + 4e^- \longrightarrow 2H_2O + 4OH^-$ (2)

In the absence of oxygen, hydrogen ions get involved in this reaction at the cathode instead of oxygen and complete the electrical circuit ($2H^+ + 2e^- \longrightarrow H_2$).

Overall reaction is given by the equation:

$$2Fe^0 + 2O_2 + 4H^+ \longrightarrow 2Fe^{2+} + 4H_2O \quad (3)$$

In acidic solution, H^+ ions are supplied by H_2CO_3 which is produced by the reaction of carbondioxide from atmosphere and water.

Oxidation of ions of Fe^{2+} as follows:

$$2Fe^{2+}_{(aq)} + O_{2(g)} + (4 + 2x)H_2O_{(l)} \longrightarrow 2Fe_2O_3 \,.\, xH_2O + 4H^+_{(aq)} \quad (4)$$

Rust is represented as $2Fe_2O_3.\ xH_2O$. Carbonic acid in water dissociates forming hydronium and bicarbonate ions which causes corrosion. Acidity level is increased by the presence of gaseous pollutants such as SO_2 and NO_2 & aggravates corrosion problems. Prevention of corrosion would be more practical than trying to eliminate it.

Factors Responsible for Corrosion:

- ***Reactivity of the metal:*** More active metals having high oxidation potential values are readily corroded.
- ***Existence of moisture and air:*** Moisture and air content accelerates corrosion phenomena. Gases like CO_2 and SO_2 in the air enhances the process of corrosion. When iron placed in a vacuum, it doesn't rust.
- ***Presence of electrolyte:*** Electrolyte exerts a vital influence in the increasing corrosion rate (e.g.: iron rust sooner in saline water compared to pure water).
- ***Strains in metals:*** Corrosion takes place more rapidly at bends, scratches and cuts in the metal.
- ***Occurrence of impurity:*** Even a small amount of impurities in metal boost the probability of corrosion. Pure metal doesn't corrode easily.

Types of Corrosion

There are different types of corrosions known, but there is no universally conventional classification. Generally, the following categorization is adopted [4,5]

and it depends on the grain structure of metals, its composition or temperature for deformation.

***Galvanic corrosion*:** This is the most commonly found and one of the useful forms of corrosion which tend to arise when metals have dissimilar affinities to corrode when they contact in a corrosive electrolyte (conductive path) or with diverse electrochemical potentials (Fig. 3.5). It can be dry or wet, chemical or electrochemical. In galvanic corrosion cell, the anode is the more active metal (more negative) and its corrosion rate is more. The cathode is the more noble (more positive) metal and its corrosion rate is less. A uniform decrease in the volume of metals takes place at a result of chemical action and soluble corrosion products are formed. When stainless steel is in contact with aluminium alloys (if galvanic corrosion happens) acceleration of corrosion of aluminium occurs. The main principle behind dry cell construction is galvanic corrosion. The negative side is that it may also occur at unwanted vicinity making the metal susceptible to damage.

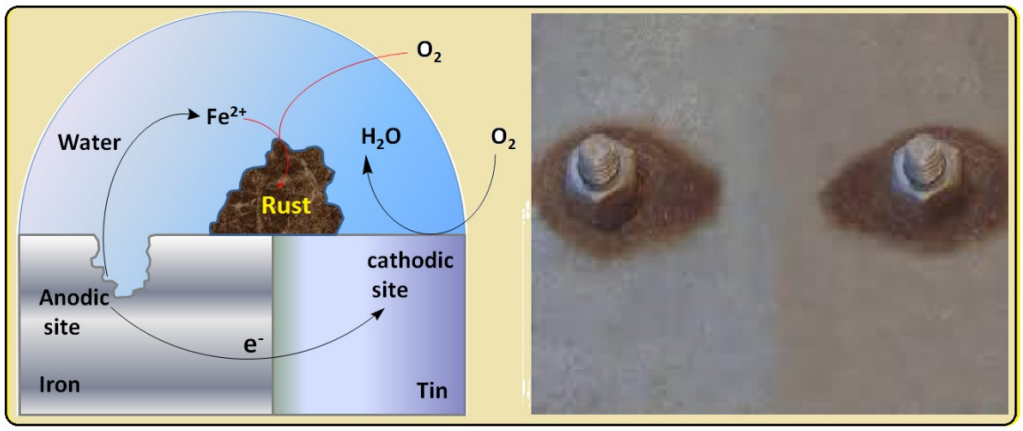

Fig. 3.5: Galvanic corrosion

***Pitting corrosion*:** "Self-nucleating" type crevice corrosion called pitting corrosion (Fig. 3.6), begins at occluded cells. Its prediction, detection and characterization are difficult. A galvanic cell is created on the metal surface because of pinholes, crack,

chemical attack, local straining etc. The crack segment on the metal surface acts as anode. A pit penetrates vertically downward and is developed by the corrosion at the anodic area which penetrates downward and forms a pit, hence named as pitting corrosion. Peripheral impurities such as scale, sand and dust implanted on the surface of metal leads to pitting. Corrosion of stainless steel and aluminium in chloride medium causes pitting.

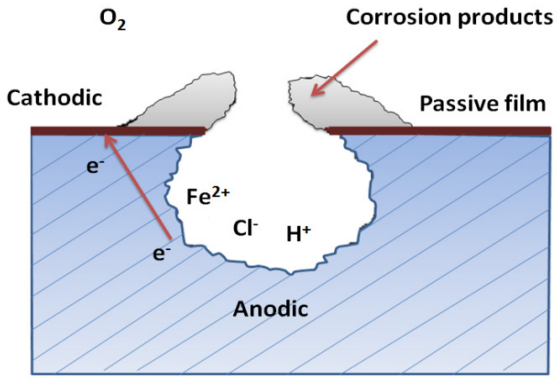

Fig. 3.6: Pitting corrosion in steel

***Crevice corrosion*:** It results from the different concentration of ions between two areas of metal and is a localized form of corrosion. Deviation in the local environment in the crevice i.e., increases in pH, depletion of oxygen and increase in halide ions (Cl^-) may cause the development of this type of corrosion. Proper joint designs minimize crevice corrosion. Usage of materials like plastic, glass, wood, asbestos and wax may contribute to crevice corrosion. Fig. 3.7 shows its mechanism and it is electrochemical in nature.

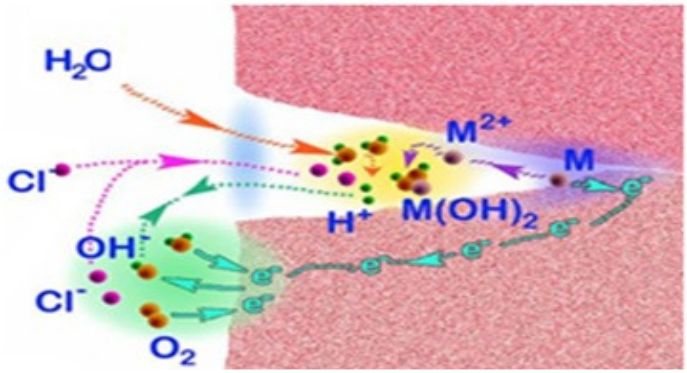

Fig. 3.7: Mechanism of crevice corrosion

***Microbiological corrosion*:** Corrosion caused by the metabolic activity of various microorganisms is called microbiological corrosion and it is commonly referred to as microbiologically influenced corrosion (MIC) or bio-corrosion (Fig. 3.8). In the oil industry, 40% of pipeline metal corrosion is due to microbes. The microorganisms can develop in an environment with or without oxygen and are classified as aerobic and anaerobic respectively. Bacteria, fungi, algae, diatoms etc. are capable of forming films resulting in microbiologically influenced corrosion. Such a film maintains concentration gradients of dissolved salts, gases, acids etc. As a result, local biological concentration cells are developed on the surface leading to microbiological corrosion.

Fig. 3.8: Microbiologically influenced corrosion (MIC) or bio-corrosion

***Inter-granular corrosion*:** This occurs along grain boundaries, especially where the material is sensitive to corrosion attack. Corrosive liquids possess a selective character of attacking only at grain boundaries and leaving the grain interior untouched or only slightly attacked (Fig. 3.9). Material containing grain boundaries shows more anodic electrode potential, undergoes corrosion in the particular corroding medium and affects the mechanical properties of metals while bulk remains intact. This may be due to the precipitation of certain compounds at the grain boundaries.

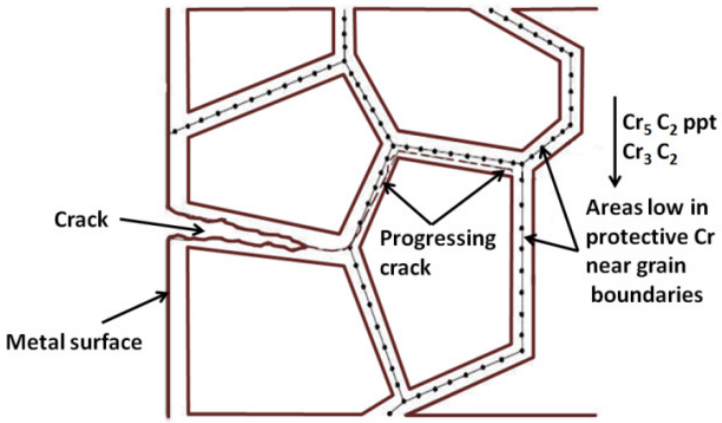

Fig. 3.9: Inter-granular corrosion of stainless steel

***Stress corrosion cracking (SCC)*:** Stress corrosion is a permutation of a corrosive environment and the tensile stress acting on the surface of a metal and this may be external or internal (Fig. 3.10). It may originate from residual stress from welding, machining, grinding etc. and also from external stress. The fraction under stress performs as an anode and the rest as a cathode, developing a galvanic system and resulting in the corrosion of the anodic fraction.

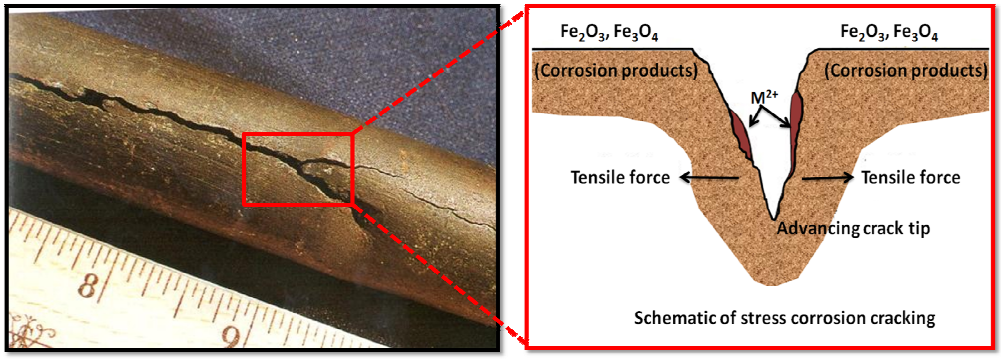

Fig. 3.10: Schematic representation of stress corrosion cracking

Prevention of Corrosion

There are several ways to protect the metal from corrosion.

- ***Barrier protection:*** To prevent corrosion, the metal surface can be protected from direct contact with the surroundings by coating it with paint, oil, enamel or a thin

protective layer of corrosion-resistant metal. Coatings provide a hurdle between moisture from surroundings and metal. E.g. brass tinning.

- ***Sacrificial protection:*** The corrosion of metal can be prevented by covering its surface with the layer of a more active metal like magnesium, zinc or aluminium. The more active metal act as the anode and iron act as cathode in the electrochemical cell set up. The covering metal gets consumed in the course of time, but the nearby exposed surfaces of iron do not rust as long as the sacrificial anode is present.
- ***Cathodic protection:*** Preventing metal surface from corrosion by making its surface as cathode in an electrochemical cell. Fuel pipelines, steel, tanks, ships, offshore oil platforms and steel pier piles are regularly sheltered in this approach.
- ***Anodic protection:*** Protection is done by applying an anodic current on the structure of the metal. Mainly this technique is employed in an aggressive atmosphere and protects the materials exhibiting passivity (e.g. stainless steel).
- ***Avoid exposure to corrosive agents:*** These methods include safeguarding the metal from rainwater or moisture by storing it indoors. Treating the feed water inside water boilers with softener prevent corrosion.
- ***Proper monitoring of metal surface:*** Routine observation for cracks and crevices which can lead to corrosion on the metal surface is to be done and preventive measures are to be adopted because these can lead to corrosion and use corrosion-resistant bars for construction.
- ***By forming insoluble phosphate or chromate coating*:** Treating the surface with phosphoric acid forms an insoluble phosphate coating that prevents corrosion. A thin chromate layer is also used.

- ***Anodization:*** It is another surface treatment, where the metal to be protected is bathed in a specific substance leading to a rigid and resilient film oxide layer and this layer which is thicker than a passivation film resists the corrosion process.
- ***By using corrosion inhibitors:*** Using an inhibitor is one of the best options to fight corrosion. Vast scientific studies have been conducted to develop and explore various corrosion inhibitors [6–12]. They work by making a coating on metal and prevent the access of corrosive agents to the metal surface. Compounds like ethylene glycol, formaldehyde, sodium molybdate, quaternary ammonium salts and glutaraldehyde revealed to restrict biofilm formation and microbial activity. Effectiveness of a corrosion inhibitor primarily depends on the composition of the quantity of H_2O and flow area and characteristics. Inhibition is facilitated by the formation of a coating, most commonly a passivation layer which blocks contact of the corrosive substance onto metal. The inhibitor may be chemically adsorbed onto the metal surface which forms a protective thin film or it may react with a potential corrosive component forming a complex.

Inorganic substances such as chromates, phosphates, silicates etc have been used as effective as inhibitors towards metallic corrosion. Also, organic compounds and natural extracts are used as inhibitors, which diminish metal dissolution rate in acid medium. There are four distinctive mechanisms proposed [13,14] to explain the inhibitory characteristics of organic species viz., (i) electrostatic interactions existing across charged species and the metal (ii) interaction between the π-electrons of the metal and inhibitor (iii) interactions between metal and uncharged electron pairs in the molecule and (iv) a permutation of various mechanism. Greater the affinity of an inhibitor to form a strong coordination bond with the metal, greater is the inhibition efficiency. Molecules

with phosphorous, sulphur, nitrogen and oxygen are found to have a strong tendency to avert corrosion [15].

Organic molecules having electron lone pairs on the heteroatoms such as P, S, N and O atoms have proved, both theoretically and practically, that they can perform as admirable corrosion inhibitors in aggressive solutions by improved adsorption on the metal surface [16,17]. Generally, effectiveness of organic inhibitors depends up on the aromaticity, efficiency (electron density) at the centres of adsorption [18,19], molecular size, number of sites of adsorption on the surfaces [20] etc; Organic molecules bearing sulfur and nitrogen behave as wonderful inhibitors against corrosion in both HCl and H_2SO_4 acidic medium [21]. Inhibitors having heteroatoms in their structures pursue the opposite order of their electronegativities and their efficiencies followed the order O < N < S < P [22,23].

There are different types of inhibitors: Anodic inhibitors form a protective oxide film and cause a large anodic shift. Eg:-molybdates, chromates, tungstates and nitrates. Cathodic inhibitors decrease reaction at cathode by limiting the diffusion of reducing species to steel/ metal surface, eg: Zn and polyphosphate inhibitors and oxygen scavengers. Mixed inhibitors reduce both cathode and anode reactions, eg: phosphates and silicates. Volatile inhibitors of corrosion are carried from source to corrosion site by volatilization, eg: In boilers, hydrazine or morpholine are transported with steam. Green corrosion inhibitors are more economical, easily available and eco-friendly than toxic organic inhibitors. Natural products are a good source, where most of them contain necessary elements such as O, C, S and N which are active in organic compounds and forms a protective film to hinder the corrosion. eg: natural honey, onion, potato, tulsi etc.

Literature survey established that imidazole azo derivatives, benzotriazoles and their derivatives, quaternary imidazoline derivatives, benzaldehyde, quinoline derivatives,

quaternary salts of benzenethiol alkaloids, triazoles, pyridine bases, thiourea, derivatives of chloroanilines, toluidine etc., have noticeable inhibitory action [24–28].

An efficient inhibitor must assure some conditions [29]:

a) It must prove the fine ability of protection while used in very small concentration.

b) It should be long-range effective.

c) It must retain its efficiency in varying conditions of operations like higher velocity and temperature.

d) Inhibitor should have minimum toxicity level.

e) There should not be any severe change in corrosion rate when altering inhibitor dosage.

f) It should be capable to guard the surface of metal from both localized and uniform corrosion.

g) Products formed from inhibitor during reactions or inhibitor itself, must not form any deposits–specially at the areas where heat transfer processes take place.

Schiff Base Corrosion Inhibitors - A Review

Literature survey pointed out that many scientists synthesized and studied different categories of Schiff bases for their inhibition capacity against corrosion of carbon/mild steel in aggressive media. Few of the Schiff bases showed their efficiency in aggressive medium against the corrosion of zinc and copper.

In 2003, M. Hosseini, et al. investigated corrosion inhibition studies of two novel Schiff bases,viz., N,N′-ortho-phenylene(salicylaldimine-2-hydroxy-1-naphthaldimine) and N,N′-ortho-phenylene(salicylaldimine-acetylacetone imine) for mild steel in 0.5M H_2SO_4 by electrochemical impedance spectroscopy (EIS) and Tafel polarization [30]. At

400ppm concentration, these two novel ligands function as good inhibitors with maximum efficiencies of 97–98%.

In 2011, M. T. Muniandy, et al. investigated the corrosion inhibition effect of N, N′-bis(4-bromobenzylidene)-1,3-diaminobenzene,N,N′-bis(2-hydroxy-5-bromobenzylide ne)-1,3-diaminobenzene and N,N′-bis(2-hydroxybenzylidene)-1,3–diamino benzene on aluminium alloy in HCl medium (0.5M) [31]. Inhibition ability of these Schiff bases are approximately similar in this acid medium and was proved by gravimetric weight loss measurements, potentiodynamic polarization (PDP) techniques and scanning electron microscopic (SEM) analysis. The polarization studies exposed that, all inhibitors are mixed type. Predominantly its action was cathodic and inhibition efficiencies were found to enhance linearly with its concentration. On aluminium surfaces, all molecules followed Langmuir adsorption isotherm and SEM studies indicated that a protective layer was developed on the aluminium surface and performance of inhibition strongly depends on the types of functional group substituted on benzene ring.

In 2011, M. D. Shah, et al. revealed the activity of inhibition of tribenzylidene and trisalicylidene derivatives of triethylenetetramine in HCl medium on zinc metal [32]. Molecules showed 96-100% of inhibition efficiency at very low (1%) concentrations in different molar solutions of HCl medium (0.5M and 1M). The efficiency of the trisalicylidene derivatives decreased after 2 hours when temperature increased from 35-65ºC, but the efficiency of other inhibitor remains approximately constant at 99.7%. The activation energies of corrosion were higher in the presence of inhibitors than in the blank. The spontaneity of adsorption of the inhibitor on the metal surface was evident from the negative values of heat of adsorption and free energy of adsorption. Cathodic polarization was found to be predominant in electrochemical studies. Langmuir isotherm was obeyed on both anodic and cathodic sites by these molecules.

M.Q. Mohammed, et al. synthesized three Schiff bases by the condensation reactions of cinnamaldehyde with 2-aminophenol, acrolein with 2-aminophenol and cinnamaldehyde with phenylenediamine in 2011 [33]. These ligands were identified by CHN, ^{1}H NMR, UV-Vis and IR analyses. Studies include the use of these ligands as corrosion inhibitors on carbon steel in 0.5M HCl media.

S.P. Fakrudeenet, et al. evaluated the corrosion inhibition efficiencies of N,N'-bis(3-methoxysalicylidene)-1,4-diaminophenelyne (MSDP), N,N'-bis (salicylidene)-1, 4-diamino phenelyne (SDP) and on an alloy (AA6061) by gravimetric weight loss method and SEM micrography in 1M hydrochloric acid medium in 2012 [34]. From the studies, it is revealed that the inhibition efficiency of these Schiff bases (MSDP, SDP) and alloy (AA6061) increases with increase in concentration. Efficiency of these ligands varied with temperature and time of immersion in solution. The adsorption of these molecules on the surface of alloy followed the Freundlich isotherm and the mechanism of inhibition was suggested based on thermodynamic parameters.

Singh, et al. studied the corrosion inhibition effect of some Schiff base compounds namely, hexane 1,4-diaminebis-isatin (HDBI), ethylenediaminebis-isatin (EDBI), and thiocarbohydrazidebis-isatin (TCBI) by gravimetric weight loss, electrochemical impedance spectroscopy, potentiodynamic polarization, scanning electron microscopy and atomic force microscopy in 2012 [35]. Frumkin isotherm was most suited isotherm for these three inhibitors. TCBI showed highest efficiency followed by EDBI and HDBI and led to a conclusion that a competent corrosion inhibitor should have planarity, large size, and unoccupied d-orbital along with an extensive number of π-electrons.

In 2013, S. Junaedi, et.al., investigated the corrosion inhibitory influence of 1,5 dimethyl-4-((2-methylbenzylidene)amino)-2-phenyl-1*H*-pyrazol-3(2H)-one in aggressive

medium on mild steel employing EIS, PDP, EFM and OCP techniques [36]. Highest occupied molecular orbital energy (E_{HOMO}), lowest unoccupied molecular orbital energy (E_{LUMO}) and dipole moment (μ) were determined and discussed.

In 2015, Kannan, et.al. reported the corrosion inhibitory effect of N,N-bis(2-hydroxyacetophenylidene)-2-hydroxy-1,3-propanediamine (LACOH) and N,N-bis (salicylidene)-2-hydroxy-1,3-propanediamine (LOH) in 2M HCl medium at 303K [37]. These inhibitors appeared to follow the Langmuir adsorption isotherm.

M. R. Vinutha and T.V. Venkatesha reported an article which enumerates numerous inhibitors accustomed to combat corrosion in aggressive medium in 2016 [38]. By economic, technical, safety and environmental terms, corrosion control is an important activity and, in this article, the literature on corrosion inhibitors has been reviewed and discussions were made on their efficiency and properties. They reported the nature of the media and metals along with the physicochemical, electronic and structural properties which having prominent roles while explaining the mechanism. Further, they inferred that the presence of S, O and N heteroatoms in the structure of ligands, surfactants and phytochemicals acting as the most efficient inhibitors within their CMC concentration.

In 2018, D. M. Jamil, et al. studied the inhibition efficiencies of relatively stable and inexpensive Schiff bases, namely 3-((4-(dimethylamino)benzylidene) amino)-2-methylquinazolin-4(3*H*)-one and 3-((4-hydroxybenzylidene)amino)-2-methyl quinazolin-4(3H)-one, by weight loss method in acid medium [39]. To compare the effects of N, N-dimethylamino and hydroxyl substituents on corrosion inhibition efficiency, density functional theory calculations were conducted which provide insight for designing novel molecular structures with improved corrosion inhibition efficiencies.

In 2020, P. Shetty reported a review of the corrosion inhibition activities of a variety of reported Schiff bases on the disintegration of mild steel in aggressive media [40]. During pickling, an undue deterioration of metal happens which can be controlled by the addition of a suitable inhibitor to this pickling solution. The relationship of structure and corrosion inhibition activity of Schiff base ligands are highlighted in this paper which finds valuable practical applications in different industrial fields. It helps the researchers to develop novel corrosion inhibitors for performing inhibitors in acid media.

Heterocyclic Schiff Base Inhibitors- A Review

In 2004, Dhayabaranet, et al. studied tetrazole derivatives, namely, 1-(9′-acridinyl)-5-(4′-hydroxy phenyl) tetrazole, 1-(91-acridinyl)-5-(4′-aminophenyl) tetrazole and 1-(9′-acridinyl)-5-(4′-chlorophenyl) tetrazole as corrosion inhibitors for commercial mild steel in 1M hydrochloric acid medium by weight loss studies [41]. Thermodynamic parameters like entropy of adsorption, heat of adsorption, activation energy and free energy of adsorption have been calculated at 303K, 318K and 333K to study the adsorption characteristics of tetrazole derivatives.

R. Upadhyay and S. Mathur have studied the corrosion inhibitory outcome of novel Schiff bases viz.N-(furfurilidine)-4-methylaniline, N-(furfurilidine)-4-methoxy aniline, N-(salicylidine)-4-methoxyaniline, N-(cinnamalidine)-2-methylaniline and N-(cinnamalidine)-4-methoxy aniline on mild steel in sulphuric acid solutions by thermometric and mass loss methods in 2007 [42]. Results obtained by both methods are in good agreement with each other and maximum inhibition performances were shown at high concentration of the Schiff's base.

In 2008, G. Elewady studied characteristics of corrosion inhibition of 2,6-dimethylpyrimidine-2-amine and its derivatives in HCl medium on carbon steel

corrosion via gravimetric techniques and EIS studies [43]. At 0.005M concentration, N-benzylidene-4,6-dimethylpyrimidine-2-amine displayed highest inhibition efficiency of 92.78 %.

In 2014, Gopi, et al. reported the corrosion inhibition behaviour of phosphano and benzotriazole and their derivatives at various temperatures ranging from 30-60°C in groundwater using PDP, scanning electron microscopy (SEM) and X-ray diffraction on mild steel [44]. At optimum concentration, an excellent inhibition efficiency of 99.59% was reported.

In 2015, L.O. Olasunkanmi et. al., studied mild steel corrosion in hydrochloric acidusing some quinoxaline derivatives namely 1-(3-phenyl-5-(quinoxalin-6-yl)-4,5-di hydro-1H-pyrazol-1-yl)propan-1-one,1-[3-phenyl-5-quinoxalin-6-yl-4,5-dihydro pyrazol -1-yl]butan-1-one and 2-phenyl-1-[3-phenyl-5-(quinoxalin-6-yl)-4,5-dihydro pyrazol-1-yl] ethanol using EIS and PDP techniques [45]. Studies were supported by Monte-Carlo simulation and quantum chemical calculations.

In 2016, P. Singh, et.al.,analysed the inhibition and adsorption effects of quinoline derivatives such as 2-amino-7-hydroxy-4-(p-tolyl)-1,4 dihydroquinoline-3-carbonitrile, 2-amino-7-hydroxy-4-phenyl-1,4-dihydroquinoline-3-carbonitrile, 2-amino-4-(4-(dimethyl amino)phenyl)-7-hydroxy-1,4-dihydroquinoline-3-carbonitrile, 2-amino-7-hydroxy-4-(4-methoxyphenyl)-1,4-dihydroquinoline-3-carbonitrile using gravimetric weight loss studies, EIS and PDP techniques [46]. Among the studied inhibitors, 2-amino-4-(4-(dimethylamino)phenyl)-7-hydroxy-1,4-dihydroquinoline-3-carbonitrile exhibited maximum inhibition efficiency of 98.19 % at 150 mg/L. Surface morphology was studied using SEM, X-ray photoelectron spectroscopy (XPS) and atomic force microscopy techniques.

Tasic, et al. investigated the synergistic inhibition effect of corrosion on benzotriazole with gelatine and potassium sorbate on copper in an acidic sulphate medium by conventional gravimetric and electrochemical studies in 2016 [47]. The maximum inhibition efficiency of 99 % was displayed due to the synergistic effect by the effective adsorption of molecules.

In 2019, I. Benmahammed, et al. studied (1Z)-N′-(4-bromophenyl)-2-oxo-N-quinolin-8-ylpropane hydrazonamide and (1Z)-2-oxo-N′-phenyl-N-quinolin-8-yl propane hydrazonamide as corrosion inhibitors in 1 M HCl medium on carbon steel by conventional gravimetric weight loss techniques, electrochemical studies, energy dispersion X-ray spectroscopy (EDS), scanning electron microscopy (SEM) coupled with atomic force microscopy, AFM studies etc.,[48]. The temperature effect was supported and different thermodynamic parameters were considered along with the synergetic effect and hydrodynamic effect. With increased rotation speed, corrosion inhibitory efficiency was decreased and the used additives adsorb cooperatively by forming a protective layer on the surface of metal. The theoretical calculations by DFT and MD simulation are in good correlation with the results obtained by the experimental measurements.

A. Mishra, et al. reviewed the collection of major investigations which illustrated the anticorrosive effect of imidazole derivatives in different electrolytes in 2020 [49]. Mostly, these derivatives acted on interface and behaved as mixed type corrosion inhibitors. They interact with the metal surface by charge sharing (donor-acceptor) interactions. Their adsorption mechanism obeyed the Langmuir adsorption isotherm.

Sulphur Containing Schiff Base Inhibitors-A Review

In 2004, M. Özcan, et al. investigated the effects of corrosion of mild steel in 0.1M H_2SO_4 using thiourea and its derivatives like phenylthiourea and methylthiourea by considering the concentration of thioamides [50]. These molecules are similar structure on one side (thiocarbonyl group) and altered on the other. Data obtained using the techniques of EIS (electrochemical impedance spectroscopy) and R_p (polarisation resistance) revealed that these molecules showed good corrosion inhibition. Phenylthiourea was the most efficient derivative and thiourea was the least.

In 2004, A. Yurt, et al. revealed the inhibition capacity of ligands containing heterocyclic substituents namely, 2-((1E)-2-az-2-pyrimiadine-2-ylvinyl)thiophene, 2-((1Z)-1-aza-2-(2-pyridyl)vinyl)pyrimidine, 2-((1E)-2-aza-2-(1,3-thiazol-2yl)vinyl) thiophene, 2-((1Z)-1-aza-2-(2-thienyl)vinyl)benzothiazole in 0.1M hydrochloric acid by AC impedance and PDP studies on carbon steel [9]. Adsorption mechanism of inhibitors obeyed the Temkin isotherm.

In 2007, H. H. Hassan, et al. carried out a comparative study of 5-amino-3-mercapto-1,2,4-triazole, 5-amino-1,2,4-triazole, 1-amino-3-methylthio-1,2,4-triazole and 5-amino-3-methylthio-1,2,4-triazole as inhibitors in 0.1M HCl solution for mild steel corrosion at 20°C [51]. To study the metal corrosion behaviour of these inhibitors at different concentrations, potentiodynamic polarization and electrochemical impedance spectroscopy (EIS) techniques were used. Open circuit potential (OCP) was measured as a function of time and these results are in close agreement with the results obtained from impedance and polarisation measurements. These studies were established that 5-amino-3-mercapto-1,2,4-triazole was the most efficient inhibitor.

In 2011, F. Bentiss and M. Lagrenée reported the relationship between corrosion inhibition properties and electronic parameters of thiadiazole, oxadiazole and

triazole derivatives [52]. Results showed that planar compounds have better adsorption than twisted or puckered molecules.

In 2011, S. Issaadi, et al. tested the corrosion inhibition of two thiophene based Schiff bases 4,4′-bis(3-carboxaldehydethiophene)diphenyldiiminoethane and 4,4′-bis (3-carboxaldehydethiophene)diphenyldiimino ether on mild steel in 1M HCl medium using electrochemical studies like EIS and PDP techniques [53]. The polarisation studies and adsorption studies were established that they were performed as mixed type (anodic/cathodic) inhibitors and satisfied the Langmuir's adsorption isotherm.

In 2012, C. Loto, et al. reviewed the inhibitive effect of thiadiazole and thiourea derivatives. Heterocyclic and organosulphur compounds and derivatives have so many practical applications [54]. The effects of these molecules on the corrosion of metallic alloys were appraised in diverse journals by different experimental techniques. It is concluded from the complete discourse presented, thiadiazole and thiourea derivatives fulfil the basic requirements for a competent corrosion inhibitor.

In 2014, Djamel Daoud, et al. analysed the inhibitory action of the molecule (NE)-N-(thiophen-3-ylmethylidene)-4-({4-[(E)-(thiophen-2-ylmethylidene)amino] phenyl}m-ethyl)aniline on the corrosion of mild steel (X52) in 1M sulfuric acid and 1M hydrochloric acid [55]. They have used the methods like weight loss, PDP, EIS, DFT to explain the correlation between inhibition efficiency and quantum chemical calculations of the investigated compounds.

In 2016, A. Aouniti, et al. studied the corrosion inhibition and adsorption behaviour of (*E*)-2-methyl-N-(thiophen-2-ylmethylidene)aniline at mild steel in 1M HCl using gravimetric weight loss and electrochemical methods at 308 K [56]. Inhibition efficiency was increased with increase in the concentration of thiophene Schiff base. The potentiodynamic polarization studies revealed that this novel

thiophene Schiff base acted as a mixed-type inhibitor. The inhibition was proposed to occur due to the adsorption of the components of the thiophene derivatives on the mild steel surface which were approximated by invoking the Langmuir adsorption isotherm model. DFT method, theoretical and experimental correlation results were also discussed.

In 2018, A. Singh, et.al., investigated the corrosion inhibitive action of thiopyrimidine derivatives viz, 5-cyano-2-thioxo-6-(p-tolyl)-2,3dihydropyrimidin-4-one, 6-(4-(dimethylamino)phenyl)-5-cyano-2-thioxo-2,3-dihydropyrimidin-4-one and 5-cyano-6-phenyl-2-thioxo-2,3-dihydropyrimidin-4-one, 5-cyano-6-(4-methoxyphenyl) -2-thioxo-2,3-dihydropyrimidin-4-one on the corrosion of mild steel in aggressive medium using EIS and PDP techniques [57]. Maximum inhibition efficiency of 97% was exhibited by 6-(4-(dimethylamino)phenyl)-5-cyano-2-thioxo-2,3-dihydro pyrimidin-4-one at 200 mg/L. All these inhibitors are mixed type with predominant control of cathodic reaction.

Polynuclear Schiff Base Inhibitors– A Review

In 2011, I. Obot, et. al., synthesized and characterized novel phenanthroline derivative, 2-mesityl-1H-imidazo[4,5-f][1,10]phenanthroline [58]. Its corrosion inhibition performance was studied in sulphuric acid medium on low carbon steel by electrochemical and quantum chemical techniques. UV-visible absorption spectrum of this molecule displayed the formation of an iron-inhibitor peak.

In 2012, Baskar et. al. synthesized three biphenyl compounds namely(2E)-1-(biphenyl-4-yl)-3-(4-hydroxyphenyl)prop-2-en-1-one, (2E)-3-(4-aminophenyl)-1-(biphenyl-4-yl)prop-2-en-1-one and (2E)-1-(Biphenyl-4-yl)-3-(4-nitrophenyl)prop-2-en-1-one, characterised and investigated their inhibition efficiency against corrosion by weight loss, PDP and EIS techniques on low carbon steel [59]. Mechanism was

supported by the surface studies (SEM-EDS) and adsorption isotherms. All biphenyl derivatives were mainly found to be cathodic nature.

In 2014, K. Shaju et al. investigated the inhibitory effect of (s)-2-(anthracene-9 (10H)-ylideneamino)-5-guanidinopentanoic acid on carbon steel (CS) in 0.5M sulphuric acid medium using different corrosion monitoring techniques [60]. Addition of KI to this medium enhances the corrosion inhibition efficiency of this ligand (synergistic effect) and the results established that the ligand acted as a mixed type inhibitor. Surface morphology of the metal (CS) was evaluated by SEM analysis.

Pyridine Derivatives of Schiff Base Inhibitors- A Review

In 1995, Ekpe U. J. et al. studied the corrosion inhibitory action of methyl and phenyl thiosemicarbazone derivatives, 2-acetylpyridine-(4-methylthiosemicarbazone) (2AP4MTSC) and 2-acetylpyridine-(4-phenylthiosemicarbazone) (2AP4PTSC) on mild steel in HCl medium using weight loss and hydrogen evolution techniques [61]. 2AP4PTSC displayed a maximum efficiency of 80.67% than 2AP4MTSC. The kinetic treatment of the results revealed that corrosion resistance found to increase with inhibitor concentration and decrease with temperature. The first-order type of mechanism was deduced and inhibition process was attributed to physisorption.

In 1999, E. Ebenso, et al. reported the effect of functional groups of some thiosemicarbazone and amide derivatives of pyridine on their corrosion inhibition efficiency using hydrogen evolution and weight loss techniques [62]. 2-acetylpyridine-(4-methyl)thiosemicarbazone,2-acetylpyridine-(4phenyl)thiosemicarbazone, urea, thio urea, semicarbazide, thiosemicarbazide, acetamide, thioacetamide, methoxy benzaldehydethiosemicarbazone, benzilthiosemicarbazone and benzointhiosemi carbazone were the compounds employed for this study. Molecules having thiocarbonyl group exhibited higher inhibition efficiency and the corrosion inhibition mechanism

depends on the total molecular structure of the inhibitor, nature and spatial relationship of the different functional groups

In, 2004, M. Lashkari, et al. studied the molecular behaviour of some pyridine derivatives as corrosion inhibitors of aluminium and iron in aggressive media. Three conditions were used for these calculations; metal cluster, isolated inhibitor molecule and polarized-continuum media. The extents of charge transfer (ΔN) and chemical potential (μ) of the inhibitor were determined. A linear correlation between these two parameters and the inhibition efficiencies are also demonstrated in this article [63].

In 2004, P. C. Okafor, et al. established the corrosion inhibition of aluminium in HCl solution by some thiosemicarbazone derivatives; 2-acetylpyridine-(4-phenyl-iso-methylthiosemicarbazone), 2-acetylpyridine-(4-phenylthiosemicarbazone) and 2-acetyl pyridine-(4-phenyl-iso-ethylthiosemicarbazone) by weight loss and hydrogen evolution techniques [25]. This paper elucidates the effects of inhibitor concentration, temperature and the molecular structure on corrosion inhibition efficiency. The inhibition efficiency increased with inhibitor concentration, while their functions get reversed and became accelerators at very low concentration.

In 2005, Abd El-Maksoud and A. S. Fouda, introduced some pyridine derivatives as corrosion inhibitors for carbon steel in acidic medium and their efficiency was studied by electrochemical polarization method (potentiodynamic, Tafel extrapolation) as well as weight loss method [64]. Results established that all these compounds acted as good inhibitors and inhibition efficiency was found to depend on the nature and the concentration of the inhibitor. The presence of substitution in the pyridine ring has significant role in the percentage of inhibition and the adsorption of these compounds obeys Langmuir adsorption isotherm.

In 2007, Kandemirli F. and S. Sagdinc, carried out the quantum chemical and corrosion inhibition studies to examine the relationship between quantum chemical calculations and the efficiencies of urea, thiourea, acetamide, thioacetamide, semicarbazide, thiosemicarbazide, methoxybenzaldehyde-thiosemicarbazone, 2-acetyl pyridine-(4-methyl)-thiosemicarbazone, 2-acetylpyridine(4phenyl)thiosemicarbazone, benzointhiosemicarbazone and benzilthiosemicarbazone [65]. The quantum chemical calculations were employed using DFT, ab-initio molecular orbital and semi-empirical methods to determine various quantum chemical parameters such as highest occupied molecular orbital energy (E_{HOMO}), lowest unoccupied molecular orbital energy (E_{LUMO}), the energy gap between E_{HOMO} and E_{LUMO} ($\Delta E_{HOMO-LUMO}$), dipole moments (μ) etc.

In 2012, Ghazoui A, et al. investigated the corrosion inhibition of imidazo derivatives namely, 2-phenylimidazo[1,2-a]pyridine and 2-(methoxyphenyl)imidazo[1,2-a]pyrimidine and on C38 steel in 1M HCl by weight loss, PDP and EIS techniques [66]. Thermodynamic data for the adsorption progression were discussed and calculated. Kinetic parameters like pre-exponential factor, activation energy, entropy and enthalpy of activation were estimated from the effect of temperature on the inhibition and corrosion processes.

In 2014, V. P. Raphael, et al. investigated the corrosion resisting capacity of 3-acetylpyridine semicarbazone (3APSC) on carbon steel in hydrochloric acid medium using weight loss measurements, electrochemical impedance spectroscopy (EIS) and potentiodynamic polarization studies [67].

In, 2016, P. Mourya, et al. studied the consequence of iodide ions on corrosion inhibition of 1, 4, 6-trimethyl-2-oxo-1, 2- dihydropyridine-3-carbonitrile on carbon steel in sulphuric acid medium using gravimetric and electrochemical techniques and

established that its adsorption followed Langmuir isotherm and showed good protection efficiency [68].

In 2018, W. Zhang, et al. investigated the adsorption and corrosion inhibition properties of pyridine-2-aldehyde-2-quinolylhydrazone for Q235 steel in acid medium by PDP and EIS techniques [69]. The protective layer formed on the steel surface was examined by surface analysis techniques (SEM, EDX, SECM). The adsorption of the compound followed Langmuir adsorption isotherm and contained both physical and chemical adsorptions.

In 2019, N.N. Hazani, et al. synthesised 2-acetylpyridine-4-ethyl-3-thiosemi carbazone and it's tin (IV) complex and investigated their corrosion inhibition behaviour on mild steel in 1M HCl solution by weight loss measurement, potentiodynamic polarization, electrochemical impedance spectroscopy (EIS), and scanning electron microscopy (SEM) [70]. The polarisation study showed that both synthesised compounds are mixed-type inhibitors and the electrochemical impedance study revealed that the presence of inhibitors resulted to increase the charge transfer resistance.

Indole Derivatives of Schiff Base Inhibitors- A Review

In 2008, G. Avci investigated the corrosion inhibition of indole-3-acetic acid on mild steel in 0.5M HCl medium containing the desired concentration of inhibitor at various temperatures using PDP, EIS and PRM measurements [71]. The experimental results indicated that corrosion potential shifted towards a more negative potential region in the presence of indole-3-acetic acid than that of blank solution. Inhibition efficiency was about 77% with 1.7×10^{-3} M inhibitor and increasing to about 93% at 1×10^{-2} M inhibitor concentration. Potentiodynamic polarization measurements showed that in the presence of inhibitor, the current at anodic and cathodic regions have smaller value than that of the blank solution at almost all potentials. Activation

energy (E_a), enthalpy (ΔH_{ads}), Gibbs free energy (ΔG_{ads}) and entropy (ΔS_{ads}) were calculated.

In 2010, M. Lebrini carried out a comparative study of 1-methyl-9H-pyrido [3,4-b]indole (harmane), 9H-pyrido[3,4-b]indole (norharmane) as corrosion inhibitors for C38 steel in 1M HCl medium at 25°C using potentiodynamic polarization and electrochemical impedance spectroscopy (EIS) techniques [72]. The OCP as a function of time was also established. Anodic and cathodic polarization curves showed that harmane and norharmane are mixed-type inhibitors and they followed Langmuir adsorption isotherm model. Potential of zero charge (PZC) of the C38 steel in the inhibited solution was estimated by the EIS technique. Raman spectroscopy established that indole molecules strongly adsorbed on the steel surface.

In 2012, Paul Aby et al. investigated the corrosion inhibition efficiency of 3-formylindole-3-aminobenzoic acid on mild steel (MS) in 1M HCl solution using gravimetric weight loss measurements, electrochemical impedance spectroscopy (EIS) and potentiodynamic polarization (PDP) studies [73]. Even at low concentrations, the ligand exhibited good inhibition on mild steel in HCl medium. The adsorption of inhibitor on the surfaces of the corroding metal followed Langmuir isotherm. Polarization studies revealed that the molecule act as a mixed type inhibitor. Thermodynamic parameters like K_{ads} and ΔG^0_{ads} were calculated using Langmiur adsorption isotherm.

In 2014, A. Fouda, et al. investigated the influence of 2-oxyindole and indole on the rate of corrosion of α-brass in 1M HNO_3 using gravimetric weight loss, potentiodynamic polarization, electrochemical impedance spectroscopy (EIS) and electrochemical frequency modulation (EFM) techniques [2]. It was found that the investigated compounds behave as inhibitors. The adsorption of these ligands on the

α-brass surface followed Langmuir's adsorption isotherm and electrochemical results showed that all the investigated ligands act as mixed-type inhibitors. Results obtained from electrochemical techniques were in good agreement [74].

Scope and Objectives of Present Investigation

Steel with carbon content varying between 0.05 to 2.1 % by weight is termed as carbon steel (CS). It is used in research and development, defence, mega projects, various industries like oil industry, nuclear industry, petro-chemical industry, pulp and paper industry etc. Resistance to wear and tear, toughness and high strength are their important properties. The combination of these properties is utilized in the manufacture of train wheels, railway tracks, crankshafts and gears and machinery parts. The consequences of corrosion which is a serious problem worldwide have escalated rapidly. It is clear from the literature survey that there is great urge for expedited research in the fields of metallic corrosion generally and particularly in carbon steel in attributed to its practical significance. Carbon steel is well prone to corrosion by an environment with aggressive medium, particularly during pickling or acid cleaning. Many additives including organic compounds alter the corrosion rate of metals like iron, copper and aluminium when added to the working media.

Many organic molecules have been extensively screened for their corrosion inhibition efficiencies on various metals in acidic media. The quest for novel potential corrosion inhibitors is still continuing in the present decade. One of the most practical, effective and economic corrosion inhibitors are the organic compounds containing heteroatoms in their molecular structures. The development of novel corrosion inhibitors containing heteroatoms such as sulphur, oxygen and nitrogen is one of prime interests in chemical industries address the problems of corrosion and to diminish the economic liability in the case of equipment. Till now, several review articles have been published

depicting elaborately the application of P, N and O atoms; but, a thorough literature survey revealed that corrosion inhibition studies of organic molecules bearing sulphur atoms are scarce. This part of thesis aims to study the applications of novel sulphur containing Schiff bases as corrosion inhibitors. Sulphur-containing compounds are greatly preferred for preventing the metallic dissolution, due to the high polarisability of the sulphur atom. So the present investigation is intended to realize novel potential sulphur containing organic inhibitors, especially towards carbon steel corrosion.

Seven novel sulphur containing Schiff base inhibitors, (E)-(N-anthracene-9-ylmethylene)-5-(4-nitrophenyl)-1,3,4-thiadiazol-2-amine (A9CNPTDA), (E)-5-(4-nitro phenyl)-N-((pyridine-2-yl)methylene)-1,3,4-thiadiazol-2amine (P2CNPTDA), (E)-5-(4-nitrophenyl)-N-(1(pyridine-3-yl)ethylidene)-1,3,4-thiadiazol-2-amine (3APNPTDA), (E) -5-(4-nitrophenyl)-N-(1(pyridin-2-yl)ethylidene)-1,3,4-thiadiazol-2-amine (2APNPTDA), N-(anthracen-9(10H)-ylidene)-5-(4-nitrophenyl)-1,3,4-thiadiazol-2-amine (ANNPTDA), N-((1H-indol-3-yl)methylene)thiazol-2amine (I3A2AT) and (13E)-N1,N2-bis((thiophene -2-yl)methylene)cyclohexane-1,2-diamine (T2CDACH) were synthesized and a detailed procedure for the synthesis of these inhibitors are explained in chapter 2. The present work was designed in order to explore the inhibition efficiencies of these 'S' containing heterocyclic Schiff bases as corrosion inhibitors on carbon steel (CS) in aggressive medium (1M HCl and 0.5M H_2SO_4). The behaviour of CS in the presence of these heterocyclic compounds was investigated by electrochemical measurements and gravimetric studies. Electrochemical impedance spectroscopy, potentiodynamic polarization and electrochemical noise studies were employed for the detailed analysis. Quantum chemical studies were also performed. The mechanism of corrosion inhibition by these sulphur-containing heterocyclic Schiff bases was another consideration of this part which will be addressed via the evaluation of the adsorption as well as

thermodynamic parameters and was further verified by surface morphological studies using scanning electron microscopy.

The entire work on corrosion inhibition studies are well documented in this part as two chapters. Chapter 12 describes the corrosion inhibition investigations of CS in the presence of 'S' containing heterocyclic Schiff bases in 1M HCl medium. Corrosion inhibition response of these Schiff bases on CS in 0.5M H_2SO_4 are well explained in chapter 13. Both these chapters comprise of the weight loss measurements, electrochemical measurements, surface morphological studies and quantum chemical studies in detail. Lastly a brief summary on these finding is depicted following by important references.

CHAPTER 11
MATERIALS AND METHODS

Corrosion inhibition effectiveness of novel 'S' containing heterocyclic Schiff bases was investigated by adopting conventional mass loss or gravimetric investigations [75], electrochemical methods like Tafel polarization analysis [76], electrochemical impedance spectroscopy (EIS) [77], electrochemical noise studies [78] and theoretical calculations such as quantum chemical studies [79]. Scanning electron microscopy [80], UV spectroscopy [81] and Fourier transform infrared spectroscopy [82] were engaged to analyze the surface morphological studies of the metal specimen.

It is not a monotonous job to craft a natural corrosive environment for the experimental settings in a laboratory. For mimicking the corrosive environment, we have customary to espouse accelerated corrosion environment, since corrosion is not only a natural and slow observable fact and to monitor the decay rate of steel is a very prolonged process. Before execution of corrosion inhibition tests, surface treatments of metal specimens were performed to make them free from grease and oxides are crucial. The preparation of metal specimens, aggressive solutions (acidic medium) and different techniques adopted for the assessment of corrosion inhibition efficiencies of these 'S' containing heterocyclic Schiff bases are specified in detail.

Metal Specimens

Carbon steel (CS) specimen dimensions (1cm long x 1cm breadth x 0.155 thickness) were used for conventional gravimetric experiments. The weight % (Chemical composition; C,0.55%; Mn,0.08%; Si,0.02% ; P,0.04%; S,0.012%) and the remainder Fe (confirmed by EDX method) of the CS worn throughout the investigation. Before weight loss and electrochemical investigations, CS specimen was cleaned underneath running

distilled water and abraded using diverse grades of silicon carbide emery papers (grade 100-1200), washed with detergent and dried. The precise surface area of the carbon steel specimens was exactly measured using screw gauge and vernier callipers. The cleaned specimen was engrossed in acetone for 10s, washed, dried using tissue paper and weighed. The specimens were conserved in desiccators with the intention to keep away from the contact of the environment till use. After immersing carbon steel specimens in aggressive medium in the absence and presence of inhibitors in diverse concentrations for a preset time, metal specimens were carefully removed, dried and then weighed.

Aggressive Solutions

Stock solutions having 1M HCl and 0.5M H_2SO_4 were prepared by the dilution of the accurate quantity of respective concentrated acids (AR grade) and using double distilled water. Stock solutions of each 'S' containing heterocyclic ligands were prepared by weighing precise amounts of these with corresponding acids and diluted to diverse concentrations (0.2mM–1.0mM). 50ml and 100ml acid solutions were used in gravimetric studies and electrochemical investigations respectively.

Methods

Gravimetric measurements were done following ASTM standards. Aggressive solutions having different concentrations of sulphur-containing heterocyclic Schiff base inhibitors were prepared, finely polished carbon steel (CS) specimens were engrossed in these solutions and the weight loss of steel specimens was calculated after 24h A blank trial was also done without the addition of the inhibitors. Duplicate experiments were carried for ensuring the reproducibility of results and the average values were recorded. The corrosion rate of carbon steel and the percentage of inhibition efficiencies of each sulphur-containing heterocyclic Schiff base inhibitors

were estimated by the following equations. The rate of corrosion was expressed in 'mm/y' and the percentage of inhibition efficiencies of each sulphur-containing heterocyclic Schiff base inhibitor were calculated using equations (1) and (2) respectively.

$$\text{Rate of corrosion, } W = \frac{K \times \text{Wt.loss (grams)}}{\text{Area in sq.cm} \times \text{Time in Hrs} \times \text{Density}} \quad (1)$$

where 'K'= 87600 (This factor used to alter cm/hour into mm/year), Density of CS specimen is 7.88g/cc

The inhibition efficiency (η) or Percentage of inhibition is given by

$$\eta = \frac{W - W'}{W} \times 100 \quad (2)$$

where W and W' are the corrosion rate of the CS specimen without and with sulphur-containing heterocyclic Schiff base inhibitors respectively [83].

Comparison studies of the inhibition efficiency of the synthesized heterocyclic Schiff bases with their parent amine for a period of 24 hrs explore the function of azomethine linkage in the corrosion inhibition ability of heterocyclic Schiff bases.

Adsorption Isotherms

The mechanism of action of inhibition of Schiff bases on the metal surface is not entirely disclosed by the researchers and later it was proved that adsorption is the main reason for the inhibitory action of these molecules [84,85]. It may be physical adsorption, chemical adsorption or both. Adsorption isotherms have a significant role in shaping the inhibition mechanism [86,87]. The extend of corrosion inhibition can be explained by considering the adsorption isotherms. These isotherms characterize the molecular interactions with the reactive sites on the specimen surface. Langmuir, Freundlich, Frumkin and Temkin are the common adsorption isotherms. The finest fit isotherm is

accepted with the support of correlation coefficient and all isotherms were tried with the help of following equations

Langmuir adsorption isotherm $\frac{C}{\theta} = \frac{1}{K_{ads}} + C$ (3)

Freundlich adsorption isotherm $\theta = K_{ads}C$ (4)

Temkin adsorption isotherm $e^{f\theta} = K_{ads}\, C$ (5)

Frumkin adsorption isotherm $\frac{\theta}{1-\theta}\exp(f\theta) = K_{ads}\, C$ (6)

where C is the inhibitor concentration, θ is the fractional surface coverage, f is the molecular interaction parameter and K_{ads} is the adsorption equilibrium constant. Among the tried isotherms, most suitable one which has the highest correlation coefficient value (R^2) was considered for explaining the adsorption mechanism.

The relation between adsorption equilibrium constant K_{ads} and the standard free energy of adsorption ΔG^0_{ads} given by the equation,

$\Delta G^0_{ads} = -RT\ln(55.5\, K_{ads})$ (7)

where the constant value 55.5 is the molar concentration of water, R is the ideal gas constant and T is the temperature in Kelvin. The value of K_{ads} and ΔG^0_{ads} were obtained from different adsorption isotherms.

Surface Analysis

The changes in the morphology of the carbon steel surface monitored by surface analysis help to illustrate the mechanism by which the synthesized compounds diminish the rate of corrosion [88]. This was done by taking SEM image (scanning electron microscopic images) of the surfaces of untreated bare metal (CS), metal engrossed in acid medium (24h) and metal engrossed in synthesized inhibitor solution (24 h). For taking SEM-EDAX the Model-JEOL 6390LA/OXFORD XMX N (0.5-30KV) accelerating voltage and Magnification x 300000) was used.

Temperature Studies

The evaluation of thermodynamic corrosion parameters (activation energy (E_a), enthalpy of corrosion (ΔH*), the entropy of corrosion (ΔS*) and Arrhenius parameter (A) in the gravimetric weight loss study was evaluated in different temperatures (30-60°C). The activation energy for the corrosion progression in the absence and presence of these synthesized sulphur containing Schiff bases was assessed by Arrhenius equation.

Rate of Corrosion; $K = A \exp\left(\frac{-Ea}{RT}\right)$ (8)

where A is the frequency factor, E_a is the activation energy, R is the gas constant and T is the temperature (Kelvin). The plot logK Vs 1000/T have to be a straight line. According to this equation, slope of the line will be $-E_a/2.303R$ (activation energy evaluated from this slope) and intercept will be log A.

Transition state theory [89] can be used for the assessment of the enthalpy and entropy of activation (ΔH*, ΔS*), which corresponds to the equation,

$$K = \left(\frac{RT}{Nh}\right) \exp\left(\frac{\Delta S*}{R}\right) \exp\left(\frac{-\Delta H*}{RT}\right) \quad (9)$$

where N is the Avogadro number and h is the Planks constant. This equation can be modified to an equation for straight line (y = mx + c)

$$log\ \frac{K}{T} = log\ \frac{R}{Nh} + \frac{\Delta S}{2.303\ R} - \frac{\Delta H}{2.303\ RT} \quad (10)$$

The enthalpy of the reaction can be obtained from the slope, $-\Delta H/2.303R$ and entropy of the reaction acquired from the intercept, $(\log\frac{R}{Nh} + \frac{\Delta S}{2.303\ R})$ of the line on y axis.

Electrochemical Impedance Spectroscopy

AC impedance methods or electrochemical impedance spectroscopy (EIS) are extensively exploited in modern days for corrosion experiments [90–96] as a

sophisticated and precise method. Mechanistic and kinetic information on inhibition investigations can be attained by impedance measurements. The response of the system offers information concerning the responses occurring at the interface. The detection of electric and dielectric properties of components under inquiry is made viable by the system. By means of suitable equivalent electrical circuits [97], electrochemical scrutinisation can be performed.

Iviumcompactstat-e system associated with a superior version of 'IviumSoft' software was employed for the electrochemical analysis. This makes it easier and possible steps to derive an appropriate equivalent circuit, computation of current densities and resistance. Assemblies of three-electrode was used as the electrochemical cell in which a saturated calomel electrode (SCE) was used as the reference electrode, a platinum electrode of area $1cm^2$ was used as the auxiliary or counter electrode and well-polished metal surface of exposed area ($1cm^2$) towards the corroding medium was employed as the working electrode for analysis.

The dimension of the capacitance (C_{dl}) in the constituency of the electrical double layer formed between oppositely charged ions in the aggressive medium and the charged carbon steel surface can be regarded as correspondent to an electrical capacitor. Corrosion inhibitors in the aggressive medium form an adsorption layer on the electrode (CS) surface. The electrical capacity decreases with an increase in the concentration of the inhibitor.

A small and steady sinusoidal current was applied during the measurement of impedance and along with the phase angle and the resulting current was measured. The real and imaginary fractions of impedance were derived by this method. The real constituent of the impedance, $Z'(\omega)$ corresponds to the resistance and the imaginary constituent, $Z''(\omega)$ corresponds to capacitance and the relation between these two

constituents are

$Z(\omega) = Z'(\omega) + jZ''(\omega)$

where Z(ω) is the impedance, Z'(ω) is given by $Z_0\cos\Phi$ and Z''(ω) is given by $Z_0\sin\Phi$, Z_0 is the magnitude of the impedance and j is the imaginary number √-1

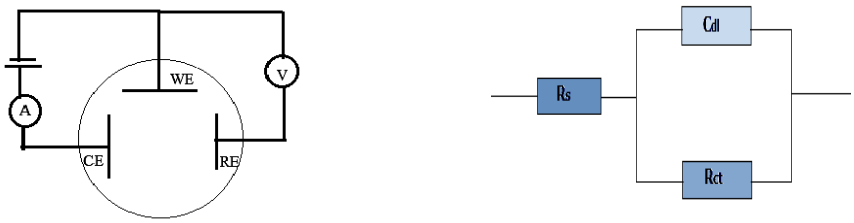

Fig. 3.11: Equivalent circuit

Impedance data can be well represented by diverse forms of plots such as Nyquist (Cole-Cole) plot, Impedance plot and Bode plot and all forms provide considerable benefits for establishing definite characteristics of an exact system. The commonly used Nyquist plots are achieved by plotting the square of the real fraction of impedance against the square of the imaginary part. The ohmic resistance or solution resistance, R_s, is the resistance between the reference electrode and the working electrode, which is given by the impedance at elevated frequencies of the semicircular Nyquist plot. At the leftmost end of the semicircle, the frequency achieves its high limit of the semicircle and at the rightmost end, it achieves its low limit, where the impedance observed is the sum of R_s and R_{ct} (charge transfer resistance at the electrode-solution interface). Subsequently, the inhibition efficiency of the synthesized molecule can be deliberated using equation (11) [30].

$$\eta_{EIS}\,\% = \frac{R_{ct} - R'_{ct}}{R_{ct}} X100 \qquad (11)$$

where R'_{ct} and R_{ct} are the charge transfer resistances of working electrode (CS) in the absence and presence of inhibitor respectively.

In Bode plots, the magnitude of impedance (|Z|) and phase angle (θ), are plotted against frequency. The absolute impedance (Z) is acquired from the equation,

$$|Z| = \sqrt{Z'^2 + Z''^2} \quad (12)$$

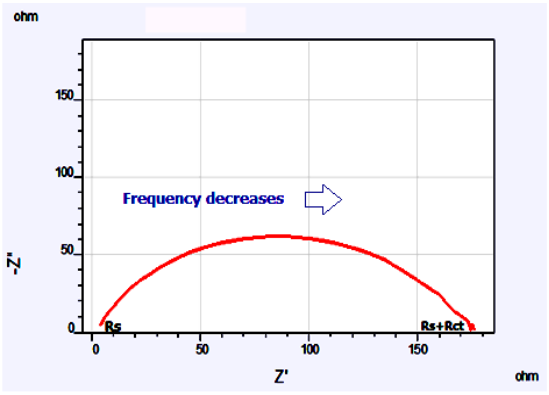

Fig. 3.12: Nyquistplot

The Bode plot is a time-consuming substitute of the Nyquist plot which helps to avoid longer times for the measurement of low frequency. The curve obtained from impedance plot ie log|Z| versus log frequency provides the value of R_s and R_{ct}. The cut-off point of this curve reclines on a straight line which has a slope of -1. Extrapolating this line to the y-axis at logf = 0 or f=1 provides outcome value of C_{dl}.

$$|Z| = \frac{1}{C_{dl}} \quad (13)$$

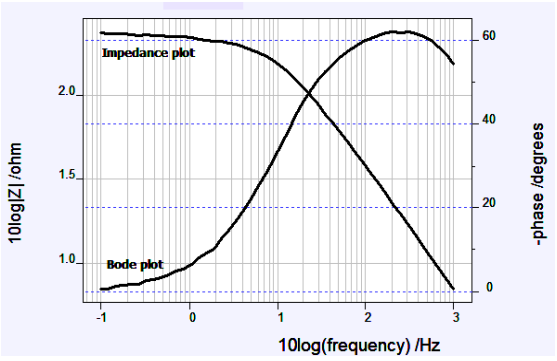

Fig. 3.13: Bode and impedance plots

The plot of 'θ' versus log f, shows a peak which equivalent to f θ^{max} representing the maximum phase shift value and from which C_{dl} can be intended. Frequency breakpoints allied with every step are the trait of impedance and Bode plots.

Potentiodynamic Polarization Studies

Polarization studies can be divided into two i) Linear polarization studies and ii) Tafel extrapolation studies. The Polarization technique associated with the alteration in the potential of the working electrode and the produced current is measured as a function of potential or time [98–100].

Linear polarization technique

The equation analogous to the Butler-Volmer equation can be used to explain the polarization reaction of a metal (carbon steel specimen)

$$i = i_{corr}[e\left(\frac{\eta}{\beta a}\right) - e\left(\frac{\eta}{\beta c}\right)] \quad (14)$$

where 'i' is the net current density across the metal specimen and electrolyte boundary, 'i_{corr}' is the corrosion current density (Acm^{-2}), $'\eta'$ is the overpotential (difference between $E_{measured}$ and E_{corr}). Depending on the mechanism of reaction, β_a and β_c are the anodic and cathodic constants and are specified by

$$\beta_a = \frac{RT}{(1-\propto)nF} \quad (15) \qquad \beta_c = -\frac{RT}{\propto nF} \quad (16)$$

It is established from Equation (14) that the charge transfer process occurred at the interface constituted by the metal and solution is the rate-determining step (slowest step) in the electrochemical process of corrosion. Experimentally this relation is observed between the potential of an electrode under corrosion (in the absence of competing redox reactions) and applied electrochemical current density. The significance of this relationship depends on the single charge transfer controlled anodic

and cathodic reactions. This equation brings the support of the electrode which undergo corrosion where electrochemical polarization method is applied.

Linear polarization mode depends on the practical and theoretical authentication that the applied current density is linear as a function of the potential of the electrode and potentials are very near to $E_{corr,}$ +/- 10mV. This is exemplified in Fig. 3.14.

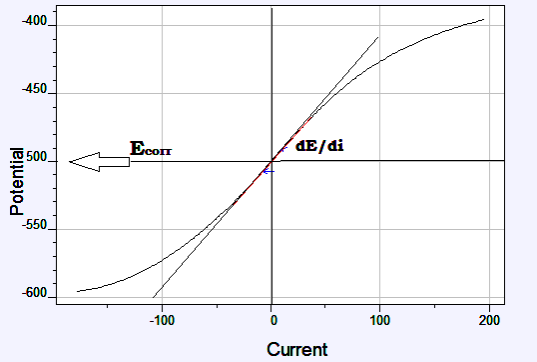

Fig. 3.14: Linear polarization plot

Slope is $\frac{\Delta E}{\Delta i}$ and has the unit of resistance (R_p), which is known as polarization resistance. Thus sometimes this approach is known as polarization resistance technique. When equation (14) undergo mathematical linearization, the famous Stern and Geary equation (11) is obtained, which indicates that the slope is inversely related to i_{corr} and is given by the equation

$$i_{corr} = \left[\frac{b_a b_b}{2.303(b_a b_b)}\right]\frac{\Delta i}{\Delta E} = \frac{B}{R_p} \qquad (17)$$

where 'b_a' and 'b_b' are called Tafel slopes (anodic and cathodic). Current density, i_{corr} in the form of corrosion rate can be measured with the aid of equation 17, where values of R_p and B are identified. For evaluating corrosion inhibition efficiency, linear polarization technique is employed in the manner that, whenever increasing the inhibitor concentration, polarization resistance (R_p) have the affinity to enhance. The rate of charge transfer process decreases on the corroding surface with the adsorption of inhibitors and

this practice boosts the polarization resistance or diminishes the corrosion rate. The polarization resistance values were acquired by the scrutiny of the slope of linear polarization curves in the vicinity of corrosion potential of blank and diverse concentration of the inhibitors [101,102]. The inhibition efficiency was considered from the polarization resistance, using the equation

$$\eta_{R_p}\% = \frac{R'_p - R_p}{R'_p} X100 \quad (18)$$

where 'R'_p' and 'R_p' are the polarization resistances with and without inhibitors respectively.

Tafel extrapolation technique

Tafel equation discloses the relationship between logarithmic value of current density and the applied potential. Using the equation 19, Tafel equation can simply be deduced. For an anodic (metal dissolution) process, the current density (i) is obtained by Tafel's law. The equation must assure the clause $\left(\frac{\eta_a}{\beta_a}\right) \gg 1$

$$i = i_{corr} e \left(\frac{\eta_a}{\beta_a}\right) \quad (19)$$

On taking the logarithm of the equation (19),

$$\eta_a = -\beta_a \ln i_{corr} + \beta_a \ln i_{corr} \quad (20)$$

Converting into logarithm to base 10 and defining the anodic Tafel constants a and b, then $\eta_a = a_a + b_a \log i_a$ (21)

where $a_a = -2.303\beta_a \log i_{corr}$ and $b_a = 2.303\beta_a \log i_a$

Likewise for cathodic process, $\left(\frac{\eta_b}{\beta c}\right) \ll 1$

$$i = -i_{corr} e \left(-\frac{\eta_c}{\beta c}\right) \quad (22)$$

Then $\eta_c = a_c - b_c \log i_c$ (23)

where $a_c = -2.303\beta_c \log i_{corr}$ and $b_c = 2.303\beta_c \log i_c$

The plot of potential of the electrode versus the logarithm of current density confers a straight line and termed as Tafel lines. The slope of a Tafel plot, 'b' provides the mechanism of electrode process and the intercept 'a' at $\eta = 0$ offer the exchange current density. The information of the rate constant is given by this model.

A way to measure i_{corr} value is the method of extrapolating the linear fragments of potential-current density curves. This practice is based on the law that the samplings (specimens) were made to operate as cathode of the electrochemical cell consisting the corrodent. Cathode potential-current density curve was plotted over a potential range E_{corr} to $E_{c.}$ In the same way, anodic potential-current density is attained in the path away from E_{corr} and at this moment the sampling (specimen) performes as anode. The attained cathodic and anodic potential-current density curves consist of linear sectors, regarded as Tafel constituency. By the extrapolation of these linear fragments of cathodic and anodic curves (Fig. 3.15), Tafel lines criss-cross at the point of coordinates E_{corr} and $logi_{corr}$ and thus the value corrosion current density achieved. Subsequently, the percentage of inhibition efficiency is calculated using the equation

$$\eta_{pol}\,\% = \frac{I_{corr} - I'_{corr}}{I_{corr}}\ X100 \qquad (24)$$

where i_{corr} and i'_{corr} are corrosion current densities of uninhibited and inhibited cases respectively.

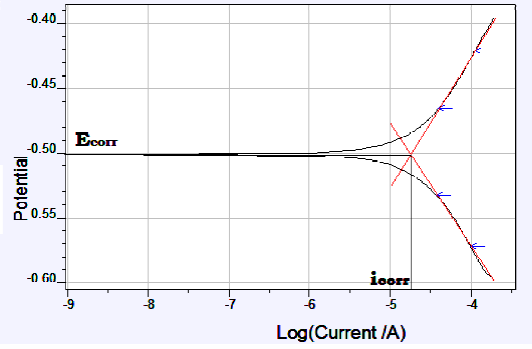

Fig. 3.15: Tafel plot

In the present investigation Tafel polarization studies of carbon steel in 1M HCl and 0.5M H_2SO_4 in the presence and absence of inhibitors conducted by recording both cathodic and anodic potentiodynamic polarization curves using Iviumcompactstat-e electrochemical system.

Electrochemical Noise Measurements

Electrochemical noise (ECN), is a common term which measures the fluctuations of current and potential allies with corrosion progression followed by metal deterioration. This technique also helps to compute the quantity of localized pitting corrosion [103–105]. The experimentation was executed in a three-electrode cell assemblage consisted of two carbon steel electrodes ($1cm^2$) used as working electrode and counter electrode/SCE was used as reference electrode [106,107] in the cell connected to Ivium Compactstat-e electrochemical system (controlled by Iviumsoft software) for a period of 1200s.

Noise is considered as a non-deterministic progression and it is an algebraic expression having random character which depicts the amplitude-time dependence of a source is unfeasible. Usually, deterministic progressions are periodic and this can be described mathematically by a varying function of time. Fluctuations observed in corrosion current values are a non-deterministic process and analysis done by statistics and probability rather than the algebraic method. Fig. 3.16 corresponds to the plot of noise current Vs time and the noise current values provide a design about the corrosion protection power of the molecules. Fig. 3.17 corresponds the pitting index curve of the sample and the amplitude of the curve point out the resistance power of the sample against localized pitting corrosion.

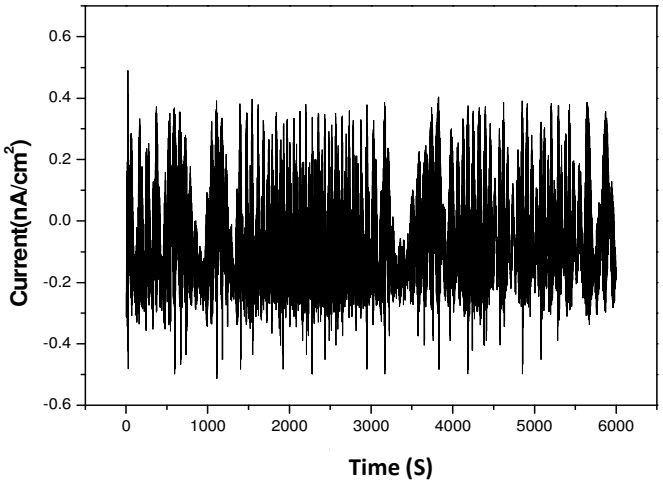

Fig. 3.16: Noise current Vs time

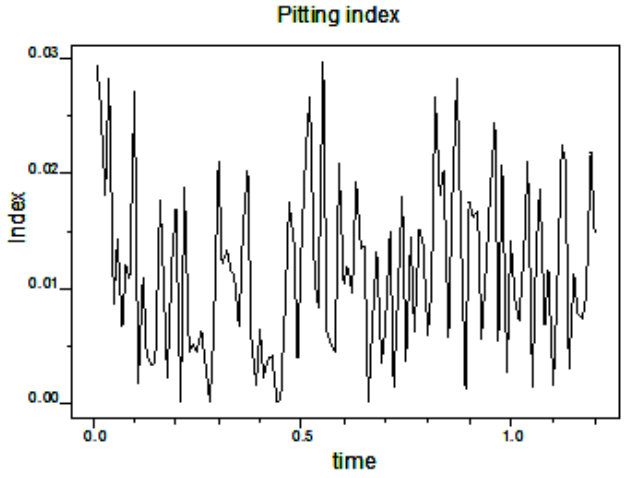

Fig. 3.17: Pitting index curve

Frequency Domain Analysis

It is understood that any complex waveform can be taken as the sum of several sinusoidal waveforms of acceptable amplitudes, periodicity and relative phase[108,109]. A spectrum is the illustration of time depending development in the frequency domain analysis and the corresponding noise measurement analysis gave the Power Spectral Density (PSD) which is given in Fig. 3.18. The PSD has diverse applications in different areas of science and technology which are showing here

- The signals of noise are significant in biomedical purposes like simulation, therapy etc;
- For acoustic measurements.
- Earthquake determination from the spectra obtained from seismographs.
- From the characteristic component analysis of the acoustic noise signals from the engine can detect its malfunction.

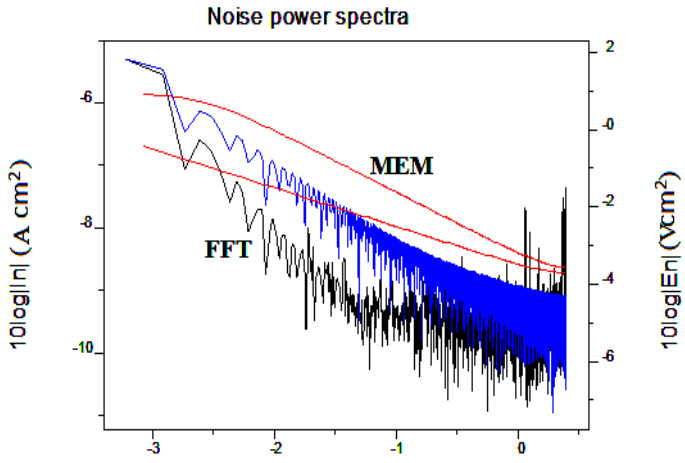

Fig. 3.18: PSD plot

Fast Fourier Transform (FFT)

In the complex Fourier series, Fast Fourier Transform is a machine calculation method and it is significantly quicker than other traditional methods. There are two major difficulties linked with investigation by FFT are aliasing and leakage. Aliasing applies to all spectral analysis methods and it is an error occurs by rate of sampling become too slow. Leakage is resulting by the basic presumption of the Fourier Transform to the fixed time record is said as periodic.

Maximum Entropy Method

In every spectral analysis mode, analysis by Fourier Transform has been measured as a basic tool [110]. It becomes precise only when long record length takes

place. When it is short, conventional spectrum estimation by smoothing may provide poor resolution. The Burg's maximum entropy method helps to improve the spectral resolution of short length records. This is achieved by the extrapolation of auto-correlation function and helps to maximize the entropy of the probability density function in each step of the extrapolation. Burg's method is data dependable method and therefore it is nonlinear. The MEM has applications in various fields in science and technology.

Quantum Chemical Studies

The corrosion inhibition response of organic molecules can be correlated with the energy of frontier molecular orbitals [111–113]. The donor-acceptor interactions (explained by HSAB concept)between the vacant d-orbitals of Fe on the surface atoms and the filled molecular orbitals of the inhibitor molecules are very significant in the preclusion of metal dissolution [114–116]. The high value of E_{HOMO} and the smallest value of E_{LUMO} and the difference in their energy (which should be low) are the vital parameters which assist the strong binding of the compounds on the metal surface. Optimisation of molecular geometry and calculations of quantum chemical studies was performed by DFT method utilizing the GAMMES software. Lee–Yang–Parr nonlocal correlation functional method (B3LYP) and Beck's three-parameter exchange functional was employed in DFT calculations [117]. HOMO (Highest occupied molecular orbital) gives information about the most vigorous (energetic) electrons containing regions and these electrons are generally likely to be donated to the electron-poor species. The LUMO (Lowest unoccupied molecular orbital) has the lowest energy and indicated the locations in a molecule which has the highest tendency to receive electrons from the electron-rich metal species. HSAB parameters such as electronegativity (χ) and chemical hardness (η) of the inhibitors were assessed by the following equations,

$\chi \approx -1/2\ (E_{HOMO} + E_{LUMO})$ (25)

$\eta \approx 1/2\ (E_{HOMO} - E_{LUMO})$ (26)

The number of electrons transferred (ΔN) implies the propensity of a ligand to donate electrons. Higher the value of ΔN, the superior is the tendency of the compound to donate electrons to the electron-deficient species. For the case of corrosion inhibitors, a higher ΔN signifies a greater tendency of interaction with the metal surface through the adsorption process. The electronegativity and chemical hardness of bulk iron are assumed as 7eV and zero respectively. The number of transferred electrons (approximate) from the molecule to atoms of iron is assessed by the subsequent equation,

$$\Delta N = \frac{\chi_{Fe} - \chi_{inhib}}{2(\eta_{Fe} + \eta_{inhib})} \quad (27)$$

Optimized geometry of newly synthesised molecules can be recognized by quantum mechanical software and this facilitates to forecast the three-dimensional arrangement of atoms in molecules which formulates them most stable form with the lowest energy.

CHAPTER 12

CORROSION INHIBITION STUDIES OF SULPHUR CONTAINING SCHIFF BASES ON CARBON STEEL IN 1M HCl

Corrosion inhibition investigations of seven novel 'S' containing Schiff base inhibitors, (E)-(N-anthracene-9-ylmethylene)-5-(4-nitrophenyl)-1,3,4-thiadiazol-2-amine (A9CNPTDA), (E)-5-(4-nitrophenyl)-N-((pyridine-2-yl)methylene)-1,3,4-thiadiazol-2-amine (P2CNPTDA), (E)-5-(4-nitrophenyl)-N-(1(pyridine-3-yl)ethylidene)-1,3,4-thiadiazol-2-amine (3APNPTDA), (E)-5-(4-nitrophenyl)-N-(1(pyridin-2-yl)ethylidene)-1,3,4-thiadiazol-2-amine (2APNPTDA), N-(anthracen-9(10H)-ylidene)-5-(4-nitrophenyl) -1,3,4-thiadiazol-2-amine (ANNPTDA), N-((1H-indol-3-yl)methylene)thiazol-2amine (I3A2AT) and (13E)-N1,N2-bis((thiophene-2-yl)methylene)cyclohexane-1,2-diamine (T2CDACH) on carbon steel were conducted by preparing inhibitor solutions in the range of 0.2mM-1mM in 1M HCl medium. Carbon steel specimens were prepared as per ASTM standards and employed for this study. To assess the capacity of inhibitors for corrosion inhibition, gravimetric weight loss measurements, potentiodynamic polarization (PDP), electrochemical impedance spectroscopy (EIS), electrochemical noise studies, quantum chemical analysis and surface morphological studies were performed and the results are documented in detail in this chapter.

Gravimetric Weight Loss Investigations

The well-polished specimens of CS were engrossed in the medium of hydrochloric acid in the absence and presence of the Schiff base inhibitors and the weight loss happened for the specimens were noted after 24h. The rate of corrosion was monitored and revealed that each heterocyclic sulphur containing Schiff base inhibitors do possess significant anticorrosive property towards the carbon steel corrosion in IM

HCl medium.

Table 3.1 represents the corrosion rates of the seven heterocyclic 'S' containing Schiff bases A9CNPTDA, P2CNPTDA, 3APNPTDA, 2APNPTDA, ANNPTDA, I3A2AT and T2CDACH in 1M HCl medium at 28^0C for 24h and established that the rates of corrosion of carbon steel specimens were noticeably decreased with the concentration of inhibitor in all cases. In the absence of Schiff bases, carbon steel specimen engrossed in the hydrochloric acid solution showed the corrosion rate of 9.19mmy^{-1}. But these seven 'S' containing Schiff bases inhibited the metallic dissolution appreciably in the acidic medium even at very low concentrations. Fig. 3.19 shows the comparison study of the corrosion rates of carbon steel specimen in the presence of varying concentrations of sulphur-containing heterocyclic Schiff base inhibitors.

Table 3.1: Corrosion rate of carbon steel in mmy^{-1} in the absence and presence of 'S' containing heterocyclic Schiff bases in 1M HCl at 28^0C for 24h

C (mM)	Corrosion rate (mmy^{-1})						
	A9CNPTDA	P2CNPTDA	3APNPTDA	2APNPTDA	ANNPTDA	I3A2AT	T2CDACH
0	9.19	9.19	9.19	9.19	9.19	9.19	9.19
0.2	0.52	1.09	0.86	1.1	1.68	0.72	1.55
0.4	0.47	0.85	0.68	1.04	1.18	0.56	1.16
0.6	0.42	0.65	0.64	0.83	0.92	0.52	0.93
0.8	0.35	0.44	0.44	0.72	0.78	0.42	0.82
1	0.18	0.29	0.35	0.41	0.43	0.22	0.45

On close assessment of the rates of corrosion, it is obvious that the carbon steel specimen exhibited an appreciably low corrosion rate in the presence of the heterocyclic Schiff base inhibitor A9CNPTDA in HCl medium and displayed an elevated value in the presence of T2CDACH. The value of the corrosion rate of CS for A9CNPTDA was 0.18mm/year at a concentration of 1mM and the rate in the presence of T2CDACH was

0.45mm/year. Values of the corrosion rate of heterocyclic corrosion inhibitors A9CNPTDA, P2CNPTDA, 3APNPTDA, 2APNPTDA and ANNPTDA, I3A2AT and T2CDACH were 0.18, 0.29, 0.35, 0.41, 0.43, 0.22 and 0.45mm/year respectively at 1mM concentration in 1M HCl medium.

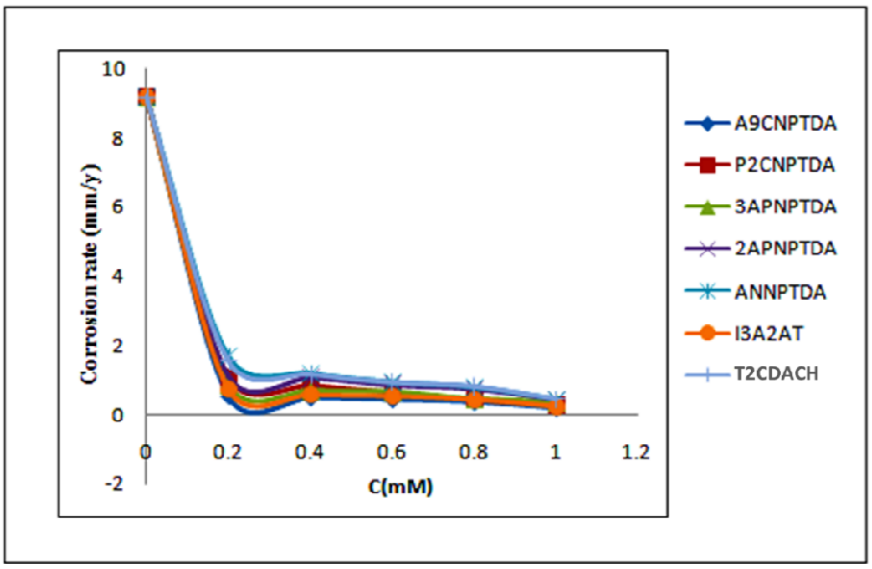

Fig. 3.19: Corrosion rates of CS with different concentration of 'S' containing heterocyclic Schiff base inhibitors in 1M HCl at 28^0C for 24h.

Corrosion inhibition efficiencies of these heterocyclic Schiff bases on carbon steel specimen were investigated in HCl medium which is depicted in Table 3.2 and a comparison of inhibition efficiencies at various concentrations are shown in Fig. 3.20. It is instantly recognizable that all 'S' containing heterocyclic Schiff bases containing azomethine linkage exhibited significant inhibition capacity against the corrosion of metals. These compounds are outfitted with active probes such as azomethine linkage, thiadiazole, thiazole, indole and thiophene moieties and aromatic rings in their structure. Lone pair of electrons on the 'N' atom and highly polarizable sulphur atom makes it a soft base and can contribute its electrons to the vacant'd' orbitals of Fe atoms (which can be considered as soft acid) efficiently. According to Pearson's concept, soft acids

strongly interact with soft bases and this soft-soft interaction is thus possible between the heterocyclic 'S' containing molecules with Fe atoms, which may be accountable for their higher inhibition efficiency. The efficiencies of these heterocyclic inhibitors were increased with the concentration.

Table 3.2: Corrosion inhibition efficiencies of 'S' containing heterocyclic Schiff bases in 1M HCl at 28^0C for 24h

C (mM)	Inhibition Efficiency (η_w%)						
	A9CNPTDA	P2CNPTDA	3APNPTDA	2APNPTDA	ANNPTDA	I3A2AT	T2CDACH
0.2	93.87	88.07	90.68	88.07	81.68	91.38	81.42
0.4	94.26	90.68	92.63	88.64	87.16	93.9	86.59
0.6	95.42	93.88	92.88	90.96	89.98	94.35	89.83
0.8	96.17	95.64	95.19	92.16	91.51	94.94	91.15
1	98.04	96.81	96.22	95.53	95.32	97.61	95.18

On examining Table 3.2, it is quite clear from the data that five heterocyclic 'S' containing Schiff bases A9CNPTDA, P2CNPTDA, 3APNPTDA, 2APNPTDA, ANNPTDA derived from 5-(4-nitro)-1,3,4-thiadiazol-2-amine (NPTDA), the Schiff base I3A2AT, derived from thiazole 2-amine and T2CDACH, which is a thiophene derivative possess excellent corrosion inhibition efficiencies at all concentrations. All of them showed outstanding corrosion inhibition efficiencies and displayed >95.18% of corrosion inhibition efficiency on CS at 1mM concentration at 28^0C.

The potential inhibition efficiency of thiadiazole derivatives of Schiff bases A9CNPTDA, P2CNPTDA, 3APNPTDA, 2APNPTDA and ANNPTDA molecules can be accredited to the presence of heteroatoms especially highly polarizable 'S' atom in the thiadiazole ring, azomethine moiety, electron-rich aromatic rings and planar structure. The highly delocalized electron clouds of the aromatic rings interacted with the metal surface deeply and thus prevent the metallic dissolution appreciably. On approach to the

metal surface, $-NO_2$ group in the heterocyclic Schiff bases derived from NPTDA is replaced by the electron-rich (activating) amino group by the reduction process. In 1854, M.A Bechamp reduced the aromatic nitro compounds into the corresponding amino compounds using Fe/HCl [118] and prepared naphthylamines from nitro naphthalenes and anilinenitrobenzene. The larger electron density around the amino group along with other factors helps the Schiff bases to adsorb on the surface of the metal firmly and can display excellent inhibition efficiency.

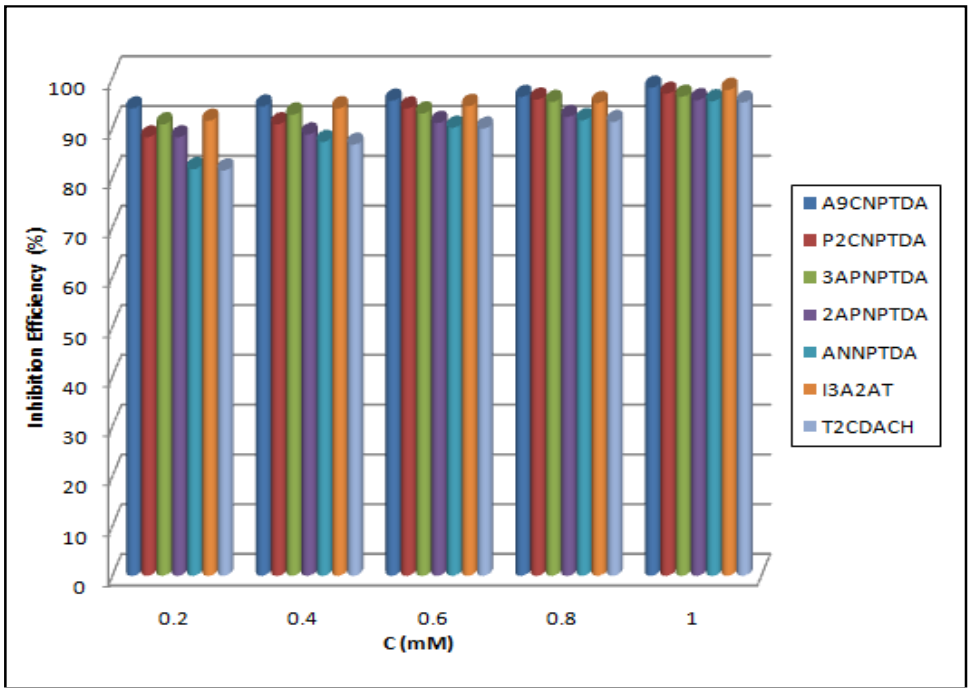

Fig. 3.20: Comparison of corrosion inhibition efficiencies (η_w%) of 'S' containing heterocyclic Schiff bases on CS in 1M HCl at 28^0C for 24h

On the assessment, it is obvious from the data that the heterocyclic polynuclear Schiff base A9CNPTDA showed pronounced corrosion inhibition efficiency compared to all other heterocyclic Schiff bases at every concentration and a maximum efficiency of 98.04% was exhibited at 1mM concentration. The remarkable corrosion preventing ability of this ligand can be interrelated with its molecular structure. Presence of highly delocalized π electron cloud of the aromatic rings in the aldehyde fraction, highly

polarisable ‘S’ atom, lone-pair of electrons of two N atoms of the thiadiazole moiety and one phenyl group attached to it together with highly conjugated azomethine linkage makes A9CNPTDA so electron-rich and help the molecule to bind metal atoms on the carbon steel surface efficiently. In addition to this, the molecule possesses almost planar structure which was deep-rooted by the optimized geometry calculation and favoring strong binding on the carbon steel surface.

Even though there is a structural similarity between the polynuclear heterocyclic Schiff bases A9CNPTDA and ANNPTDA, corrosion inhibition efficiency of ANNPTDA is relatively low compared to that of A9CNPTDA. It is not only due to the presence of an sp^3 carbon atom in the aromatic ring, but also there is a slight deviation from its coplanarity. In addition to the less extensive conjugation and aromatic nature, the presence of strained azomethine linkage also caused to decrease its corrosion inhibition efficiency.

One of the key factors for the elevated inhibition efficiency of heterocyclic pyridine derivatives P2CNPTDA, 3APNPTDA and 2APNPTDA molecules is the presence of pyridine ring in addition to thiadiazole moiety, azomethine linkage and a phenyl group. Maximum inhibition efficiency of 96.81, 96.22 and 95.53% was exhibited by P2CNPTDA, 3APNPTDA and 2APNPTDA respectively at 1mM concentration. On comparing the inhibition efficiencies of P2CNPTDA and 2APNPTDA in HCl medium, 2APNPTDA showed comparatively low η_w%. In these molecules, azomethine linkage starts from the second position of the pyridine ring but a severe steric hindrance is observed in 2APNPTDA due to a bulky methyl group, leading to the loss of coplanarity. But in the case of 3APNPTDA, a methyl group is at the third position with respect to ‘N’ atom of the pyridine ring. There is no steric hindrance in this molecule and planarity is maintained and so high inhibition efficiency showed by this molecule compared to

2APNPTDA.

For a period of 24h, the I3A2AT molecule showed little bit higher inhibition efficiency than the molecule T2CDACH at all concentrations and a maximum efficiency of 97.61% was achieved at a concentration of 1mM. The enhanced efficiency of I3A2AT attributed by the presence of indole and thiazole moieties, extensively conjugated azomethine linkage and electron rich aromatic heterocyclic ring contain highly polarizable 'S' atom. The decreased inhibition efficiency of T2CDACH may be due to its puckered nature of aromatic rings.

Stability of the inhibitor in aggressive medium is very essential if it is to be recommended for long time use. The consequence of time on the corrosion inhibition efficiency of these 'S' containing heterocyclic corrosion inhibitors are represented in Table 3.3.

Table 3.3: Effect of time on the corrosion inhibition efficiency of 'S' containing heterocyclic corrosion inhibitors (1mM) on CS in 1M HCl

Time (h)	Inhibition Efficiency (η_w%)						
	A9CNPTDA	P2CNPTDA	3APNPTDA	2APNPTDA	ANNPTDA	I3A2AT	T2CDACH
24	98.04	96.81	96.22	95.53	95.32	97.61	95.08
48	97.93	94.64	94.01	92.68	94.88	95.12	82.16
72	97.82	94.38	94.30	90.30	94.12	93.34	71.91
96	97.89	93.79	94.27	88.62	92.60	91.18	62.14
120	97.85	93.782	94.64	84.72	90.31	89.83	39.49

Fig. 3.21 represents the variation of corrosion inhibition efficiency with time for the inhibitor molecules at 1mM concentration. The results of gravimetric corrosion studies established that all inhibitor molecules derived from NPTDA and 2-amino thiazole exhibited predominant inhibition efficiency for a long time period. This may be due to their slow hydrolysis rate in acidic medium and prominent adsorption capability by highly active heteroatoms

Even though T2CDACH contain two thiophene ring and two azomethine linkage, its inhibition efficiency decreased with time. It is attributed by its puckered geometry and the tendency to hydrolysis which prevents the molecule to interact with the metal surface. It was confirmed by UV-Visible study that this molecule undergo fast hydrolysis into their parent compounds in 1M HCl medium (Fig. 3.22).

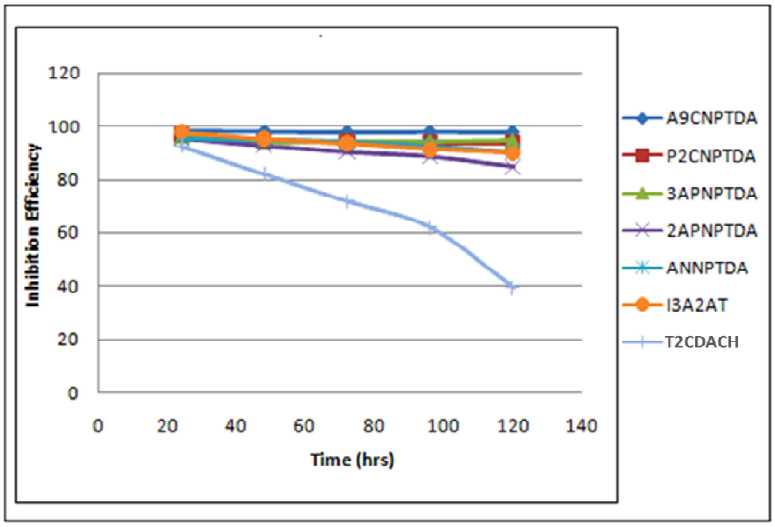

Fig. 3.21: Variation of corrosion inhibition efficiencies of 'S' containing heterocyclic Schiff base inhibitors (1mM) with time on CS in 1M HCl

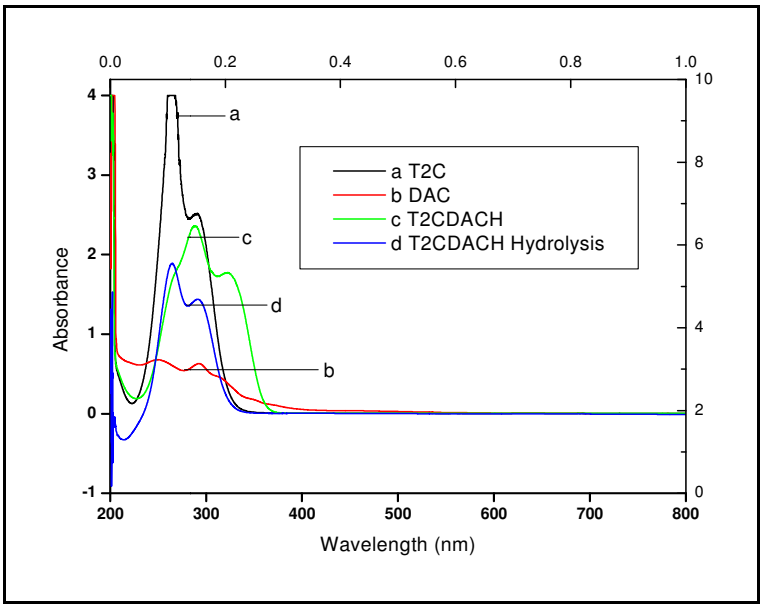

Fig. 3.22: UV-Visible spectra of a) Thiophene 2-carbaldehyde (T2C) b) 1,2 Diaminocyclohexane (DAC) c) T2CDACH at 0h and (d) T2CDACH at 48h 1M HCl

Comparison of Corrosion Inhibition Efficiencies (η_w%) of Schiff Bases With Their Parent Compounds

Corrosion inhibition behaviour of five thiadiazole heterocyclic Schiff base inhibitors A9CNPTDA, P2CNPTDA, 3APNPTDA, 2APNPTDA and ANNPTDA was compared with their parent amine 5-(4-nitrophenyl)-1,3,4-thiadiazol-2-amine (NPTDA) at three different concentrations and revealed that inhibition efficiency was remarkably higher than that of parent amine. Superior inhibitory authorities of these ligands were accredited due to the presence of extensively conjugated azomethine linkage in their structure.

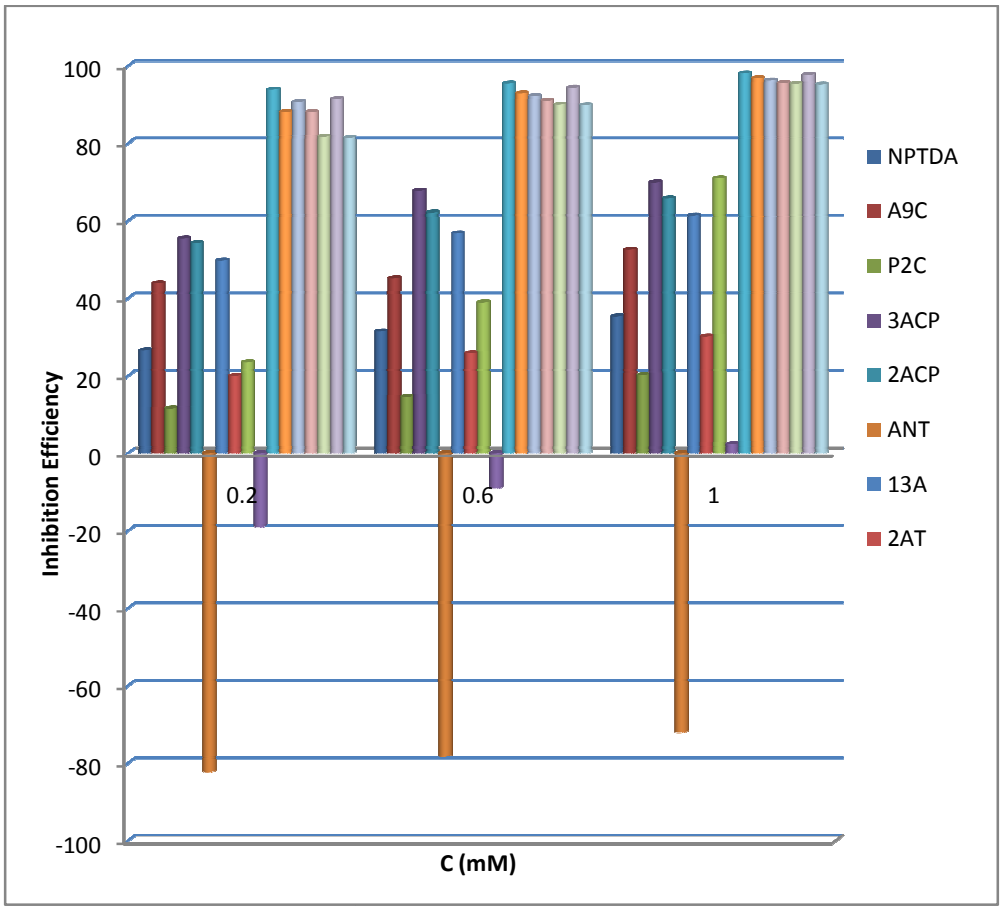

Fig. 3.23: Comparison study of corrosion inhibition efficiencies (η_w%) of 'S' containing heterocyclic Schiff bases with their parent compounds in 1M HCl

It is evident from the Fig. 3.23 and Table 3.4 that all synthesized sulphur-containing heterocyclic Schiff bases exhibit extraordinarily high inhibition efficiencies in comparison with their subsequent parent compounds Anthracene 9-carbaldehyde (A9C), Pyridine-2-carbaldehyde (P2C), 3-acetylpyridine (3ACP), 2-acetylpyridine (2ACP), Anthrone (AN), Indole-3-Carbaldehyde (I3A), 2-Aminothiazole (2AT), Thiophene-2-carbaldehyde (T2C) and 1,2-Diamino cyclohexane (DAC). This substantiates the striking aspect of electron rich azomethine (C=N) moiety present in all sulphur containing Schiff bases which hamper the mechanism of corrosion on the CS surface

Table 3.4: Corrosion inhibition efficiencies (η_w%) of parent compounds NPTDA, A9C, P2C, 3ACP, 2ACP, ANT, I3A, 2AT, T2C and DAC on CS in 0.5M HCl for a period 24h

C (mM)	Inhibition Efficiencies (η_w%)									
	NPTDA	A9C	P2C	3ACP	2ACP	ANT	13A	2AT	T2C	DAC
0.2	26.57	43.87	11.56	55.43	54.28	-82.26	49.74	19.97	23.47	-19
0.6	31.47	45.13	14.5	67.78	62.13	-78.34	56.72	25.78	38.94	-9
1	35.3	52.55	20.16	69.92	65.78	-72.06	61.36	30.17	70.96	2.3

Adsorption Isotherms

The mechanism of inhibition of these sulphur-containing Schiff bases on the surface of the carbon steel specimens can be explained by the adsorption process and the resultant surface modifications on the metal specimen under consideration. The mechanism of adsorption of these organic compounds can be explained by considering different adsorption isotherms; in which the commonly used ones are Langmuir, Freundlich, Temkin, Frumkin, Elawady, and FlorryHuggin etc. The parameters like free energy of adsorption ΔG_{ads} and adsorption equilibrium constant K_{ads} were calculated and its assessment is done by selecting the finest fit isotherm model assisted by the highest correlation coefficient (R^2).

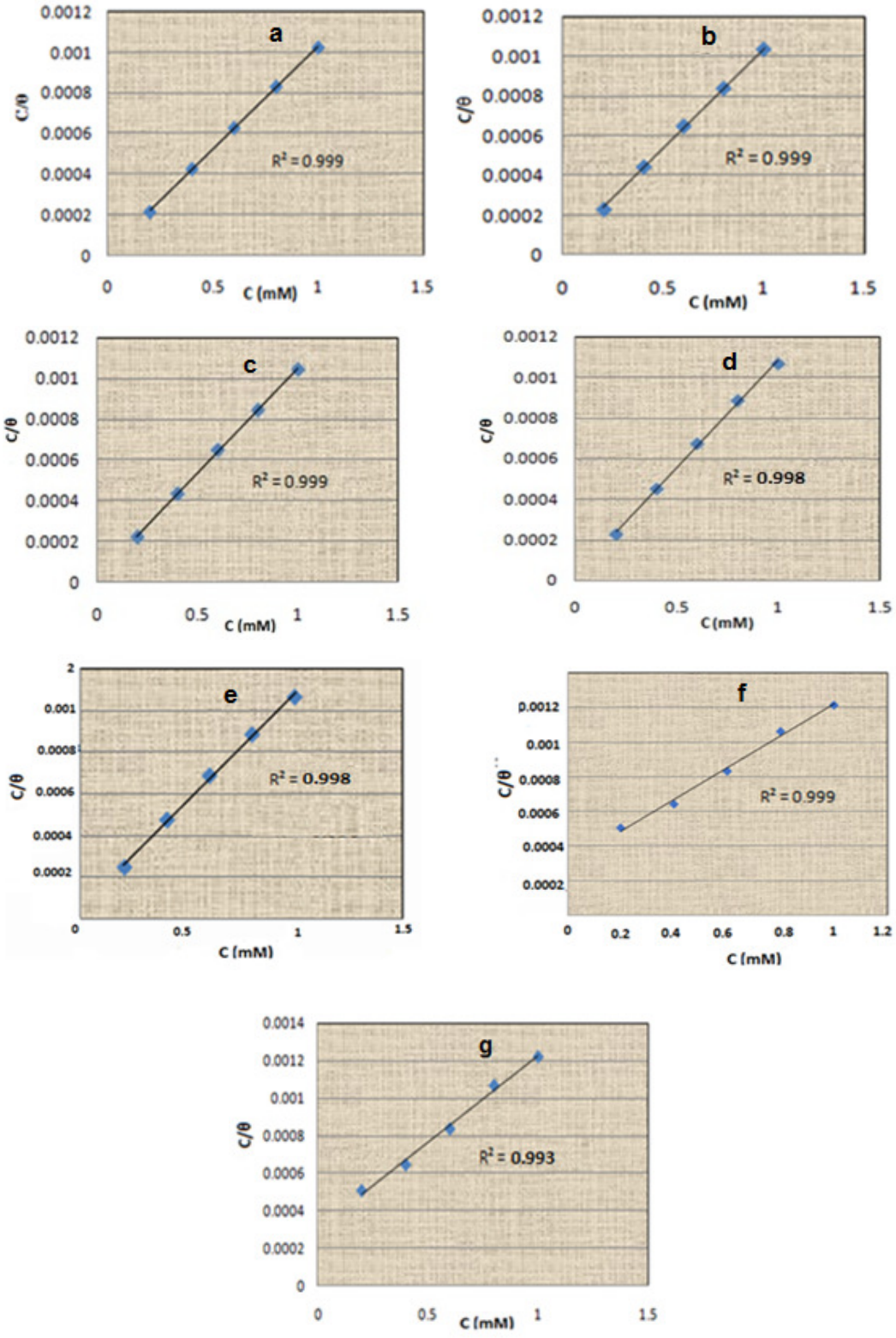

Fig. 3.24: Langmuir adsorption isotherm of (**a**) A9CNPTDA, (**b**) P2CNPTDA, (**c**) 3APNPTDA, (**d**) 2APNPTDA (**e**) ANNPTDA (**f**) I3A2AT (**g**) T2CDACH on CS corrosion in 1M HCl

From the adsorption investigations, it was found that these 'S' containing heterocyclic Schiff base inhibitors A9CNPTDA, P2CNPTDA, 3APNPTDA, 2APNPTDA, ANNPTDA, I3A2AT and T2CDACH followed Langmuir adsorption isotherm on the CS surface of during the process of corrosion inhibition. Isotherms of these inhibitors in 1M HCl are represented from Fig. 3.24 and parameters obtained from investigations are tabulated in Table 3.5

Table 3.5: Adsorption parameters of 'S' containing heterocyclic Schiff bases on CS corrosion in 1M HCl

Adsorption Parameter	Schiff bases						
	A9CNPTDA	P2CNPTDA	3APNPTDA	2APNPTDA	ANNPTDA	I3A2AT	T2CDACH
K_{ads}	58823.5	50000	47619	33334	22222.2	47128.6	3333.3
ΔG^0_{ads} ($kJmol^{-1}$)	-37.56	-37.15	-37.02	-36.14	-35.12	-37.02	-30.37

Negative values of ΔG^0_{ads} for all sulphur containing Schiff bases inhibitors point out the spontaneity of the adsorption on the surface of CS. ΔG^0_{ads} values up to -20kJ/mol indicates the electrostatic interaction between the charged heterocyclic organic inhibitors and the charged metal surface (physisorption). If ΔG^0_{ads} is more negative than -40kJ, shows a well-built adsorption of the inhibitors molecules on the surface of the metal through co-ordinate type bond, which is known as chemisorption [119]. In the present investigation, all the synthesized novel 'S' containing Schiff bases inhibitors exhibited ΔG^0_{ads} ranges between -30.37 and -37.56 kJ/mol on CS specimens in 1M HCl medium which implies that the adsorption behaviour of all the synthesized heterocyclic inhibitor molecules involves both electrostatic and chemical adsorption. The free energy of adsorptions of these heterocyclic Schiff base inhibitors, A9CNPTDA, P2CNPTDA, 3APNPTDA, 2APNPTDA and I3A2AT, were comparatively elevated than that of the other heterocyclic imines ANNPTDA and T2CDACH. The main reason is that these inhibitors are more powerfully adsorbed on the CS surface forming a monolayer through

highly conjugated azomethine linkage, highly polarisable aromatic rings. Planarity of the molecule also helped to adsorb molecules strongly.

The adsorption equilibrium constant K_{ads} also represents the extension of the adsorption happening on the corresponding surface. The above data shows that almost all heterocyclic Schiff base inhibitors derived from 5-(4-nitrophenyl)-1,3,4-thiadiazol-2-amine (NPTDA) except ANNPTDA and the Schiff bases derived from thiazole I3A2AT have relatively high K_{ads} value than heterocyclic sulphur containing Schiff base T2CDACH.

Impact of Temperature

To assess the consequences of temperature of corrosion inhibition process of these 'S' containing heterocyclic Schiff bases, gravimetric weight loss studies were performed at the temperature sequence of 303-333K. The activation energy of corrosion (E_a) with and without these inhibitors was measured by Arrhenius equation,

The rate of corrosion,

$$K = A \exp\left(\frac{-Ea}{RT}\right) \quad (28)$$

where A is the frequency factor, R is the universal gas constant and T the temperature in Kelvin scale.

Linear plots between log K and 1000/T having regression coefficients close to unity point out that the corrosion on CS in aggressive medium can be explained by a simple kinetic model. Fig. 3.25-3.31 represents the plots of log K Vs 1000/T and log (K/T) Vs 1000/T with and without these inhibitors. Enthalpy and entropy of activation (ΔH^*, ΔS^*) were calculated from the transition state theory, which can be represented by the following equation.

$$K = \left(\frac{RT}{Nh}\right) \exp\left(\frac{\Delta S*}{R}\right) \exp\left(\frac{-\Delta H*}{RT}\right) \quad (29)$$

where h is the Planck's constant and N is the Avogadro number.

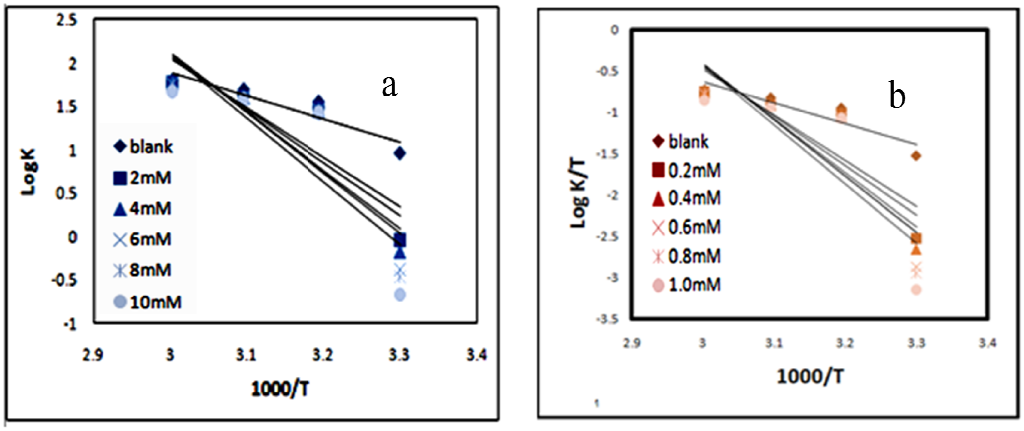

Fig. 3.25: a) Arrhenius plots and **b)** log (K/T) vs 1000/T plots of CS corrosion in the presence and absence of A9CNPTDA in 1M HCl

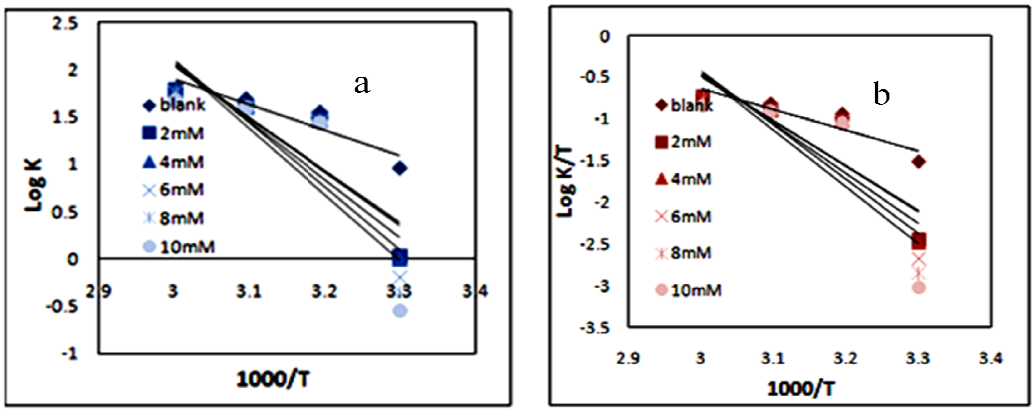

Fig. 3.26: a) Arrhenius plots and **b)** log (K/T) vs 1000/T plots of CS corrosion in the presence and absence of P2CNPTDA in 1M HCl

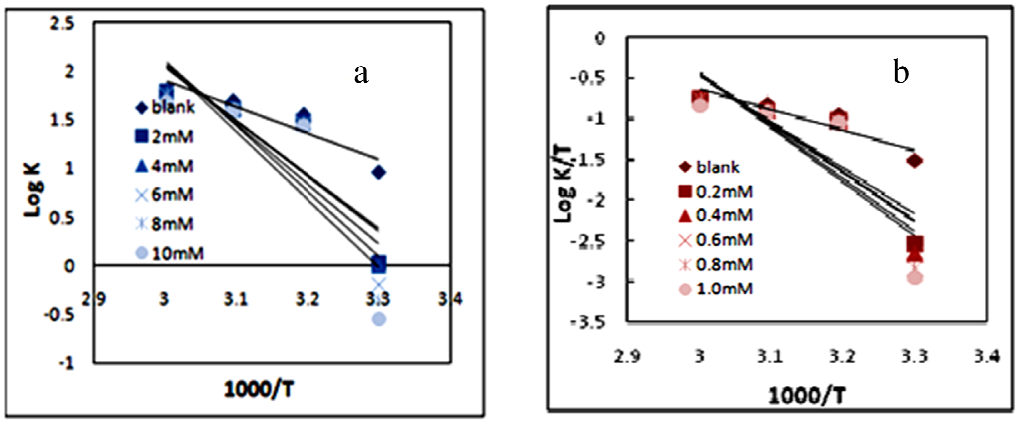

Fig. 3.27: a) Arrhenius plots and **b)** log (K/T) vs 1000/T plots of CS corrosion in the presence and absence of 3APNPTDA in 1M HCl

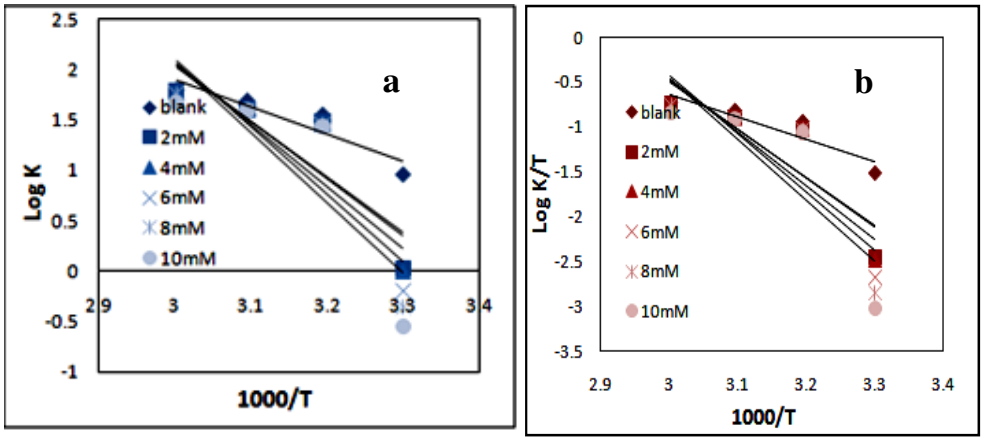

Fig. 3.28: a) Arrhenius plots and **b)** log (K/T) vs 1000/T plots of CS corrosion in the presence and absence of 2APNPTDA in 1M HCl

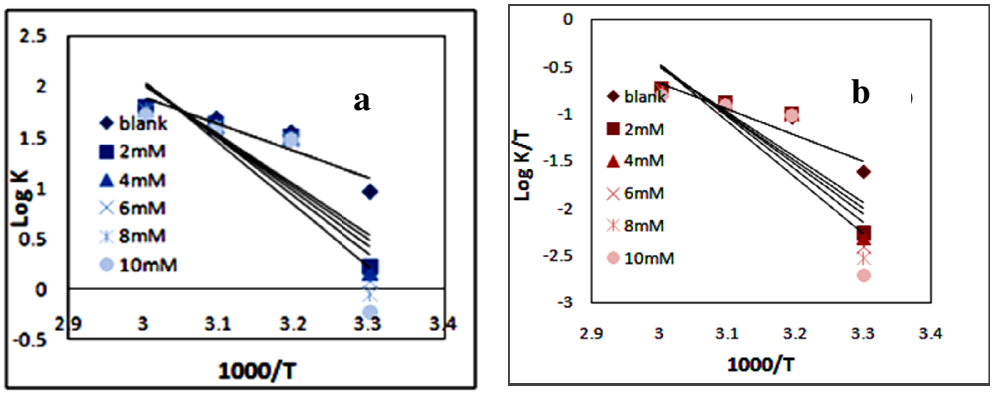

Fig. 3.29: a) Arrhenius plots and **b)** log (K/T) vs 1000/T plots of CS corrosion in the presence and absence of ANNPTDA in 1M HCl

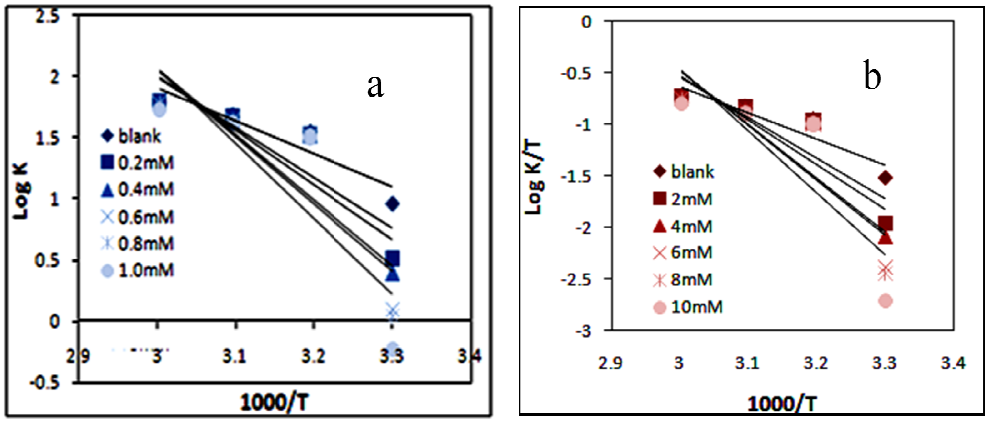

Fig. 3.30: a) Arrhenius plots and **b)** log (K/T) vs 1000/T plots of CS corrosion in the presence and absence of I3A2AT in 1M HCl

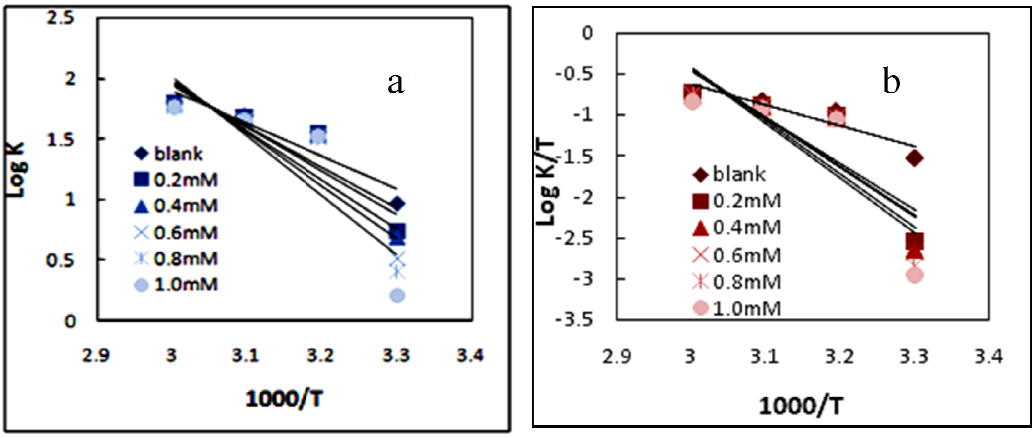

Fig. 3.31: a) Arrhenius plots and **b)** log (K/T) vs 1000/T plots of CS corrosion in the presence and absence of T2CDACH in 1M HCl

Thermodynamic parameters (entropy of activation ad enthalpy of activation) of corrosion in 1M HCl in the presence and absence of these inhibitors A9CNPTDA, P2CNPTDA, 3APNPTDA, 2APNPTDA, ANNPTDA, I3A2AT and T2CDACH are depicted in Table 3.6. Positive signs of enthalpies with a regular rise reflect the endothermic nature of dissolution and the decreasing corrosion tendency with the inhibitor. Increase of entropy values emphasizes that randomness increase for the activated complex take place than the reactant with the concentration of the inhibitor. The raise of entropy and activation energy implies that the reluctance of dissolution of metal increased with the inhibitor concentration, which can be attributed to the considerable intervention of inhibitor molecules during the metallic dissolution.

Table 3.6: Thermodynamic parameters of CS corrosion, in the presence and absence of 'S' containing heterocylic Schiff bases in 1M HCl

Schiff base	C (mM)	E_a (kJ mol^{-1})	A	ΔH* (kJ mol^{-1})	ΔS* (J mol-1 K^{-1})
Blank	0	51.33	8.73×10^{9}	48.7	-56.51
A9CNPTDA	0.2	109.23	1.48×10^{19}	107	107.29
	0.4	117.00	2.34×10^{20}	114	110.16
	0.6	128.7	1.91×10^{22}	126	113.04
	0.8	132.00	8.71×10^{22}	130	121.26
	1	140.00	1.2×10^{24}	138	133.33
P2CNPTDA	0.2	104.92	3.01×10^{18}	102	106.99
	0.4	107.33	7.24×10^{18}	105	114.37
	0.6	117.69	3.44×10^{20}	115	142.14
	0.8	127.32	1.12×1^{22}	125	175.26
	1	133.41	9.55×10^{22}	131	193.07
3APNPTDA	0.2	111.19	3.02×10^{19}	109	126.06
	0.4	117.14	2.69×10^{20}	114	144.25
	0.6	118.62	3.47×10^{20}	115	146.35
	0.8	127.62	1.26×10^{22}	125	176.22
	1	129.88	2.63×10^{22}	127	194.78
2APNPTDA	0.2	105.02	1.41×10^{18}	111	107.29
	0.4	105.96	1.68×10^{18}	114	110.16
	0.6	106.95	6.44×10^{18}	119	113.03
	0.8	109.69	1.56×10^{19}	122	121.26
	1	117.25	5.24×10^{20}	125	144.00
ANNPTDA	0.2	94.45	6.46×10^{16}	92	75.12
	0.4	97.57	2×10^{17}	95	84.51
	0.6	102.82	1.38×10^{18}	100	100.39
	0.8	109.10	1.39×10^{19}	106	119.55
	1	116.83	2.69×10^{20}	117	142.71
I3A2AT	0.2	77.70	1.45×10^{9}	55	-34.39
	0.4	112.87	2.38×10^{19}	111	143.13
	0.6	114.73	3.47×10^{19}	119	148.75
	0.8	120.5	1.16×10^{20}	121	160.22
	1	123.44	2.04×10^{20}	128	174.47
T2CDACH	0.2	64.04	9.33×10^{9}	61.4	-17.64
	0.4	67.64	3.47×10^{11}	65	-6.82
	0.6	76.01	8.13×10^{13}	73.7	19.59
	0.8	82.58	9.55×10^{14}	80	38.74
	1	93.17	3.98×10^{16}	90.5	60.18

Surface Morphological Investigations

In order to establish the mechanism of action of these heterocyclic Schiff bases A9CNPTDA, P2CNPTDA, 3APNPTDA, 2APNPTDA, ANNPTDA, I3A2ATand T2CDACH on CS surface, SEM experiments were conducted. The SEM micrographs of (a) bare CS surface (b) CS specimen immersed in 1M HCl and CS specimen immersed in 1M HCl containing 1mM concentration of (c) A9CNPTDA and (d) T2CDACH after 48 hrs of immersion time are shown in Fig. 3.32. The pits and cracks appearing in the SEM image of the bare metal specimen were due to the polishing effects. Some cracks are observed on the CS surface in T2CDACH solution. This is due to the fast hydrolysis nature of this molecule. On close examination of these images, it was clear that the CS surface undergoes severe corrosion in blank HCl solution and smoother surface was displayed by metal specimens immersed in 1M HCl in the presence of heterocyclic inhibitor A9CNPTDA at 1mM concentration. This can be attributed to the prevention of CS corrosion in aggressive medium by the formation of a protective barrier of inhibitors through adsorption process.

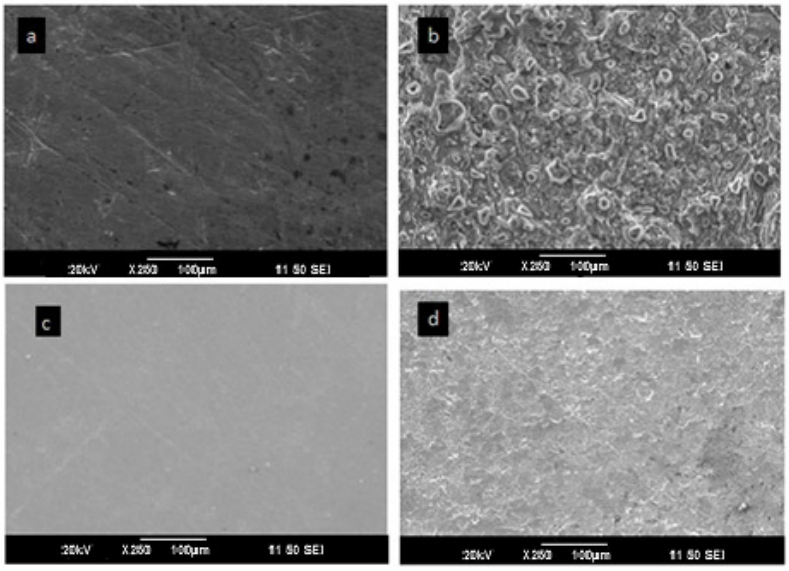

Fig. 3.32: SEM images of (a) bare CS (b) CS treated with 1M HCl (c) CS treated with A9CNPTDA (1mM) (d) CS treated with T2CDACH (1mM) for 48h.

Electrochemical Impedance Spectroscopic Studies (EIS)

The behavior of corrosion on CS in 1M HCl with and without the heterocyclic inhibitors was studied by employing impedance spectroscopic analysis. To make clear the inhibitory action of these organic ligands, CS specimens were engrossed in 1M HCl medium in the presence and absence of the inhibitors for 30 minutes prior to the experiment at 303K. Fig. 3.33 to Fig. 3.39 corresponding to the Nyquist plots and Bode plots of the sulphur-containing heterocyclic Schiff bases A9CNPTDA, P2CNPTDA, 3APNPTDA, 2APNPTDA, ANNPTDA, I3A2AT and T2CDACH respectively. The impedance (EIS) parameters such as charge transfer resistance (R_{ct}), solution resistance (R_s), double layer capacitance (C_{dl}) and percentage of inhibition efficiency ($\eta_{EIS\%}$) were calculated from these plots and documented in Table 3.7. From R_{ct} values, the percentage of inhibition efficiency was evaluated using the subsequent equation

$$\eta_{EIS}\% = \frac{Rct - R'ct}{Rct} \times 100 \quad (30)$$

where R'_{ct} and R_{ct} are the charge transfer resistances of the working electrode in acid medium in the absence and presence of the heterocyclic Schiff bases respectively.

R_{ct} is a measure of electron transfer between the acidic solution and exposed area of CS and the corrosion rate is inversely proportional to it. From Nyquist plots, it was observed that the diameter of semicircle increases with the concentration of inhibitors indicating that these 'S' containing inhibitors self-assemble on the CS surface by forming protective layer and resist the corrosion. The monolayer of inhibitors obstructs the charge transfer between the carbon steel and the acidic solution and charge transfer resistance increases with inhibitor concentration. The diminishing nature of capacitance values (C_{dl}) with the concentration of inhibitor, mainly indicates the increase in the thickness of the electrical double layer and/or decrease in local dielectric constant.

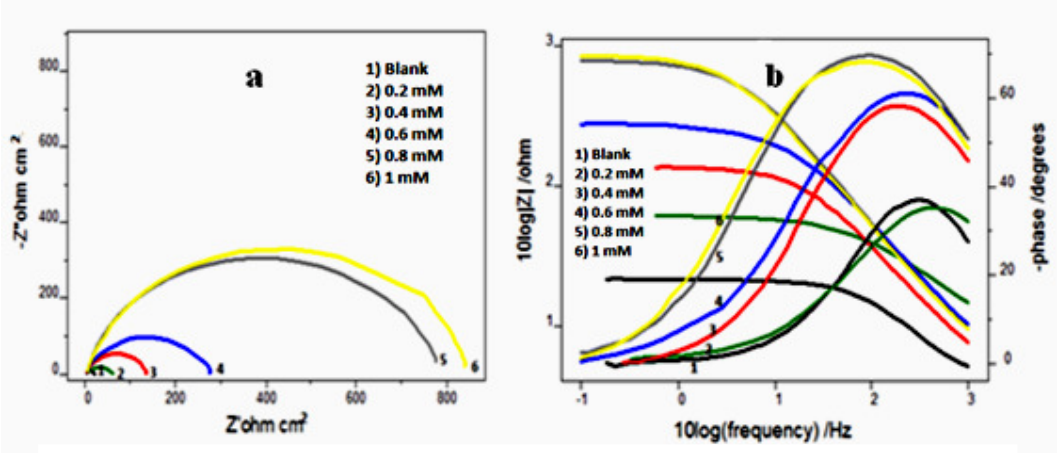

Fig. 3.33: a) Nyquist plots and **b)** Bode plots of CS corrosion in the presence and absence of A9CNPTDA in 1M HCl

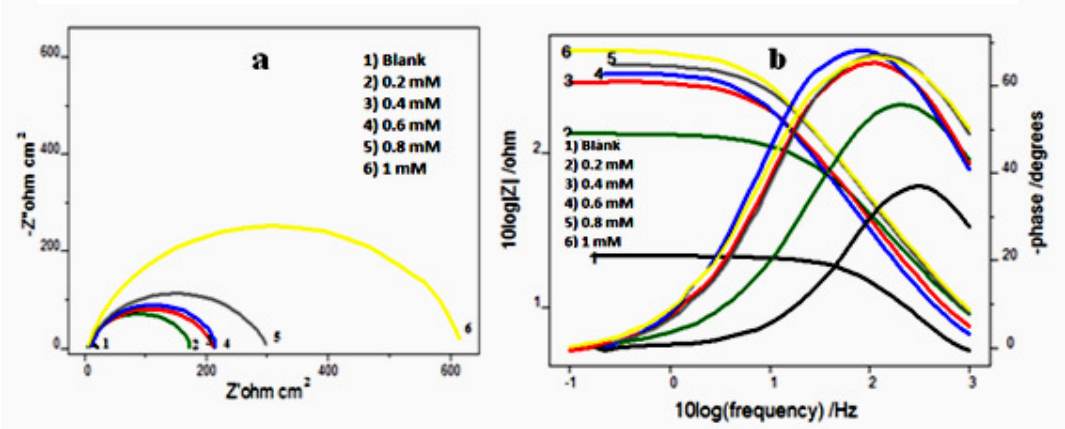

Fig. 3.34: a) Nyquist plots and **b)** Bode plots of CS corrosion in the presence and absence of P2CNPTDA in 1M HCl

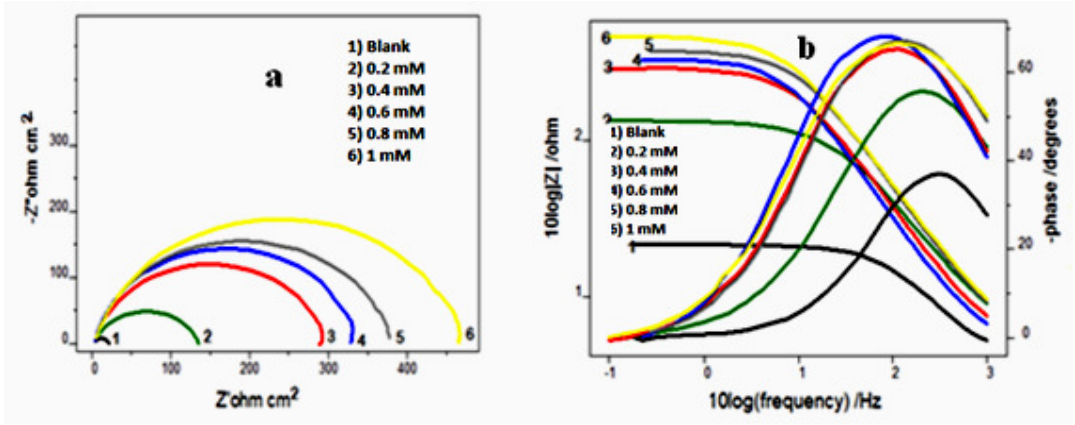

Fig. 3.35: a) Nyquist plots and **b)** Bode plots of CS corrosion in the presence and absence of 3APNPTDA in 1M HCl

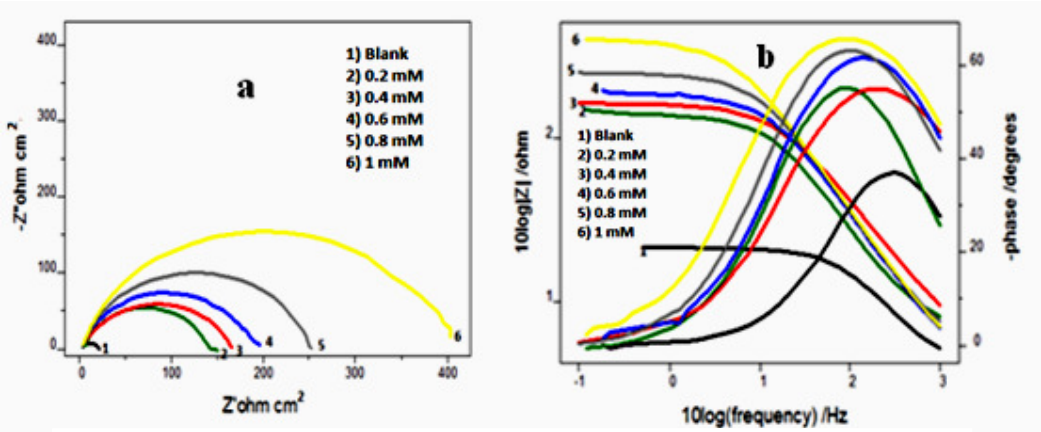

Fig. 3.36: a) Nyquist plots and **b)** Bode plots of CS corrosion in the presence and absence of 2APNPTDA in 1M HCl

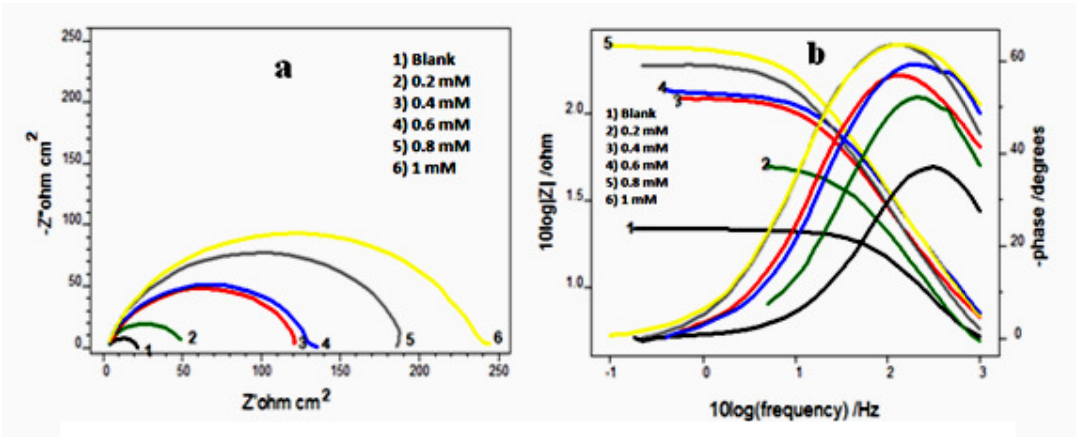

Fig. 3.37: a) Nyquist plots and **b)** Bode plots of CS corrosion in the presence and absence of ANNPTDA in 1M HCl

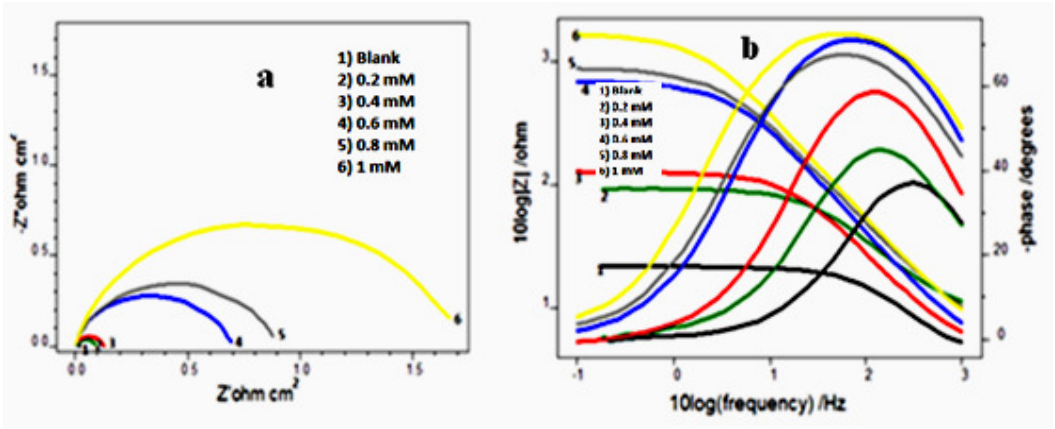

Fig. 3.38: a) Nyquist plots and **b)** Bode plots of CS corrosion in the presence and absence of I3A2AT in 1M HCl

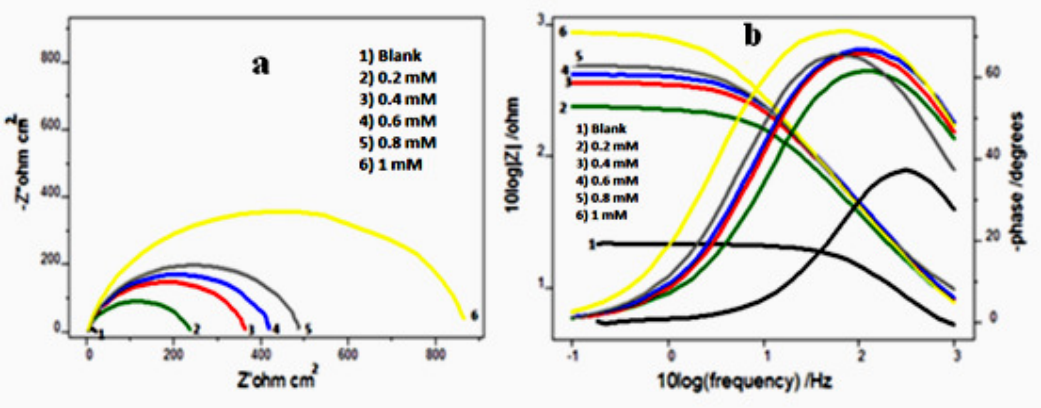

Fig. 3.39: a) Nyquist plots and b) Bode plots of CS corrosion in the presence and absence of T2CDACH in 1M HCl

From these plots, it is obvious that the impedance response of CS specimens showed a marked difference in the presence and absence of inhibitors. On examining Table 3.7, all synthesized 'S' containing Schiff base inhibitors displayed remarkable inhibition efficiency on CS even at low concentration. The weight loss results of heterocyclic Schiff bases derived from the parent amine NPTDA were in good agreement with EIS measurements. Presence of highly polarized sulphur atom from the thiadiazole moiety and the presence of azomethine linkage which is bridged through two aromatic systems enhance the delocalization of π electron cloud in these molecules and favour the interaction with CS surface. Among thiadiazole derivatives, the Schiff base inhibitor A9CNPTDA exhibited notable inhibition efficiency compared to others. Maximum efficiency of 97.9% was obtained at 1mM concentration of the inhibitor. Even at lowest concentration of 0.2mM, thiadiazole derivative A9CNPTDA exhibited 89.74% inhibition potency.

Table 3.7: Electrochemical Impedance parameters of CS corrosion in the presence and absence of 'S' containing heterocyclic Schiff base inhibitors in 1M HCl at 303K

Schiff bases	C (mM)	C_{dl} ($\mu F\ cm^{-2}$)	R_{ct} ($\Omega\ cm^{-2}$)	η_{EIS}%
Blank	0	101	16.1	-
A9CNPTDA	0.2	83.9	157	89.74
	0.4	53.0	187	91.39
	0.6	45.7	239	93.23
	0.8	47.5	712	97.73
	1.0	53.1	768	97.90
P2CNPTDA	0.2	55.5	120	86.50
	0.4	51.0	182	91.15
	0.6	83.0	194	91.70
	0.8	66.3	262	93.85
	1.0	55.2	567	97.16
3APNPTDA	0.2	52.4	115	86.00
	0.4	59.5	271	94.01
	0.6	65.7	312	94.83
	0.8	42.6	347	95.36
	1.0	45.4	431	96.26
2APNPTDA	0.2	80.3	125	87.12
	0.4	56.6	140	88.50
	0.6	62.6	167	90.35
	0.8	63.8	228	92.94
	1.0	72.2	359	95.51
ANNPTDA	0.2	84.3	29	61.80
	0.4	46.0	38.8	83.50
	0.6	73.1	68.6	85.09
	0.8	74.9	131	90.69
	1.0	73.6	208	92.47
I3A2AT	0.2	61.4	76.3	78.9
	0.4	76.7	114	85.87
	0.6	57.8	633	97.45
	0.8	57.3	800	97.98
	1.0	51.5	1540	99.6
T2CDACH	0.2	64.9	211	92.37
	0.4	55.3	334	95.17
	0.6	53.1	386	95.82
	0.8	58.1	449	96.41
	1.0	59.7	811	98.01

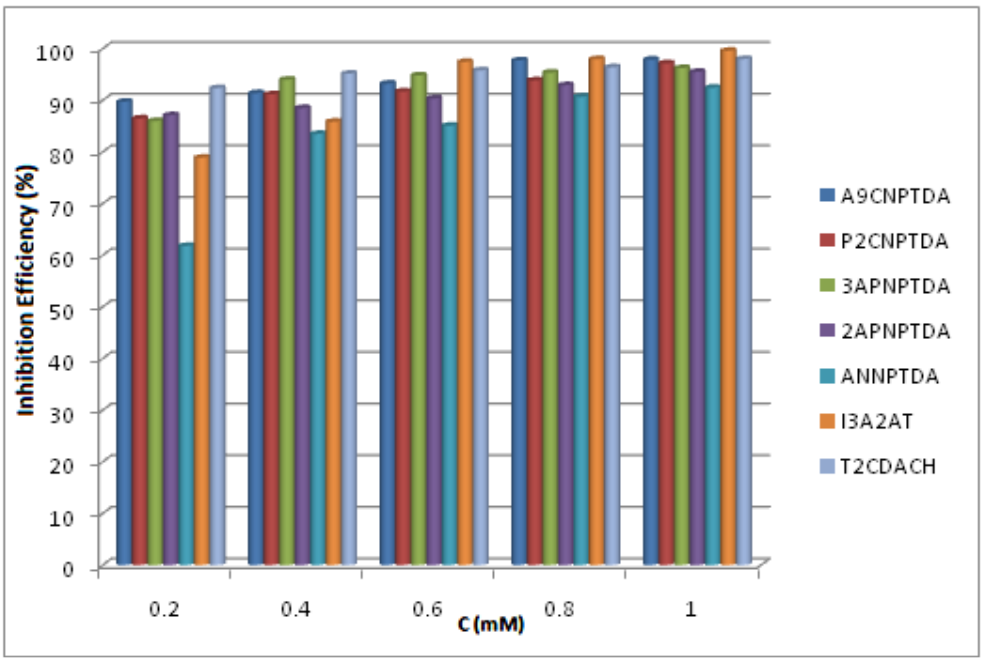

Fig. 3.40: Comparison of the corrosion inhibition efficiencies ($\eta_{EIS\%}$) of 'S' containing heterocyclic Schiff bases in 1M HCl at 28^0C

The electrochemical analysis is a quick corrosion monitoring procedure and displays the corrosion inhibition potencies of inhibitors in the early hours of treatment. Fig. 3.40 illustrate the assessment of the corrosion inhibition efficiencies of seven heterocyclic Schiff base inhibitors by EIS measurements. It is noticeable from the figure that the inhibition efficiency of the five heterocyclic Schiff base inhibitors derived from NPTDA follows the order A9CNPTDA < P2CNPTDA < 3APNPTDA < 2APNPTDA < ANNPTDA respectively. This tendency finds good harmony with the outcome obtained from the gravimetric weight loss studies. Thiazole derivative of Schiff base I3A2AT and thiophene derivative T2CDACH showed outstanding inhibition efficiency and maximum efficiency of 99.6% was obtained for I3A2AT and 98.01% for T2CDAC at 1mM concentration. The highest R_{ct} value 1540 exhibited by I3A2AT can be attributed to the presence of thiazole moiety, indole ring and azomethine linkage. As per gravimetric studies, the heterocyclic Schiff base T2CDACH exhibited low inhibitive

response on CS surface but showed outstanding inhibition by EIS measurements. From the UV-visible spectral studies, it was confirmed that T2CDACH undergo fast hydrolysis and I3A2AT undergo slow hydrolysis in hydrochloric acid medium.

Potentiodynamic Polarization Studies

To emphasize the corrosion inhibitory role of the novel 'S' containing Schiff bases on carbon steel and to verify the electrochemical site of interaction, potentiodynamic polarization studies including Tafel extrapolation analysis and Linear polarization studies were conducted. Corrosion potential (E_{corr}), corrosion current density (i_{corr}) and polarization resistance (R_p) were calculated in every analysis and by means, determined the inhibition efficiency. Tafel plots and linear polarization curves of CS in 1M HCl medium in the presence and absence of these heterocyclic Schiff base inhibitors are depicted from Fig. 3.41 to 3.47. Tafel and Linear polarization data including corrosion current density (I_{corr}), corrosion potential (E_{corr}), anodic slope (b_a), cathodic slope (b_c) and corrosion inhibition efficiency were obtained by potentiodynamic polarization studies and tabulated in Table 3.8.

On scrutiny, it was revealed that the corrosion current densities of steel specimens decreased appreciably with the concentration of inhibitors. This is because of these organic molecules obstruct the metal dissolution progression appreciably by either prevailing in the cathodic or anodic process of corrosion or they acted as mixed type inhibitors [120]. On the evaluation of Tafel and Linear polarization curves, it was established that the slope of the Tafel curves of uninhibited solution entirely different from the slope obtained in the presence of inhibitors. The outcome obtained by the potentiodynamic polarization studies were in good harmony with the electrochemical impedance studies.

Table 3.8: Potentiodynamic polarization parameters of CS corrosion in the presence and absence of 'S' containing heterocyclic inhibitors in 1M HCl

Inhibitors	Tafel Data						Polarization data	
	C (mM)	$-E_{corr}$ (mV/SCE)	I_{corr} ($\mu A/cm^2$)	$-b_a$ (mV/dec)	b_c (mV/dec)	η_{pol} %	R_p (ohm)	η_{Rp} %
Blank	0	451	1115	110	184	-	26.86	-
A9CNPTDA	0.2	471	77	70	134	93.1	259.6	90.00
	0.4	469	37.8	63	119	96.6	475.2	94.34
	0.6	479	36	61	123	96.8	494.6	94.56
	0.8	470	30.3	66	115	97.3	601.6	95.53
	1	476	12.2	52	103	98.9	1239	97.83
P2CNPTDA	0.2	444	132	76	197	88.2	175.9	84.72
	0.4	441	70.5	72	134	93.7	227.7	88.20
	0.6	448	37.3	61	132	96.7	417	93.55
	0.8	463	36.3	68	145	96.8	461.3	94.17
	1	456	21.2	68	136	98.1	882.3	96.95
3APNPTDA	0.2	453	92.2	76	164	91.7	227	88.16
	0.4	454	80.2	75	123	92.8	302	91.10
	0.6	455	66.6	72	157	94.1	320	91.60
	0.8	461	97.1	87	133	91.3	322	91.65
	1	457	22.9	58	164	97.9	785	96.57
2APNPTDA	0.2	427	204	98	185	81.7	143	81.20
	0.4	482	81	86	122	92.8	323.1	91.68
	0.6	463	84	81	121	92.5	376.2	92.90
	0.8	487	64	84	123	94.3	425.3	93.68
	1	443	48	78	128	95.7	505.4	94.68
ANNPTDA	0.2	473	492	93	151	55.9	71.88	62.63
	0.4	468	161	83	153	85.7	158.4	83.04
	0.6	472	125	73	142	88.8	193.5	86.11
	0.8	453	105	62	138	90.6	258.3	89.60
	1	483	70.4	79	125	93.7	284	90.54
I3A2AT	0.2	473	284	112	208	74.52	97.05	71.90
	0.4	467	110	73	205	90.04	216.6	87.59
	0.6	474	12.5	43	111	98.86	878.7	97.00
	0.8	460	11.1	61	116	98.99	1097	97.55
	1	480	7.6	82	102	99.31	1708	98.42
T2CDACH	0.2	471	79	73	130	93.07	285.6	90.60
	0.4	468	37.8	63	119	96.65	495.2	94.60
	0.6	469	36	61	124	96.77	512.6	94.77
	0.8	470	30.3	66	117	97.28	621.6	95.60
	1	476	12.2	52	103	98.87	1274	97.90

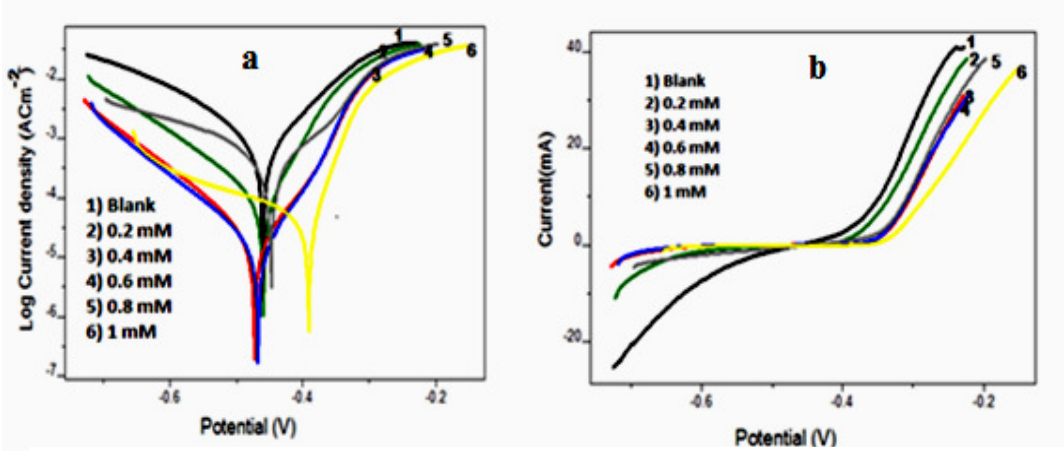

Fig. 3.41: a) Tafel plots and **b)** Linear polarization plots of CS corrosion in the presence and absence of A9CNPTDA in 1M HCl.

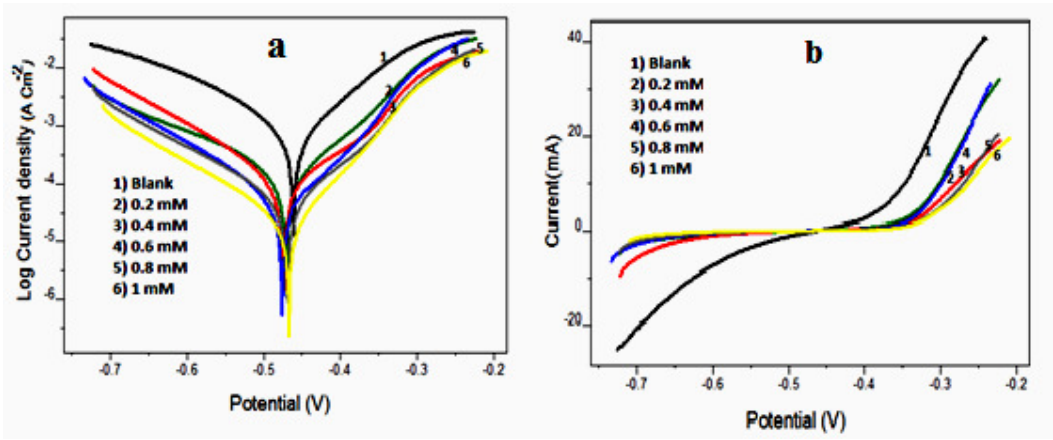

Fig. 3.42: a) Tafel plots and **b)** Linear polarization plots of CS corrosion in the presence and absence of P2CNPTDA in 1M HCl

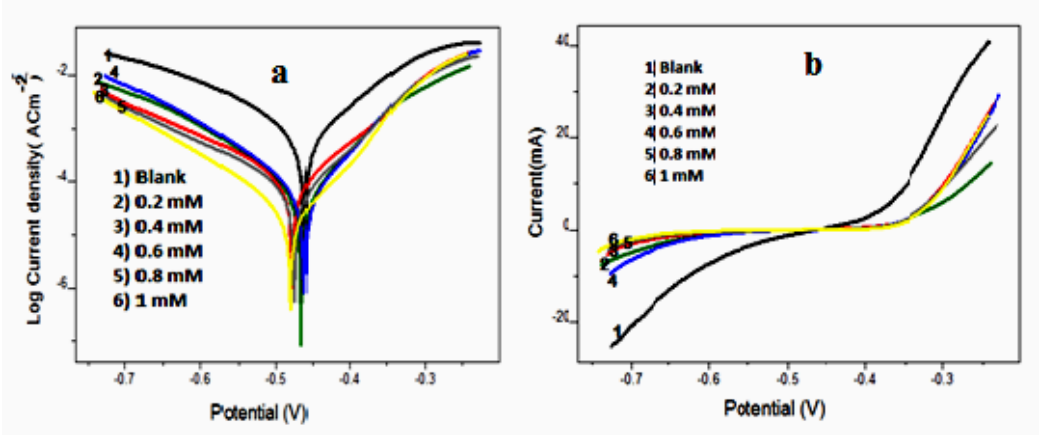

Fig. 3.43: a) Tafel plots and **b)** Linear polarization plots of CS corrosion in the presence and absence of 3APNPTDA in 1M HCl

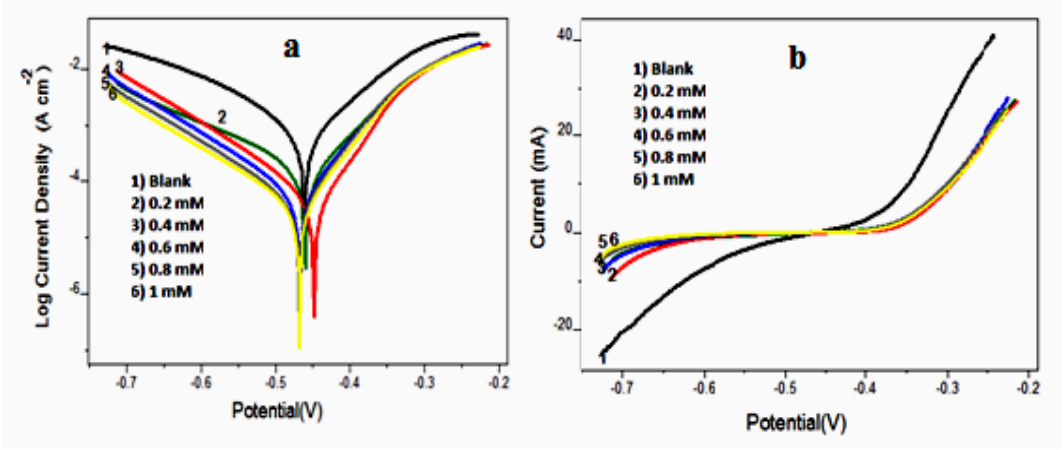

Fig. 3.44: a) Tafel plots and **b)** Linear polarization plots of CS corrosion in the presence and absence of 2APNPTDA in 1M HCl

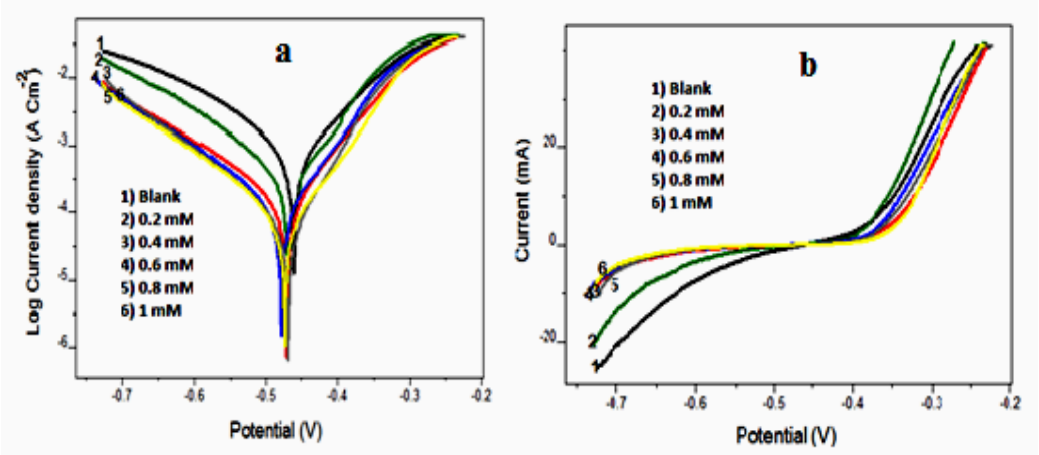

Fig. 3.45: a) Tafel plots and **b)** Linear polarization plots of CS corrosion in the presence and absence of ANNPTDA in 1M HCl

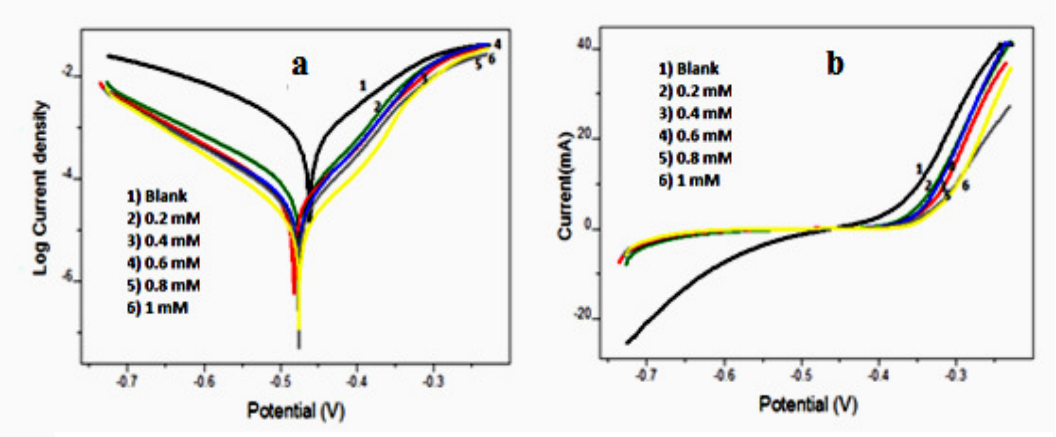

Fig. 3.46: a) Tafel plots and **b)** Linear polarization plots of CS corrosion in the presence and absence of I3A2AT in 1M HCl

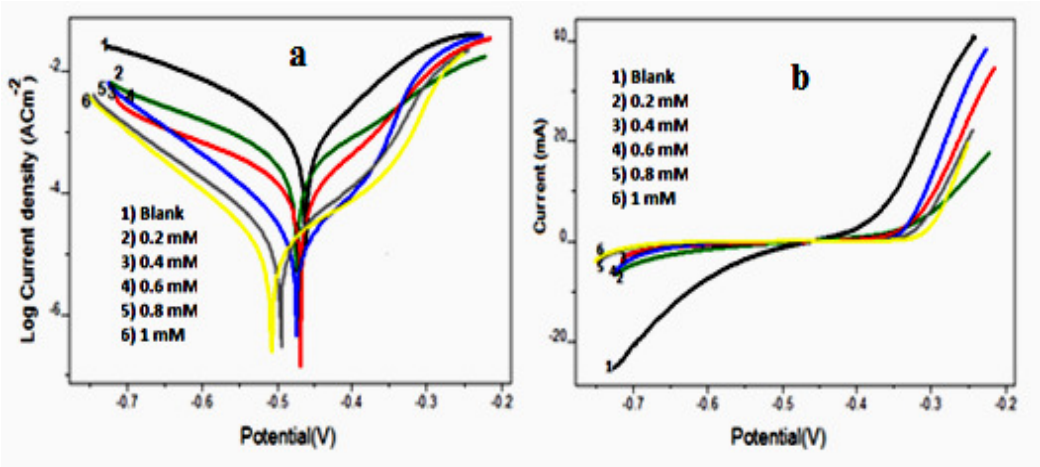

Fig. 3.47: a) Tafel plots and **b)** Linear polarization plots of CS corrosion in the presence and absence of T2CDACH in 1M HCl

A comparison between the inhibition efficiencies of these sulphur containing heterocyclic Schiff base inhibitors was done and portrayed in Fig. 3.48. Among thiadiazole derivatives, the heterocyclic Schiff base, A9CNPTDA exhibited the maximum inhibition efficiency of 98.9% at 1mM concentration. The heterocyclic Schiff bases, I3A2AT and T2CDACH, also exhibited excellent inhibition efficiencies (99.31% in the case of I3A2AT and 98.87% in the case of T2CDACH, which is higher than that obtained from the gravimetric weight loss studies. This is because, in electrochemical investigations, the contact time between the acid solution and the working electrode is about 30 minutes only whereas in the later the contact time is 24h. Generally, if the shift of E_{corr} is greater than 85 and a significant change is observed in cathodic or anodic slopes, the inhibitor can be considered as cathodic or anodic. In the present investigation, the seven heterocyclic Schiff bases namely A9CNPTDA, P2CNPTDA, 3APNPTDA, 2APNPTDA, ANNPTDA, I3A2AT and T2CDACH affects the anodic and cathodic slopes uniformly and E_{corr} values didn't alter considerably with respect to the blank (>85) and therefore these molecules can be regarded as mixed-type inhibitors.

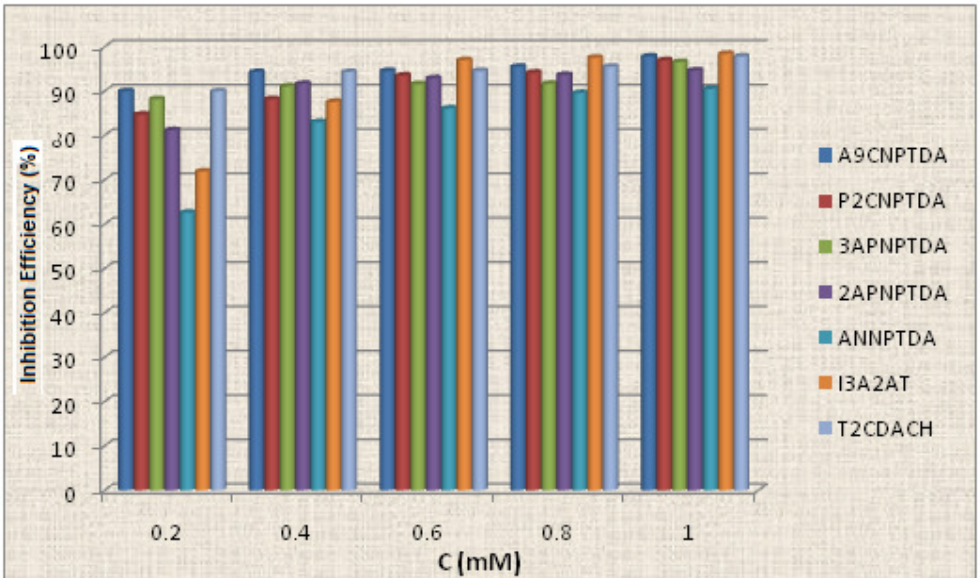

Fig. 3.48: Comparison study of corrosion inhibition efficiencies ($\eta_{pol\%}$) of 'S' containing heterocyclic Schiff base inhibitors on CS in 1M HCl at 28^0C

Mechanism of Inhibition

Organic inhibitors can prevent the metal dissolution by forming a hydrophobic film through adsorption process on the metal surface. The Capability of the inhibitor molecule mainly depends on its molecular structure and chemical composition.

The mechanism anodic dissolution of iron can be represented as follows.

i) In aqueous solutions

$$Fe + H_2O \rightarrow [FeOH]_{ads} + H^+ + e^- \quad (31)$$

$$[FeOH]_{ads} \rightarrow [FeOH]^+_{ads} + e^- \quad (32)$$

$$[FeOH]^+_{ads} + H^+ \rightarrow Fe^{2+} + H_2O \quad (33)$$

ii) In aqueous solution containing A^- (A= Cl^-, or SO_4^{2-}) ions

$$Fe + H_2O + A^- \rightarrow [FeAOH]^-_{ads} + H^+ + e^- \quad (34)$$

$$[FeAOH]^-_{ads} \rightarrow [FeAOH]_{ads} + e^- \quad (35)$$

$$[FeAOH]_{ads} + H^+ \rightarrow Fe^{2+} + A^- + H_2O \quad (36)$$

where $[FeOH]_{ads}$ and $[FeAOH]^-_{ads}$ are the adsorbed molecules which are intermediates

involved in the rate determining step of the reaction (equations 32 and 35, respectively). The following equations are the mechanism of the evolution of hydrogen in the cathode

$$Fe + H^+ \rightarrow (FeH^+)_{ads} \quad (37)$$

$$(FeH^+)_{ads} + e^- \rightarrow (FeH)_{ads} \quad (38)$$

$$(FeH)_{ads} + H^+ + e^- \rightarrow Fe + H_2 \quad (39)$$

The protonated inhibitor molecules adsorb at cathodic sites and hence reduce the H_2 gas evolution. Generally, the surface of the metal tends to have a positively charged environment in acidic media. The adsorption of negatively charged Cl^- ion will lead to the allocation of more and more negative charge and make easy the adsorption of the protonated Schiff bases on the metal surface, preventing the reduction of Fe to Fe^{2+} [121]. If one observes the features of these heterocyclic Schiff base inhibitors, many potential areas of metal–inhibitor interaction can be recognized. In this case, the binding of the compound on the metallic surface can be associated with the pi-electron cloud containing aromatic rings. In addition to this electrostatic interaction between the metal surface and the protonated inhibitor, the presence of heteroatoms which provide lone pair of electrons, interaction of π-electron cloud containing aromatic rings, azomethine moiety etc, will affect the adsorption progression. Highly polarisable sulphur atom and the unpaired electrons on the N atoms were the key factors for making a coordinate bond with the metal surface.

Besides, the highly conjugated azomethine linkage in the heterocyclic inhibitors allows the back donation of metal ‘d’ electrons to the antibonding π* orbital of the ligand and this type of interaction cannot be observed in the parent compounds. This can be defensible by the lower inhibition efficiency of the parent compounds. Fig. 3.49 illustrates the interaction of the inhibitor A9CNPTDA on the metal surface.

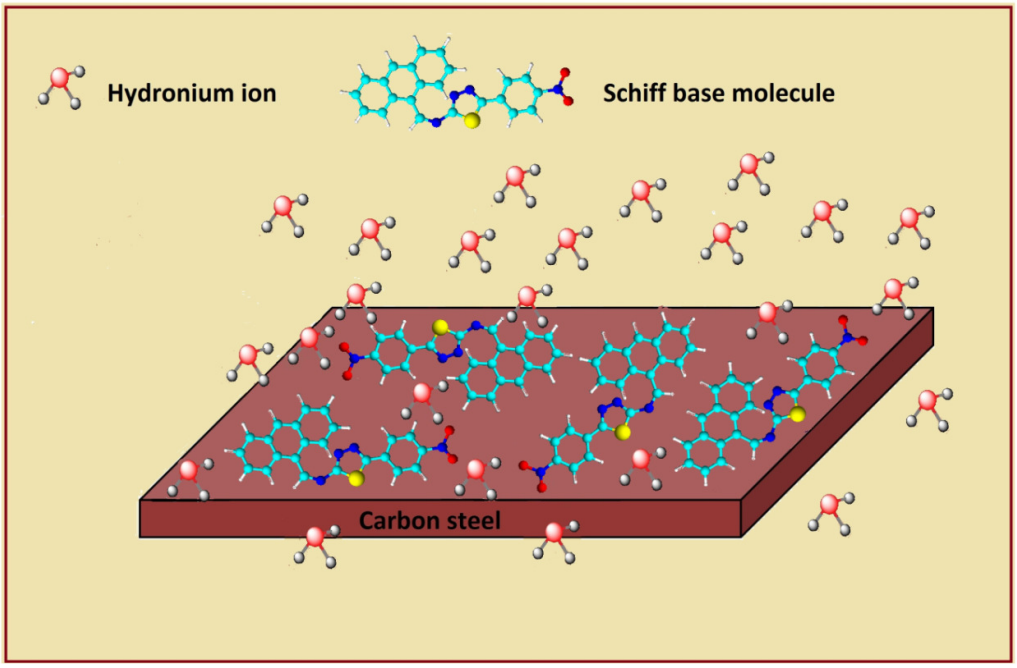

Fig. 3.49: Corrosion inhibition mechanism of A9CNPTDA molecules on CS surface

Electrochemical Noise Studies

Electrochemical noise experiments (ECN) were performed by a three-electrode cell system, which consists of SCE as a reference electrode, two carbon steel electrodes of 1cm^2 area used as working electrode and counter electrode. All ECN analyses were performed for 1200s using Ivium Compactstat-e electrochemical system.

Fig. 3.50 represents the noise current of carbon steel specimen engrossed in the acid solution with and without inhibitors. From the figure, it is obvious that at all frequencies, the noise current in the presence of inhibitors has very low value than the blank carbon steel specimen, which shows the protective corrosion power of these 'S' containing Schiff base ligands. Higher values of noise current for carbon steel specimen in uninhibited acid medium indicates appreciable localized corrosion takes place on the surface of the metal [122].

The frequency-domain analysis of noise measurement gave the Power Spectral

Density (PSD) of different systems, which are depicted in Fig. 3.51. It doesn't affect signal statistics and time. In the Ivium software, the time-dependent noise parameters were converted into PSD plots by FFT (Fast Fourier Transformation) technique. MEM (Maximum entropy method) for better spectral resolution was introduced by Burge. PSD plots in Figures revealed that the magnitude of the signals is higher for blank metal than metals with studied molecules in 1M HCl medium. These results pointed out a considerable amount of localised corrosion on carbon steel surface in the absence of these inhibitors.

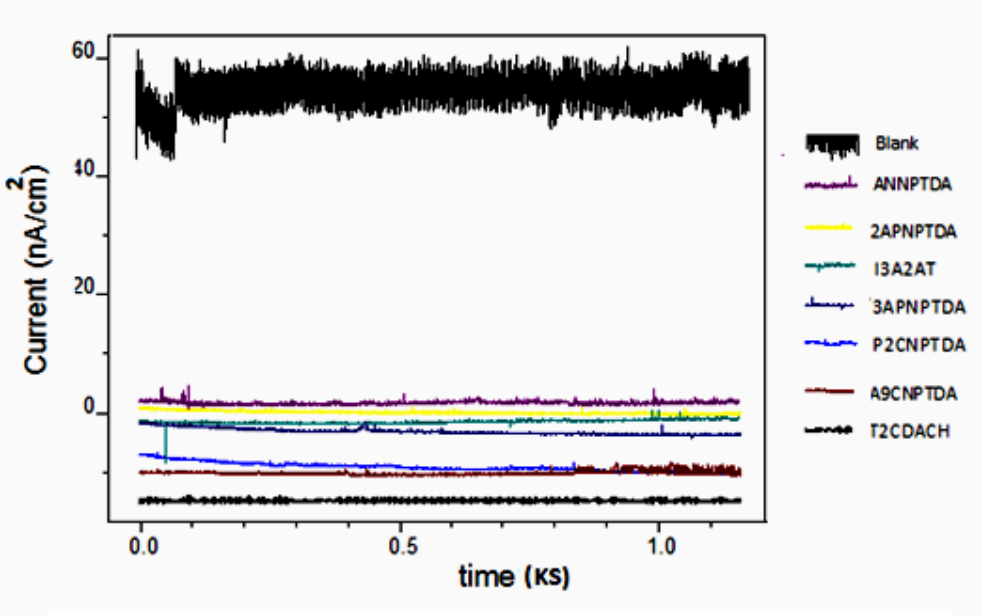

Fig. 3.50: Noise current of CS corrosion in the presence and absence of 'S' containing heterocyclic inhibitors in 1M HCl solution

Pitting Resistance Equivalent Number (PREN) or pitting index is the measurement of resistance against pitting corrosion. On analyzing the pitting index plots represented in Fig. 3.52, it is established that the amplitude of pitting index curves corresponding to the blank carbon steel specimen is lower than the specimen treated with heterocyclic Schiff base demonstrating their higher resistance towards pitting corrosion. These results are in close agreement with other electrochemical studies.

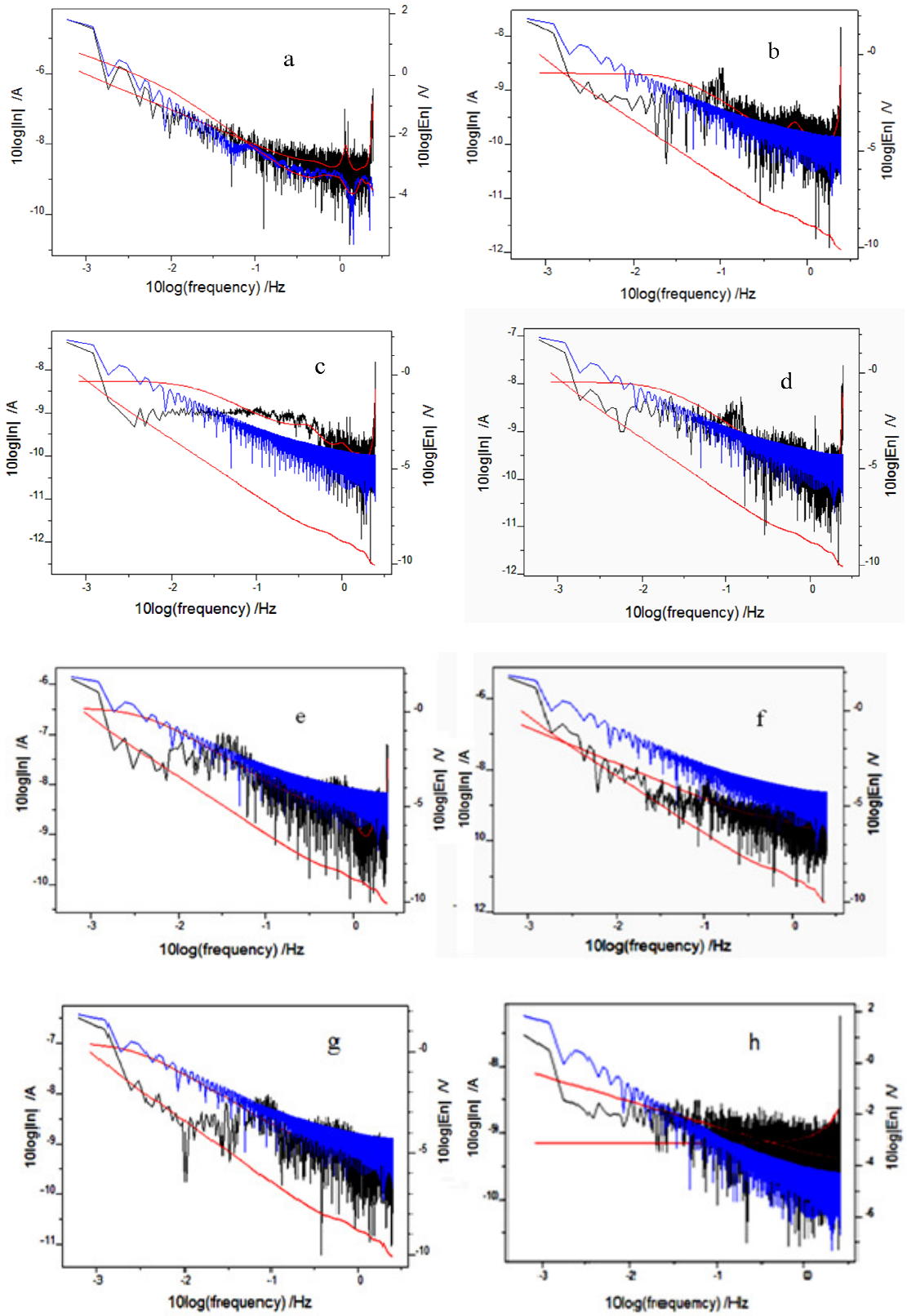

Fig. 3.51: PSD curves of CS corrosion in a) blank b) A9CNPTDA c) P2CNPTDA d) 3APNPTDA e) 2APNPTDA f) ANNPTDA g) I3A2AT h) T2CDACH at 1mM concentration in 1M HCl

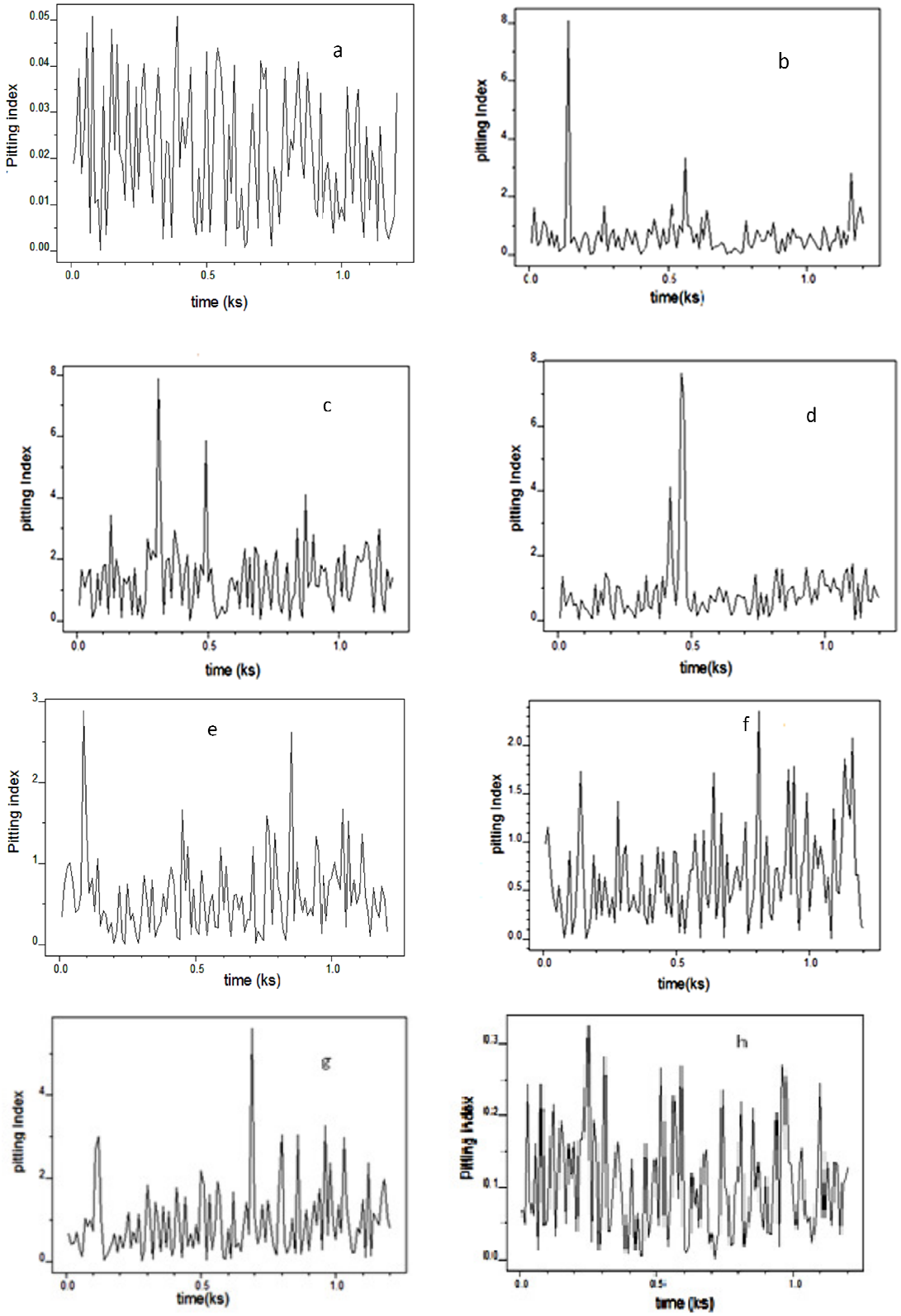

Fig. 3.52: Pitting index curves of CS corrosion in a) blank b) A9CNPTDA c) P2CNPTDA d) 3APNPTDA e) 2APNPTDA f) ANNPTDA g) I3A2AT and h) T2CDACH in IM HCl

Quantum Chemical Studies

The corrosion inhibition efficiency of these 'S' containing heterocyclic Schiff bases can be interrelated with the energies of Frontier molecular orbitals. The HSAB concept (donor-acceptor interactions) between the vacant d-orbitals of Fe atoms on the surface and the filled molecular orbitals of the molecules (inhibitors) have significant role in the prevention mechanism of metal disintegration. The highest value of E_{HOMO}, the lowest value of E_{LUMO} and the energy difference between the HOMO and the LUMO (ΔE) are the significant quantum chemical parameters which facilitate strong binding of the inhibitor molecules on the surface of metal. Energy of HOMO (E_{HOMO}) provides information about the tendency of a molecule to donate electrons to an electron-poor species. The higher E_{HOMO} indicates the greater tendency of a molecule to donate its electrons to the electron-poor species. The lowest $E_{LUMO} - E_{HOMO}$ (ΔE) value of inhibitors is an important quantum chemical parameter, it helps the ligands to bind on the metal surface strongly. Quantum chemical evaluations and Optimization of geometries of these inhibitors were carried out using DFT method by GAMMES software and B3LYP method was employed in DFT calculations. Calculated quantum mechanical parameters like E_{HOMO}, E_{LUMO}, Energy gap (ΔE), electronegativity (χ), hardness (η) and number of transferred electrons (ΔN) for the investigated inhibitors are tabulated in Table 3.9. HOMO and LUMO of inhibitors are depicted from Fig. 3.53 – Fig. 3.59 and optimized geometry of compounds established quantum mechanically represented in Fig. 3.60.

The energy gap between the Frontier orbitals ΔE, it helps to describe the static molecular reactivity. Low values of ΔE imply that the polarization and the adsorption of the molecule on the metal surface were takes place easily. Chemical hardness (η) is an important property to measure the reactivity molecular stability. A soft molecule has the small energy gap (ΔE) and they can offer electrons to the acceptor. The ΔE between

HOMO and LUMO is comparably low (2.68eV) for A9CNPTDA than other 'S' containing heterocyclic Schiff base inhibitors, implied that A9CNPTDA has high ability to accept electrons from the d-orbital of iron and high stability of the [Fe–L] complexes. It is also observed from the data that the Schiff base A9CPTDA has a low chemical hardness value (η = 1.361eV) compared to other studied molecules and thus, by being a soft molecule A9CNPTDA would enhance adsorption on the steel surface.

Table 3.9: Quantum chemical parameters of 'S' containing heterocyclic inhibitors

Inhibitors	E_{HOMO} (eV)	E_{LUMO} (eV)	ΔE (eV)	χ (eV)	η (eV)	Δ N
A9CNPTDA	-3.53	-0.843	2.68	2.204	1.361	0.836
P2CNPTDA	-3.619	-0.841	2.77	2.231	1.388	0.811
3APNPTDA	-3.592	-0.707	2.88	2.149	1.442	0.808
2APNPTDA	-3.538	-0.626	2.91	2.082	1.456	0.814
ANNPTDA	-3.565	-0.544	3.02	2.041	1.497	0.815
I3A2AT	-2.395	1.551	3.94	0.422	1.973	1.029
T2CDACH	-3.673	1.016	4.68	1.333	2.341	0.672

Table 3.8 shows that the hardness order of thiadiazole derivatives are as follows: A9CNPTDA > P2CNPTDA > 3APNPTDA > 2APNPTDA > ANNPTDA, which is in close agreement with the experimentally obtained inhibition potency. It is reported from the studies that electron transfer from an inhibitor to metal takes place easily when the N value is > 0 and < 3.6.

Among investigated compounds, it can be concluded that thiadiazole derivatives A9CNPTDA and thiazole derivative I3A2AT have the highest E_{HOMO} and ΔN value implied that they have the greater tendency to donate their electrons to the metal surface and therefore bind strongly on the metal surface. The higher value of ΔE (4.68 eV), high chemical hardness (η= 2.341eV) and low ΔN (0.672) value for thiophene based Schiff base T2CDACH which could be recognized to its lesser corrosion inhibition efficiency. These results are in good agreement with the results obtained from the gravimetric

weight loss studies.

The calculations are conducted using following equations,

$$\chi \approx -1/2\ (E_{HOMO} + E_{LUMO})$$

$$\eta \approx 1/2\ (E_{HOMO} - E_{LUMO}) \qquad \Delta N = \frac{\chi_{Fe} - \chi_{inhib}}{2(\eta_{Fe} + \eta_{inhib})}$$

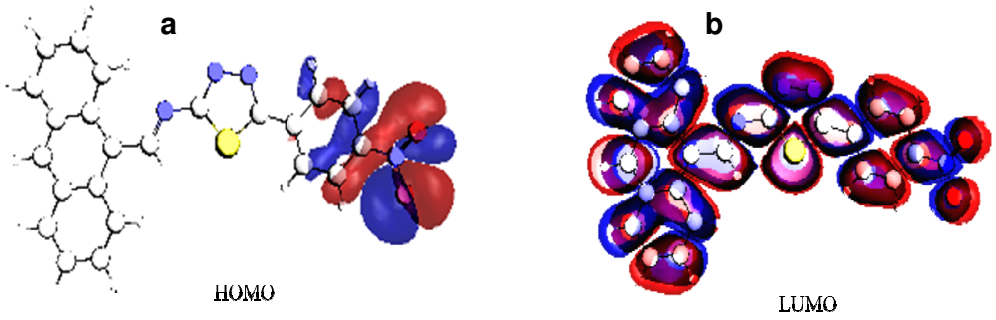

Fig. 3.53: a) HOMO and **b**) LUMO of A9CNPTDA

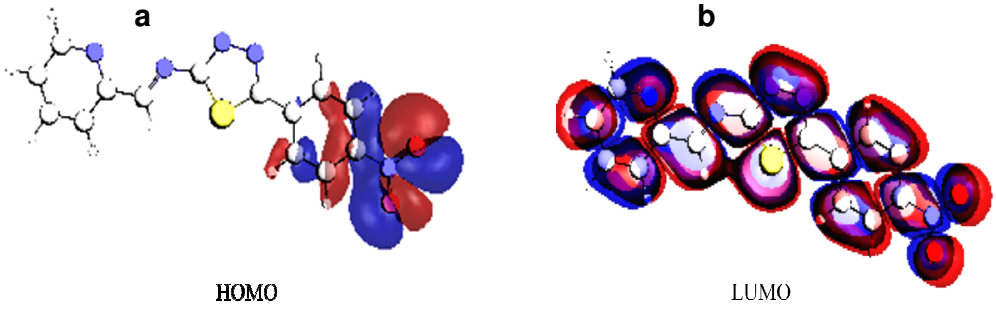

Fig. 3.54: a) HOMO and **b**) LUMO of P2CNPTDA

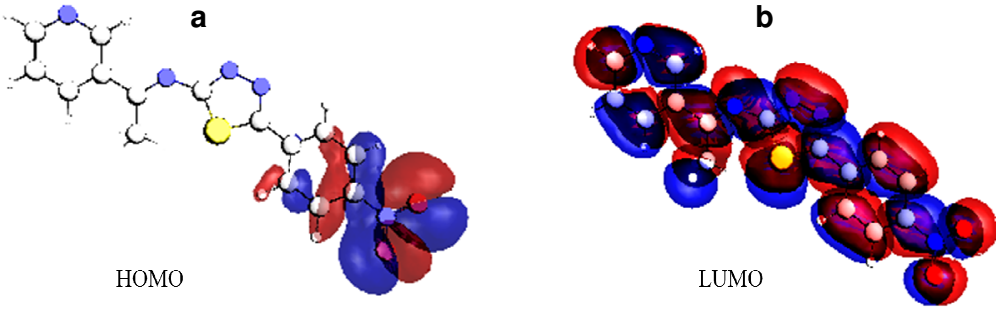

Fig. 3.55: a) HOMO and **b**) LUMO of 3APNPTDA

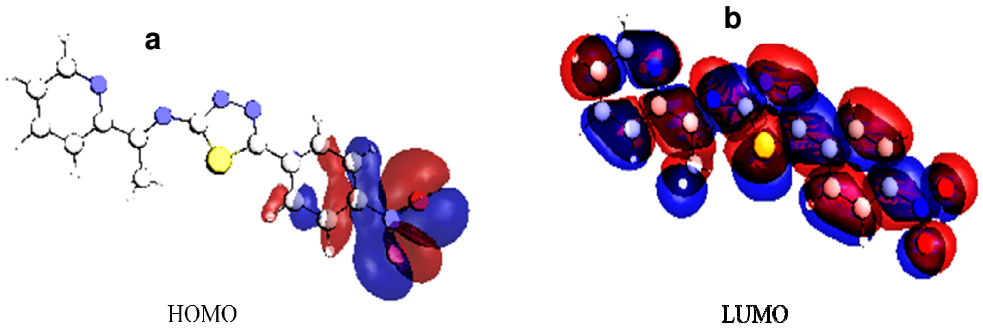

Fig. 3.56: a) HOMO and **b**) LUMO of 2APNPTDA

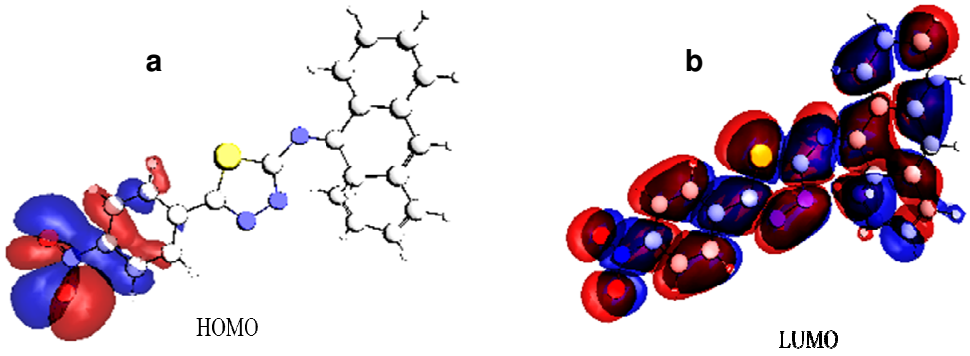

Fig. 3.57: a) HOMO and **b**) LUMO of ANNPTDA

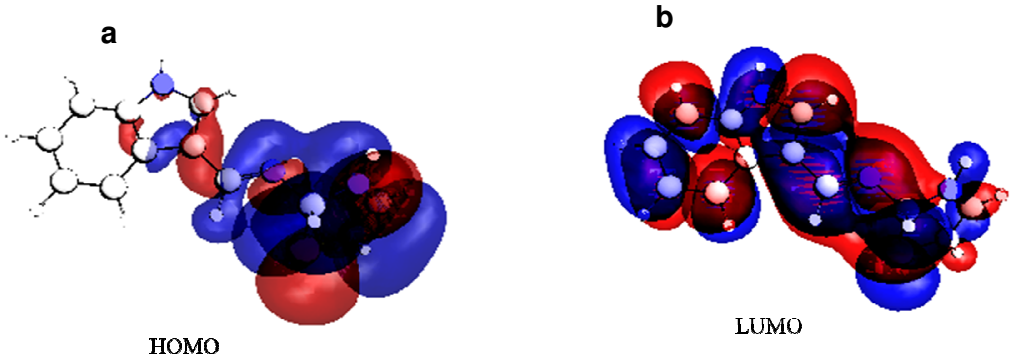

Fig. 3.58: a) HOMO and **b**) LUMO of I3A2AT

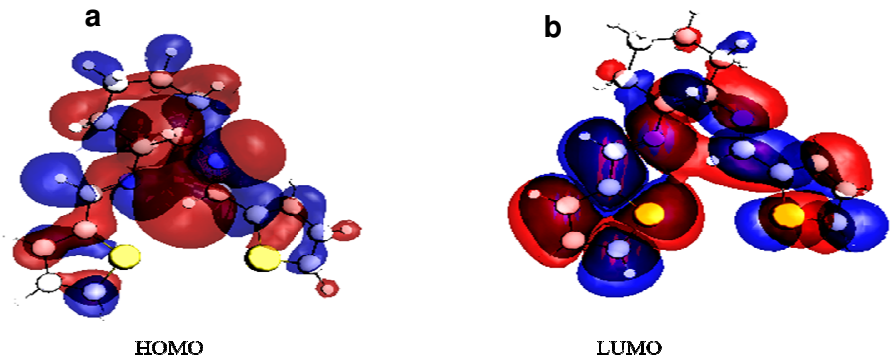

Fig. 3.59: a) HOMO and **b**) LUMO of T2CDACH

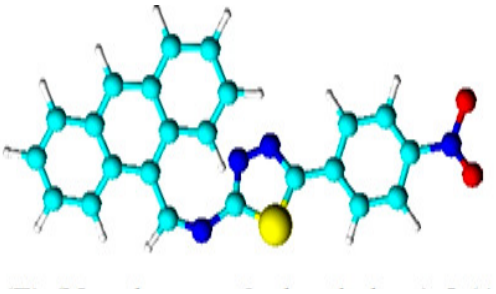

(E)-(N-anthracene-9-ylmethylene)-5-(4-nitrophenyl)-1,3,4-thiadiazol-2-amine (A9CNPTDA)

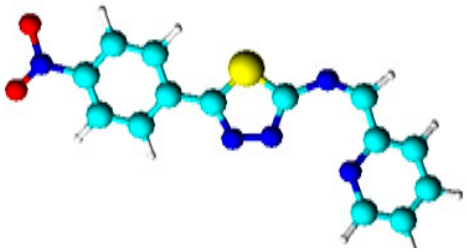

(E)-5-(4-nitrophenyl)-N-((pyridine-2-yl)methylene)-1,3,4- thiadiazol-2 amine (P2CNPTDA)

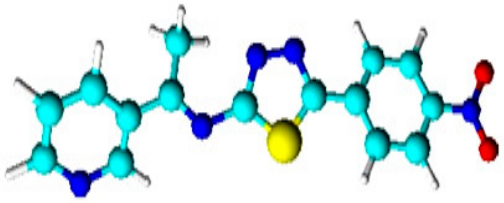

(E)-5-(4-nitrophenyl)-N-(pyridine-3-yl) ethylidene)-1,3,4-thiadiazol-2-amine (3APNPTDA)

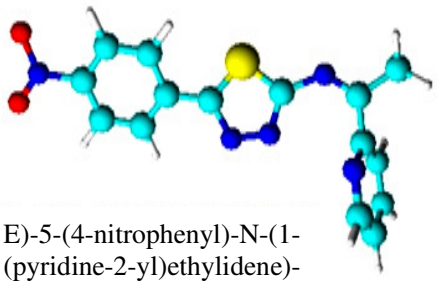

E)-5-(4-nitrophenyl)-N-(1-(pyridine-2-yl)ethylidene)-1,3,4-thiadiazol-2-amine (2APNPTDA)

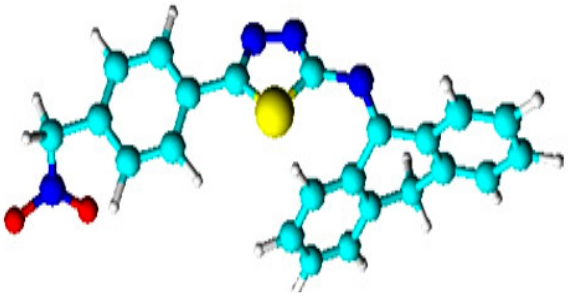

N-(anthracen-9(10H)-ylidene)-5-(4-nitrophenyl)-1,3,4-thiadiazol-2-amine (ANNPTDA)

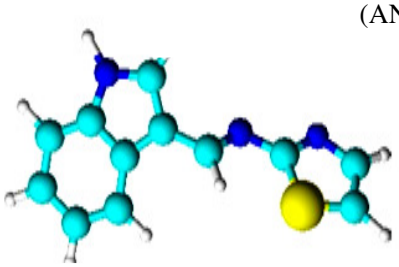

N-((1H-indol-3-yl)methylene)thiazol-2amine (I3A2AT)

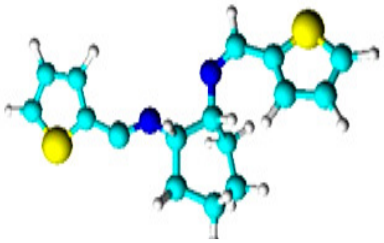

(13E)-N1,N2-bis((thiophene-2-yl)methylene)cyclohexane-1,2-diamine (T2CDACH)

Fig. 3.60: Optimized geometries of 'S' containing Schiff bases

CHAPTER 13

CORROSION INHIBITION STUDIES OF SULPHUR CONTAINING SCHIFF BASES ON CARBON STEEL IN 0.5M H_2SO_4

Investigations of corrosion inhibition response of seven heterocyclic Schiff bases including thiazole derivative, thiophene derivative and thiadiazole derivatives on carbon steel specimens in 0.5M sulphuric acid medium was established. Most adopted methods like gravimetric weight loss measurements, electrochemical impedance studies (EIS), potentiodynamic polarization studies (PDP), theoretical studies like quantum chemical calculations and surface morphological studies (SEM) were carried out for the investigation of corrosion inhibition capacity and to explain the mechanism of inhibition. In general, the inhibition competence of these heterocyclic Schiff base inhibitors in 0.5M H_2SO_4 medium was not that much prominent as in the HCl medium and it may be due to the highly aggressive nature of sulphuric acid lead to high corrosion rate of carbon steel specimens.

Gravimetric Weight Loss Measurements

Carbon steel specimens were engrossed in 0.5M sulphuric acid medium for 24h at 303K in the absence and presence of heterocyclic inhibitors. The rate of corrosion (W) and inhibition efficiencies (η_w%) are the characteristics of each heterocyclic Schiff base inhibitor which are displayed in Table 3.10 and Table 3.11 respectively. Variation of corrosion rate and the comparison of percentage of inhibition efficiency (η_w%) with concentration of heterocyclic Schiff bases are depicted in Fig. 3.61 and Fig. 3.62 respectively.

On the assessment, it is obvious that a corrosion rate of 40.64mm/y was observed for carbon steel specimens in 0.5M H_2SO_4 (blank) whereas CS in the presence of

investigated inhibitors displayed low corrosion rate. The heterocyclic poly nuclear thiadiazole Schiff base A9CNPTDA showed pronounced corrosion inhibition efficiency and low corrosion rate compared to all other heterocyclic Schiff bases at every concentration and a maximum efficiency of 90.7% was exhibited at 1mM concentration.

Table 3.10: Corrosion rates (mmy^{-1}) of CS in the presence of 'S' containing heterocyclic Schiff bases, in 0.5 M H_2SO_4 at 28^0C for 24h

C (Mm)	Corrosion rate (mmy^{-1})						
	A9CNPTDA	P2CNPTDA	ANNPTDA	3APNPTDA	2APNPTDA	I3A2AT	T2CDACH
0	40.64	40.64	40.64	40.64	40.64	40.64	40.64
0.2	11.4	13.9	23.51	22.55	24.98	12.68	19.19
0.4	9.28	12.24	20.09	21.66	23.48	10.21	11.45
0.6	7.81	10.21	16.04	20.76	22.58	6.96	7.84
0.8	6.04	8.13	15.76	19.2	20.96	6.23	6.89
1	3.74	5.23	14.76	18.82	19.59	3.95	6.04

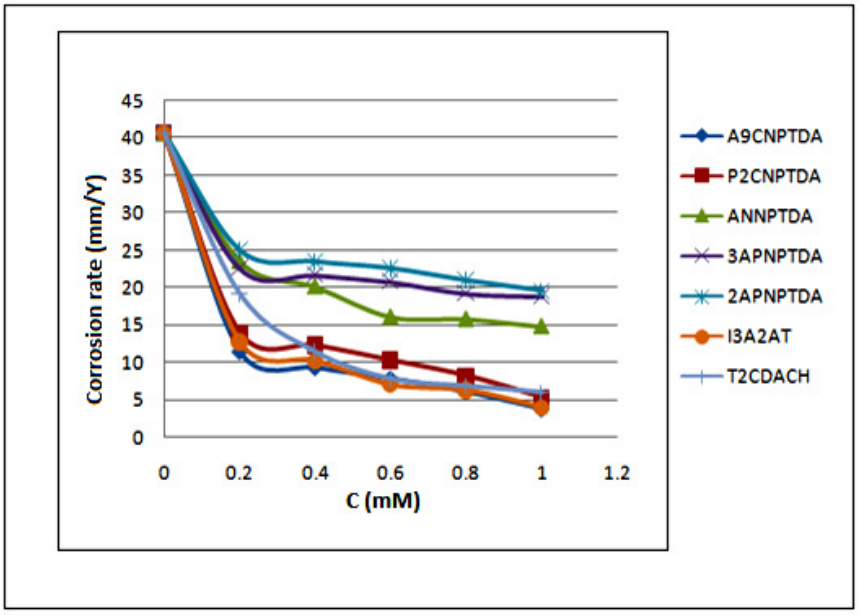

Fig. 3.61: Variation of corrosion rates of CS with the concentration of 'S' containing heterocyclic Schiff base inhibitors, in 0.5M H_2SO_4 for 24h

Table 3.11: Corrosion inhibition efficiencies (η_w%) of 'S' containing heterocyclic Schiff bases on CS corrosion in 0.5M H_2SO_4 at 28^0C for 24h

C (mM)	Inhibition efficiency (η_w%)						
	A9CNPTDA	P2CNPTDA	3APNPTDA	2APNPTDA	ANNPTDA	I3A2AT	T2CDACH
0.2	71.95	65.8	44.52	38.54	42.16	68.7	52.77
0.4	77.16	69.88	46.71	42.23	50.57	74.88	71.82
0.6	80.91	74.89	48.92	44.44	60.54	82.8	80.68
0.8	85.13	79.99	52.66	48.43	61.22	84.67	83.04
1	90.7	87.14	53.69	51.8	63.68	90.28	85.13

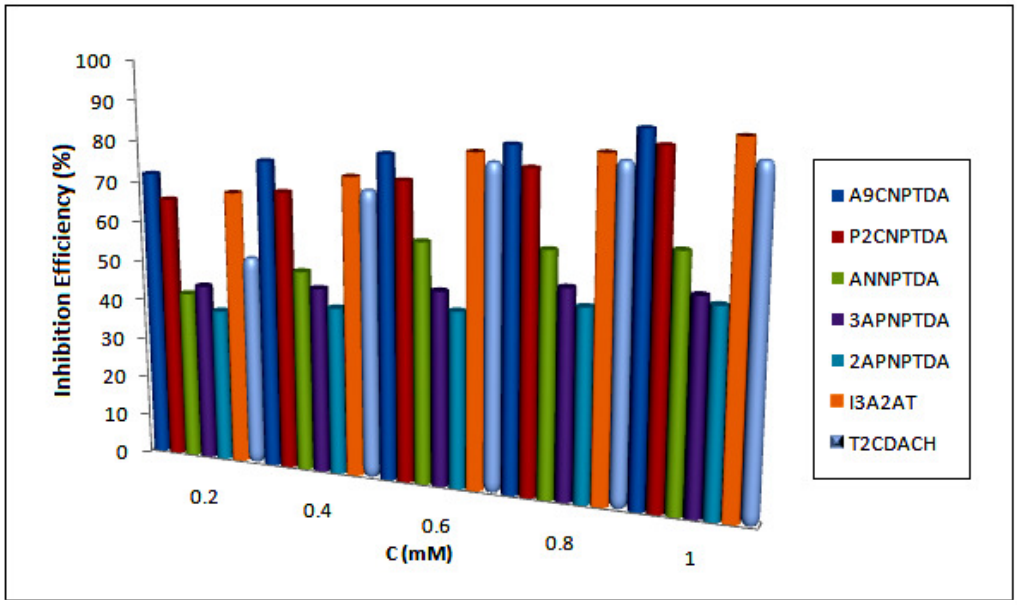

Fig. 3.62: Comparison of corrosion inhibition efficiencies (η_w%) of 'S' containing heterocyclic Schiff base inhibitors on CS corrosion in 0.5M H_2SO_4 for 24h

Among thiadiazole Schiff base inhibitors, 3APNPTDA, 2APNPTDA and ANNPTDA showed moderately low corrosion inhibition efficiency and high corrosion rate on CS surface in aggressive solution. Even though these organic molecules have dynamic corrosion inhibition probes such as a highly polarisable sulphur atom, azomethine linkage, heteroatoms and aromatic rings, they exhibited low corrosion inhibition performance, which may be recognized to i) vibrant corrosive behaviour of

H_2SO_4 medium and ii) possibility of slow hydrolysis rate of the molecules in H_2SO_4 medium.

The Heterocyclic Schiff base I3A2AT which is derived from indole-3-carbaldehyde and 2-aminothiazole and T2CDACH which is a derivative of thiophene 2aldehyde showed elevated inhibition efficiency in H_2SO_4 medium. Maximum η_w% shown by I3A2AT molecule at a concentration of 1mM was 90.28%. The maximum inhibition efficiency of I3A2AT is attributed by its adsorption employing between the electrons of the indole rings and CS surface, and it acts as a bidentate ligand in which surface coordination taking place via both the amino group and the –S– moiety from the thiazole ring. The Schiff base derived from thiophene-2-aldehyde i.e., T2CDACH showed elevated corrosion inhibition efficiency than thiadiazole pyridine derivatives and anthrone derivatives in sulphuric acid medium. The η_w% varied from 52.77 to 85.13% for concentrations 0.2 to 1mM respectively. Like other Schiff bases, T2CDACH also undergo hydrolysis but one of the hydrolysed product, thiophene 2-aldehyde exhibited higher inhibition efficiency in H_2SO_4 medium (Table 3.11).

Corrosion inhibition potencies of the 'S' containing Schiff base inhibitors were compared with their parent compounds 5-(4-nitrophenyl)-1,3,4-thiadiazol-2-amine (NPTDA), Anthracene-9-carbaldehyde (A9C), Pyridine-2-carbaldehyde (P2C), 3-Acetylpyridine (3ACP), 2-Acetylpyridine (2ACP), Anthrone (AN), Indole-3-Carbaldehyde (I3A), 2-Aminothiazole (2AT), Thiophene-2-carbaldehyde (T2C) and 1,2-Diamino cyclohexane (DAC) in 0.5M H_2SO_4 for a period 24h at different concentrations and are tabulated in Table 3.12. It can be inferred from the comparison studies that higher corrosion inhibition potencies of these heterocyclic Schiff base inhibitors were because of the presence of highly conjugated azomethine linkage.

Table 3.12: Corrosion inhibition efficiencies (η_w%) of parent compounds NPTDA, A9C, P2C, 3ACP, 2ACP, ANT, I3A, 2AT, T2C and DAC on CS in 0.5M H_2SO_4 for a period 24h

C (Mm)	Inhibition Efficiencies (η_w%)									
	NPTDA	A9C	P2C	3ACP	2ACP	ANT	13A	2AT	T2C	DAC
0.2	12.43	15.9	7.35	0.82	0.73	-85.78	38.92	12.28	22.16	-28
0.6	30.17	18.53	11.18	1.49	1.18	-80.09	43.54	14.64	34.72	-16
1	32.84	20.58	16.47	1.82	1.59	-74.93	48.65	21.87	70.03	1.68

On comparing the inhibition efficiencies of these heterocyclic Schiff bases in HCl and H_2SO_4 medium, it is obvious that they show higher inhibition efficiency in HCl medium. It is supposed that the Cl^- ions can more strongly adsorb on the metal surface than SO_4^{2-} ions and builds an excess negative charge on the carbon steel surface. It will facilitate the adsorption of protonated heterocyclic Schiff bases and reduce iron dissolution.

Adsorption Isotherms

The mechanism of interaction of these heterocyclic Schiff bases on the surface of CS specimens was demonstrated with the aid of adsorption isotherms. By considering different adsorption isotherms and the best fit model was selected with the support of correlation coefficient. Isotherms of these inhibitors in 0.5M H_2SO_4 are represented from Fig. 3.63 and parameters obtained from investigations are tabulated in Table 3.13.

From the adsorption investigations, it was found that these 'S' containing heterocyclic Schiff base inhibitors A9CNPTDA, P2CNPTDA, 3APNPTDA, 2APNPTDA, ANNPTDA, I3A2AT and T2CDACH followed Langmuir adsorption isotherm on the CS surface of during the process of corrosion inhibition in 0.5M H_2SO_4. Negative values of ΔG^0_{ads} for all sulphur containing Schiff bases inhibitors point out the spontaneity of the adsorption process. ΔG^0_{ads} values up to -20kJ/mol indicates the electrostatic interaction between the charged metal surface (physisorption) and the charged heterocyclic organic inhibitors.

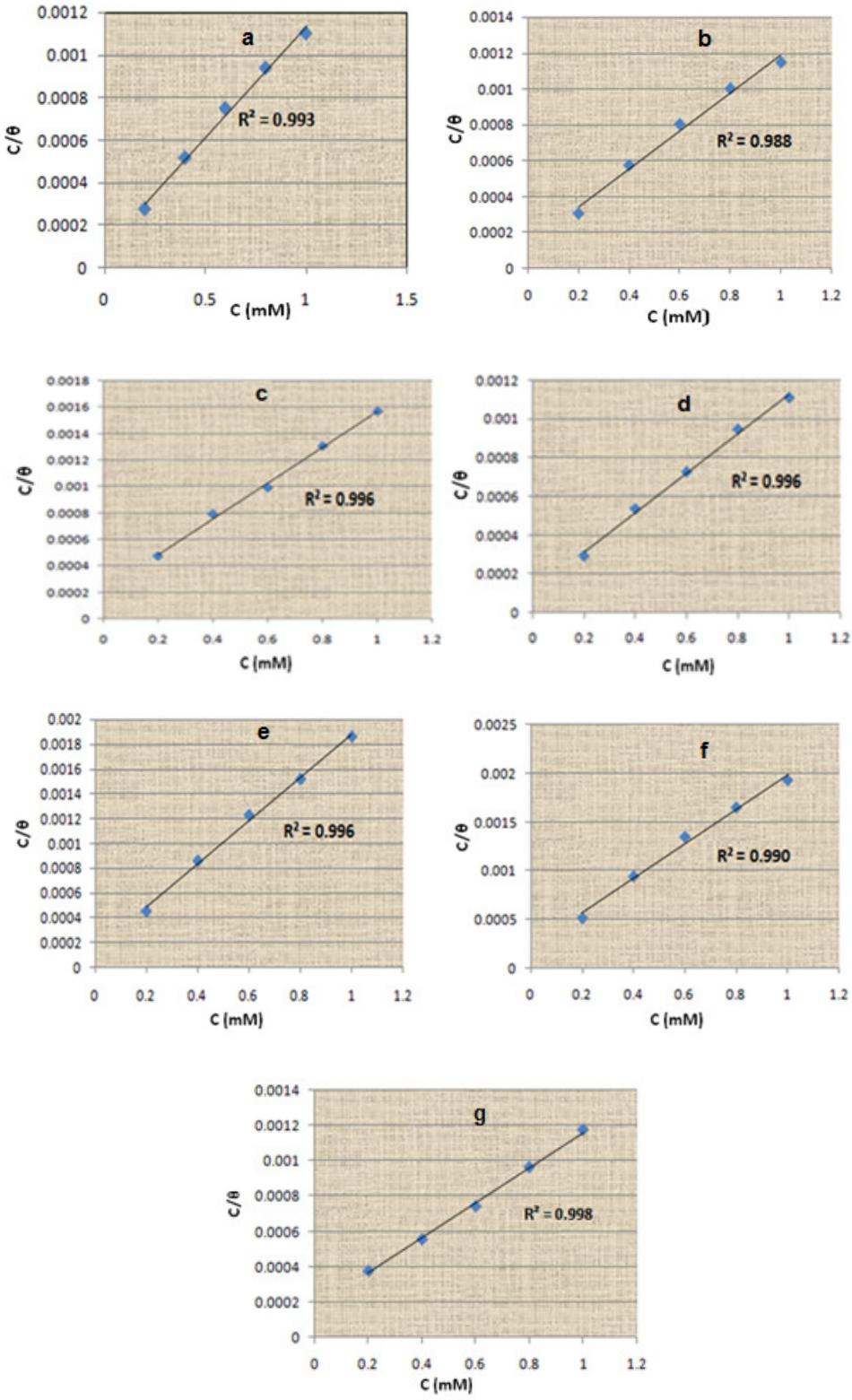

Fig. 3.63: Langmuir adsorption isotherms of (**a**) A9CNPTDA (**b**) P2CNPTDA (**c**) 3APNPTDA (**d**) 2APNPTDA (**e**) ANNPTDA (**f**) I3A2AT (**g**) T2CDACH on CS in 0.5M H_2SO_4

Table 3.13: Adsorption parameters of 'S' containing heterocyclic Schiff base inhibitors on CS corrosion in 0.5M H_2SO_4

Adsorption Parameter	Schiff bases						
	A9CNPTDA	P2CNPTDA	3APNPTDA	2APNPTDA	ANNPTDA	I3A2AT	T2CDACH
K_{ads}	10000	7633.58	7352.94	5000	4672	9090.90	6250
ΔG^0_{ads} ($kJmol^{-1}$)	-33.12	-32.44	-32.35	-31.38	-31.12	-32.88	-31.94

ΔG^0_{ads} ranges between -31.94 and -33.12kJ/mol on CS specimens in 0.5M H_2SO_4 medium which implies that the adsorption behaviour of all the synthesized heterocyclic inhibitor molecules involves both electrostatic and chemical adsorption. The free energy of adsorptions of these heterocyclic Schiff base inhibitors, A9CNPTDA and I3A2AT were comparatively elevated than that of the other heterocyclic imines. The main reason is that these inhibitors are more powerfully adsorbed on the CS surface forming a monolayer through highly conjugated azomethine linkage, highly polarisable aromatic rings etc.

Surface Morphological Investigations

In order to establish the mechanism of action of these heterocyclic Schiff base inhibitors A9CNPTDA, P2CNPTDA, 3APNPTDA, 2APNPTDA, ANNPTDA, I3A2AT and T2CDACH, SEM experiments were conducted in 0.5M H_2SO_4 on CS surface. The SEM micrographs of (a) bare CS surface (b) CS specimen immersed in 0.5M $H_2SO_4$and containing 1mM concentration of (c) A9CNPTDA and (d) ANNPTDA after 24 h of immersion time are shown in Fig. 3.64. Surface morphology of these images were clearly established that in presence of inhibitors, the damage occurred on the CS surfaces was fairly decreased whereas the surface was dangerously destroyed in the absence of inhibitor.

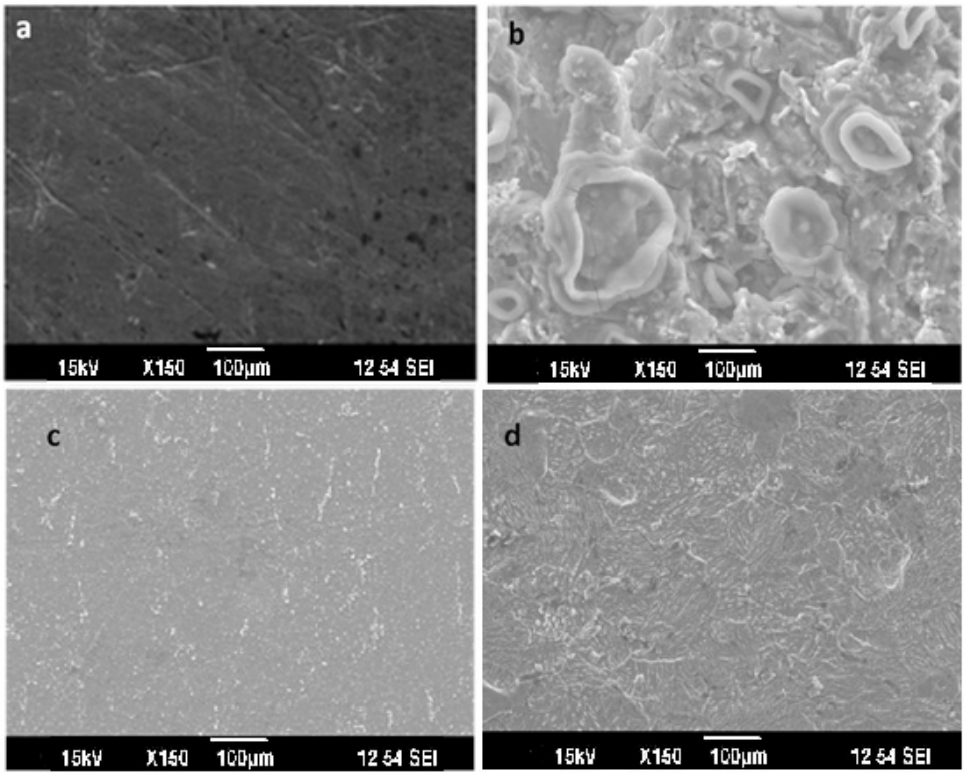

Fig. 3.64: SEM images of (**a**) bare CS (**b**) CS treated with 0.5M H_2SO_4 (**c**) CS treated with A9CNPTDA (1mM) (**d**) CS treated with ANNPTDA (1mM) for 24h

Electrochemical Impedance Spectroscopic Studies (EIS)

Iviumcompactstat-e system associated with a superior version of 'IviumSoft' software was employed for the electrochemical analysis. Assemblies of three-electrode was used as the electrochemical cell in which a saturated calomel electrode (SCE) was used as the reference electrode, a platinum electrode of area $1cm^2$ was used as the auxiliary or counter electrode and well-polished metal surface of exposed area ($1cm^2$) towards the corroding medium was employed as the working electrode for analysis.

The corrosion behaviour of CS in 0.5M H_2SO_4 with and without these 'S' heterocyclic inhibitors was studied by employing impedance spectroscopic analysis. To make clear the inhibitory action of these organic ligands, CS specimens were engrossed in 0.5M H_2SO_4 medium in the presence and absence of the inhibitors for 30 minutes prior to the experiment at 303K.

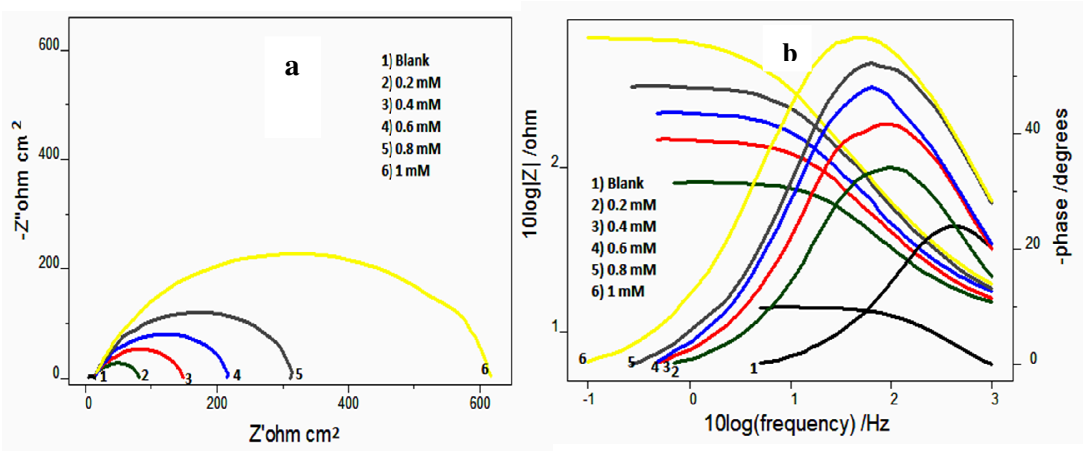

Fig. 3.65: a) Nyquist plots and **b)** Bode plots of CS corrosion in the presence and absence of A9CNPTDA in 0.5M H_2SO_4

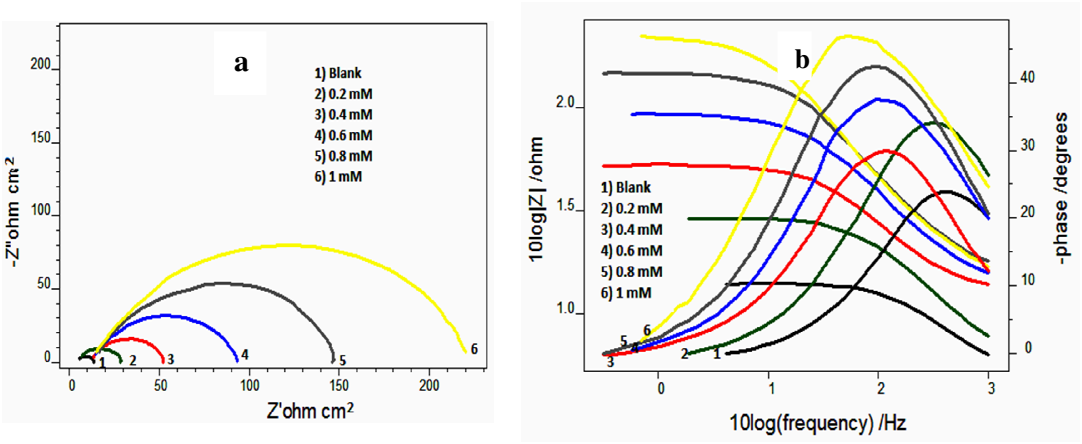

Fig. 3.66: a) Nyquist plots and **b)** Bode plots of CS corrosion in the presence and absence of P2CNPTDA in 0.5M H_2SO_4

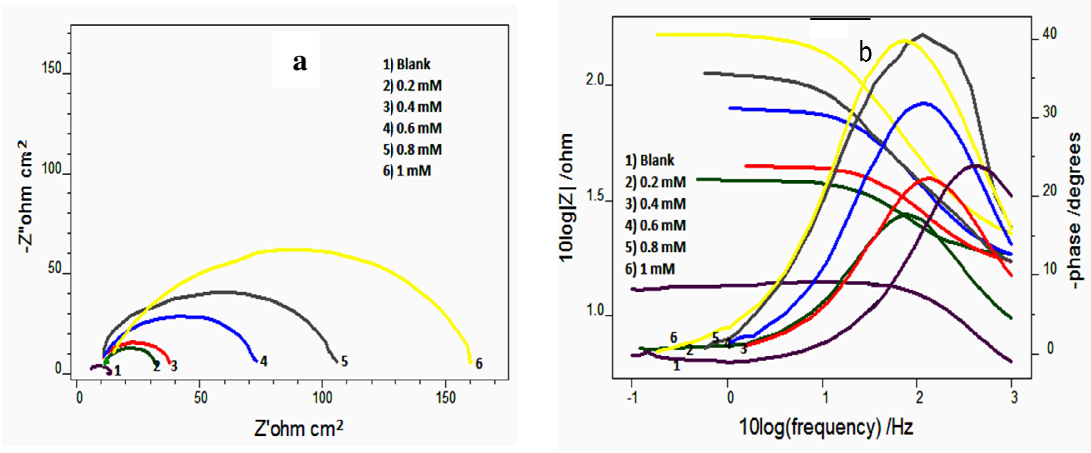

Fig. 3.67: a) Nyquist plots and **b)** Bode plots of CS corrosion in the presence and absence of 3APNPTDA in 0.5M H_2SO_4

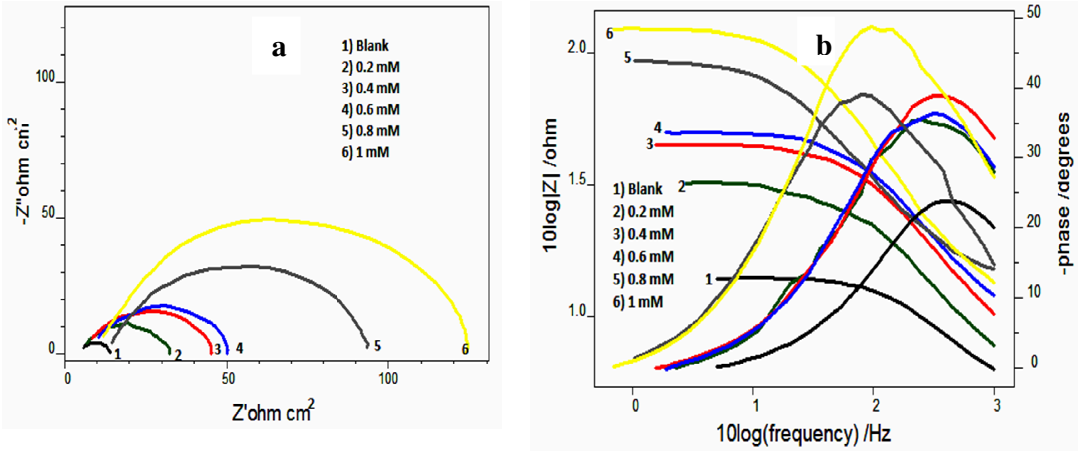

Fig. 3.68: a) Nyquist plots and **b)** Bode plots of CS corrosion in the presence and absence of 2APNPTDA in 0.5M H_2SO_4

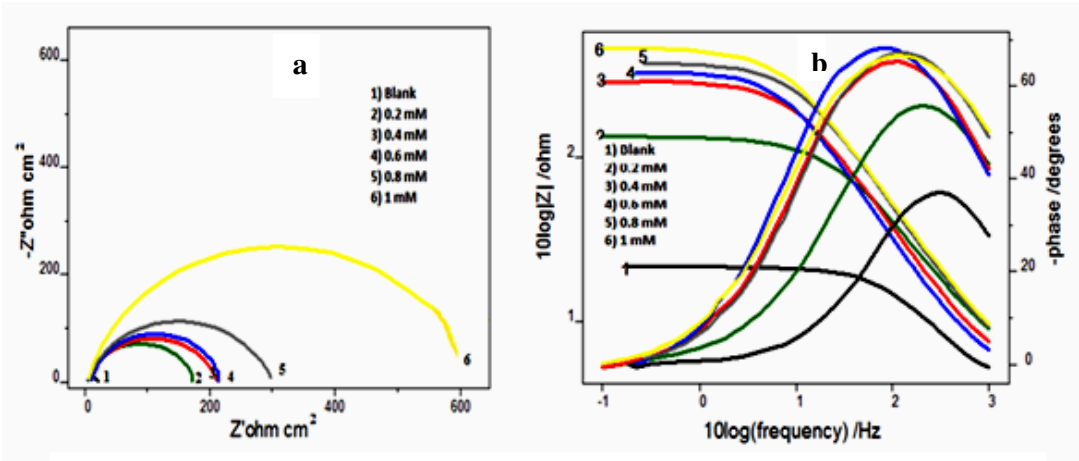

Fig. 3.69: a) Nyquist plots and **b)** Bode plots of CS corrosion in the presence and absence of ANNPTDA in 0.5M H_2SO_4

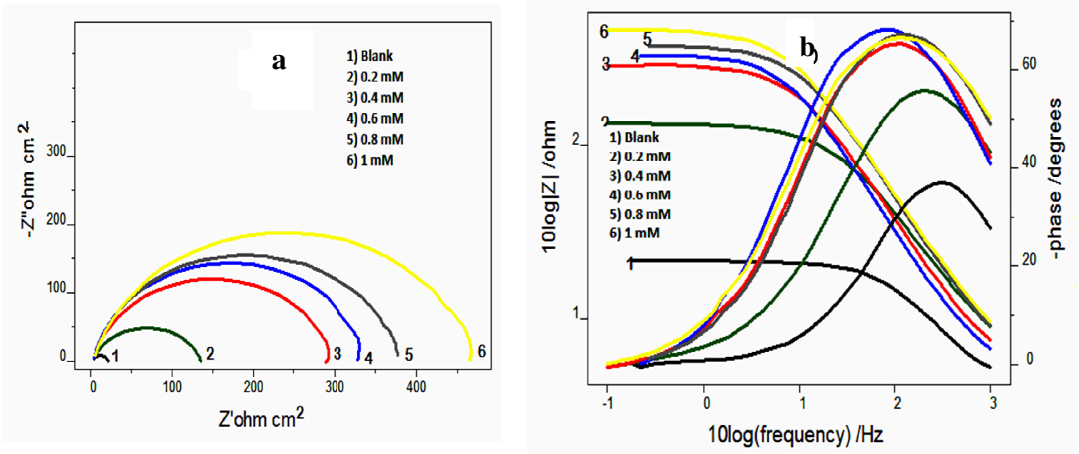

Fig. 3.70: a) Nyquist plots and **b)** Bode plots of CS corrosion in the presence and absence of I3A2AT in 0.5M H_2SO_4

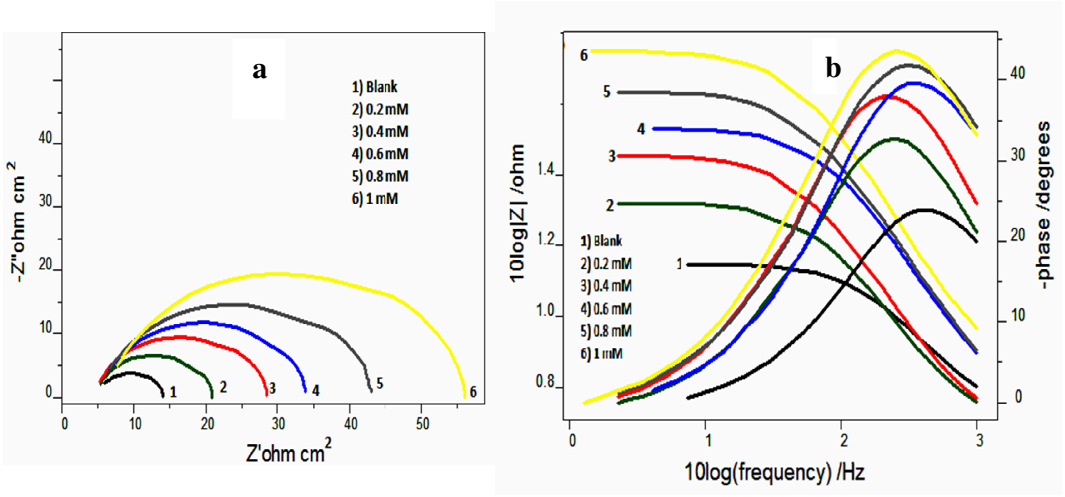

Fig. 3.71: a) Nyquist plots and **b)** Bode plots of CS corrosion in the presence and absence of T2CDACH in 0.5M H_2SO_4

Fig. 3.65 to Fig. 3.71 corresponding to the Nyquist plots and Bode plots of the 'S' containing heterocyclic Schiff bases A9CNPTDA, P2CNPTDA, 3APNPTDA, 2APNPTDA, ANNPTDA, I3A2AT and T2CDACH respectively. The impedance (EIS) parameters such as charge transfer resistance (R_{ct}), double layer capacitance (C_{dl}), solution resistance (R_s)and percentage of inhibition efficiency ($\eta_{EIS\%}$) were calculated from these plots and documented in Table 3.14. From R_{ct} values, the percentage of inhibition efficiency was evaluated using the subsequent equation

$$\eta_{EIS}\% = \frac{Rct - R'ct}{Rct} \times 100 \qquad (40)$$

where R'_{ct} and R_{ct} are the charge transfer resistances of the working electrode in acid medium in the absence and presence of these heterocyclic Schiff base indicators respectively

The value of R_{ct} is a measure of electron transfer between acidic solution and the exposed area of CS and the rate of corrosion is inversely proportional to it. From Nyquist plots, it was observed that the diameter of semicircle increases with the concentration of inhibitors indicating that these 'S' containing inhibitors undergo self-assembly on the CS

surface for forming a protective layer and resist the corrosion process. Highest value of R_{ct} is shown by thiadiazole Schiff base A9CNPTDA and a maximum efficiency of 97.81% was obtained at 1mM concentration of the inhibitor. The monolayer formation of inhibitors obstructs the charge transfer between the carbon steel and the acidic solution and charge transfer resistance increases with inhibitor concentration. The decreasing nature of capacitance values C_{dl} with the inhibitor concentration mainly indicates the increase in the thickness of the electrical double layer and/or decrease in local dielectric constant. The trend of increasing percentage of inhibition efficiency with the concentration is depicted in Fig. 3.72.

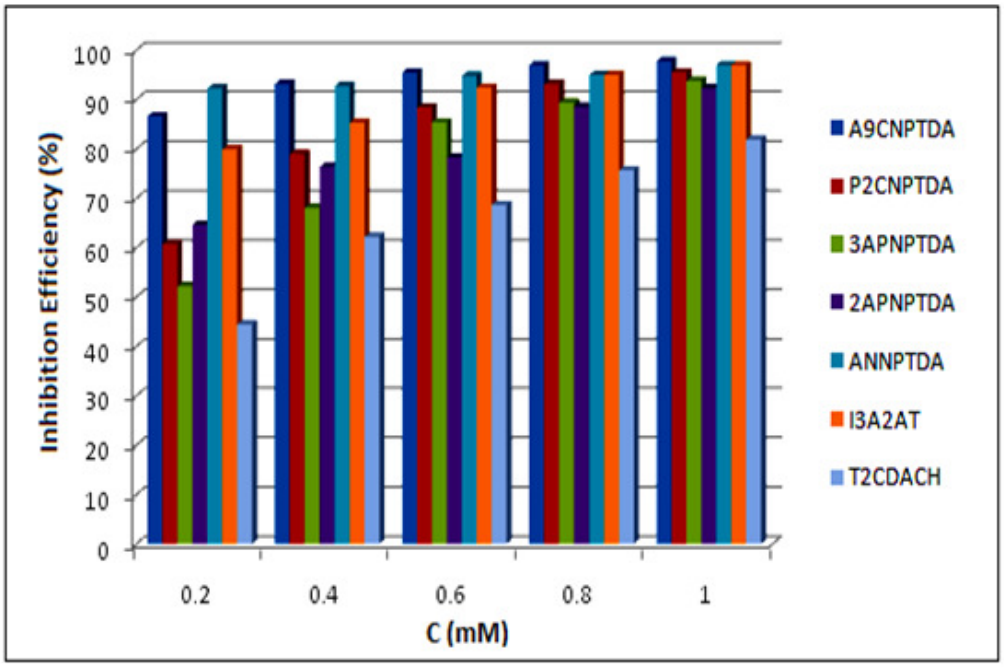

Fig. 3.72: Comparison of Corrosion inhibition efficiencies ($\eta_{EIS\%}$) of 'S' containing heterocyclic Schiff base inhibitors on CS in 0.5M H_2SO_4 at 28^0C

Table 3.14: Electrochemical impedance parameters of CS corrosion in the presence and absence of 'S' containing heterocyclic Schiff bases in 0.5M H_2SO_4

Inhibitors	C (mM)	C_{dl} ($\mu F\ cm^{-2}$)	R_{ct} ($\Omega\ cm^{-2}$)	η_{EIS}%
Blank	0	90	8.16	-
A9CNPTDA	0.2	79.2	61.2	86.66
	0.4	65.2	120	93.22
	0.6	58.3	181	95.49
	0.8	43.6	273	97.01
	1	39.5	374	97.81
P2CNPTDA	0.2	66.9	20.8	60.76
	0.4	89.9	35.9	79.03
	0.6	62.1	70.5	88.42
	0.8	52.7	120	93.2
	1	60.7	184	95.56
3APNPTDA	0.2	64.0	19.1	52.27
	0.4	87.3	25.6	68.12
	0.6	63.9	56.1	85.45
	0.8	64.7	77.4	89.45
	1	55.0	133	93.86
2APNPTDA	0.2	69.6	23.1	64.67
	0.4	43.9	34.6	76.41
	0.6	43.0	37.6	78.29
	0.8	80.7	72.0	88.60
	1	46.7	106	92.35
ANNPTDA	0.2	68.7	106	92.30
	0.4	65.1	113	92.77
	0.6	70.0	158	94.83
	0.8	71.0	164	95.02
	1	66.3	359	97.02
I3A2AT	0.2	80.0	60.9	80.00
	0.4	68.8	101	85.41
	0.6	69.7	146	92.50
	0.8	118	159	95.05
	1	59.2	312	97.01
T2CDACH	0.2	106	14.7	44.55
	0.4	97.7	21.6	62.26
	0.6	52.8	25.9	68.70
	0.8	57.0	33.6	75.74
	1	49.8	45.0	82.00

Inhibition efficiency obtained from gravimetric weight loss studies and results gained from EIS analysis are not comparable. Results from EIS studies are higher than the results obtained from gravimetric weight loss studies. Electrochemical analysis is a quick corrosion monitoring procedure and it will only show the corrosion inhibition potencies in the early hours stage of treatment. In H_2SO_4 medium, these ligands have a tendency to hydrolyze into their parent compounds and they exhibit poor inhibition efficiency for a long period of 24h. This is the main reason for the poor results of gravimetric corrosion inhibition studies than the electrochemical analysis results. Comparatively least efficiency was reported in the case of inhibitor T2CDACH and these results are similar to gravimetric weight loss studies. This is because of the inhibitor T2CDACH undergoes faster hydrolysis in H_2SO_4 medium in the early hours stage. Heterocyclic inhibitors ANNPTDA and I3A2AT showed high results in EIS analysis, but the performance of ANNPTDA in gravimetric studies are very low. The results also show the fast hydrolytic nature of this molecule in aggressive medium. Order of performances of the studied S containing heterocyclic Schiff base inhibitors in H_2SO_4 medium on can be given as A9CNPTDA > ANNPTDA > I3A2AT > P2CNPTDA > 3APNPTDA >2APNPTDA > T2CDACH.

Potentiodynamic Polarization Studies

To emphasize the corrosion inhibitory role of the novel 'S' containing Schiff bases on carbon steel and to recommend the electrochemical site of interaction, potentiodynamic polarization studies including Tafel extrapolation analysis and Linear polarization studies were conducted. Corrosion potential (E_{corr}), corrosion current density (i_{corr}) and polarization resistance (R_p) were calculated in every analysis and by means, the inhibition efficiency was determined. Tafel plots and linear polarization curves of CS in 0.5M H_2SO_4 medium in the presence and absence of these heterocyclic Schiff base

inhibitors are depicted from Fig. 3.73 to Fig. 3.79. Tafel and Linear polarization data including corrosion potential (E_{corr}), corrosion current density (I_{corr}), anodic slope (b_a), cathodic slope (b_c) and inhibition efficiency were obtained by potentiodynamic polarization studies and tabulated in Table 3.15. A comparison between the inhibition efficiencies of these sulphur containing heterocyclic Schiff base inhibitors was done and portrayed in Fig. 3.83.

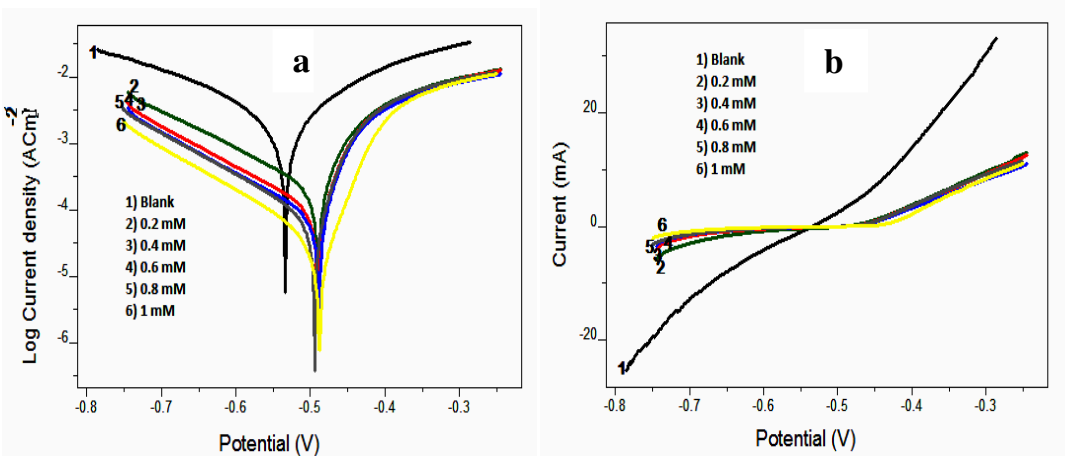

Fig. 3.73: a) Tafel plots and **b)** Linear polarization curves of CS corrosion in the presence and absence of A9CNPTDA in 0.5M H_2SO_4

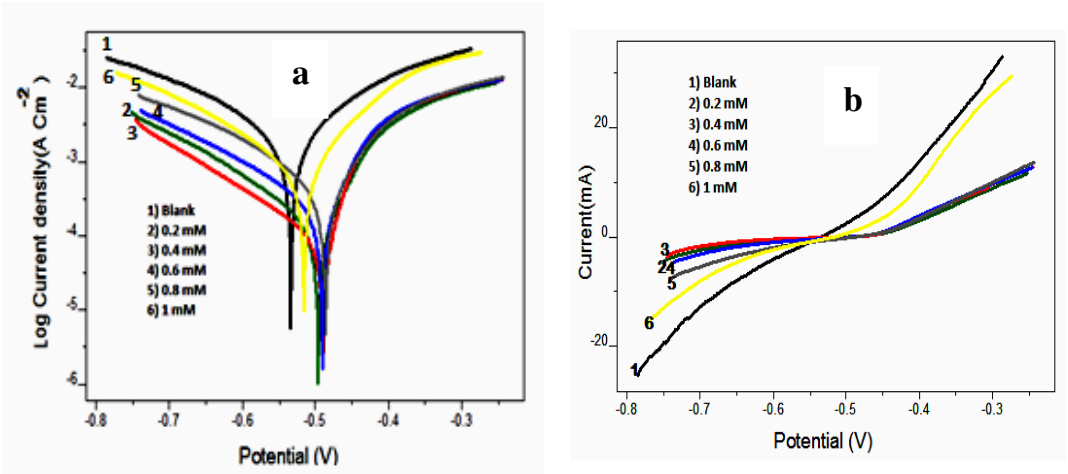

Fig. 3.74: a) Tafel plots and **b)** Linear polarization curves of CS corrosion in the presence and absence of P2CNPTDA in 0.5M H_2SO_4

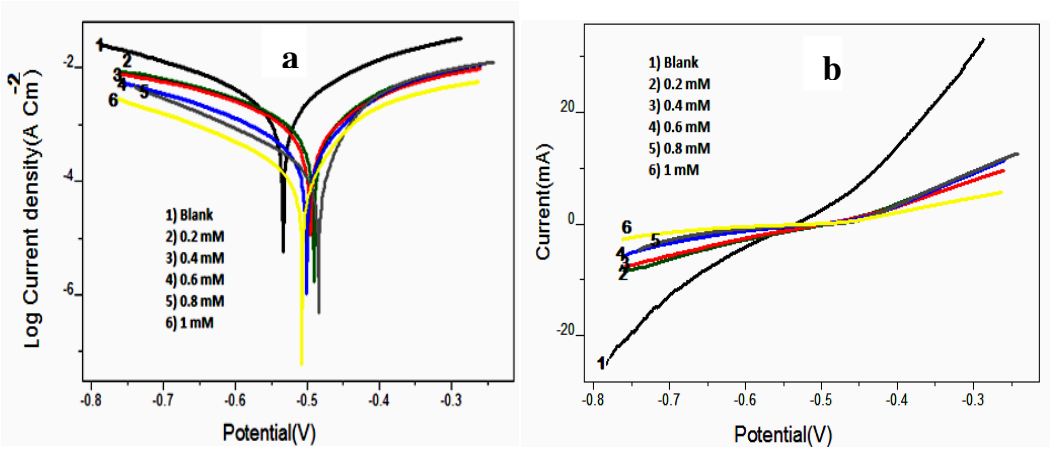

Fig. 3.75: a) Tafel plots and **b)** Linear polarization curves of CS corrosion in the the presence and absence of 3APNPTDA in 0.5M H_2SO_4

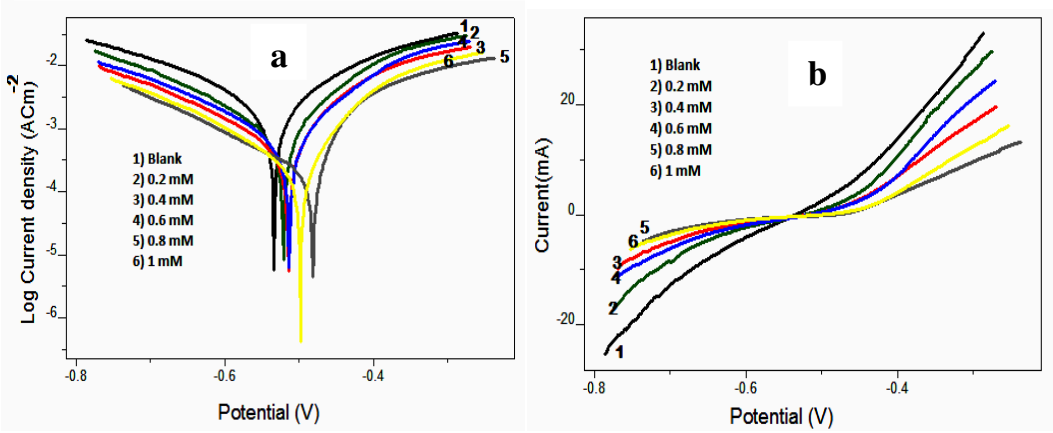

Fig. 3.76: a) Tafel plots and **b)** Linear polarization curves of CS corrosion in the presence and absence of 2APNPTDA in 0.5M H_2SO_4

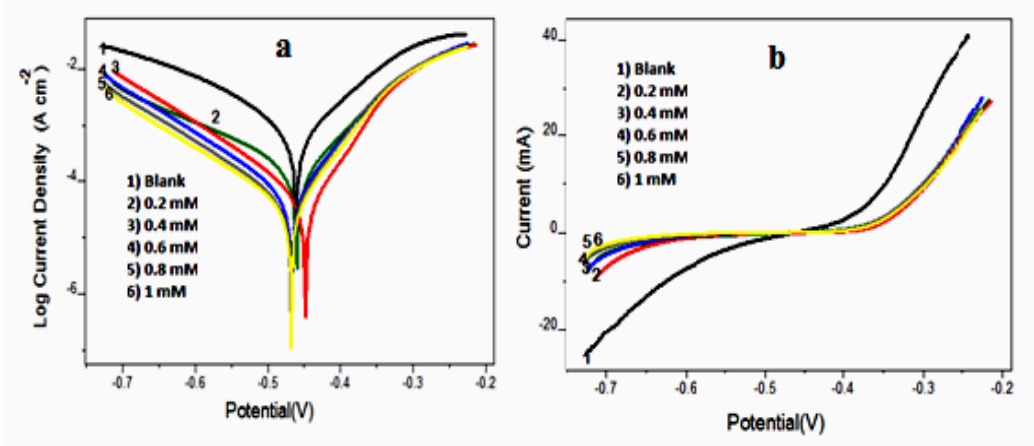

Fig. 3.77: a) Tafel plots and **b)** Linear polarization curves of CS corrosion in the presence and absence of ANNPTDA in 0.5M H_2SO_4

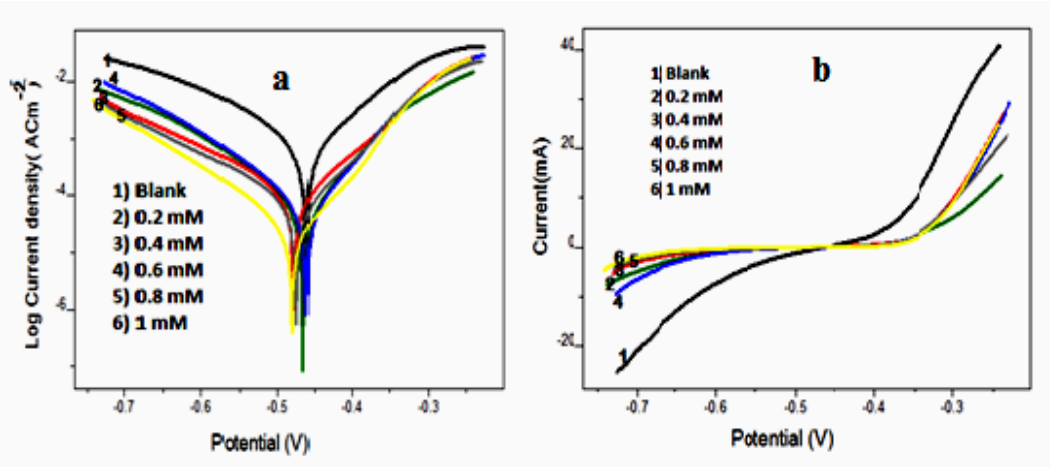

Fig. 3.78: a) Tafel plots and **b)** Linear polarization curves of CS corrosion in the presence and absence of I3A2AT in 0.5M H_2SO_4

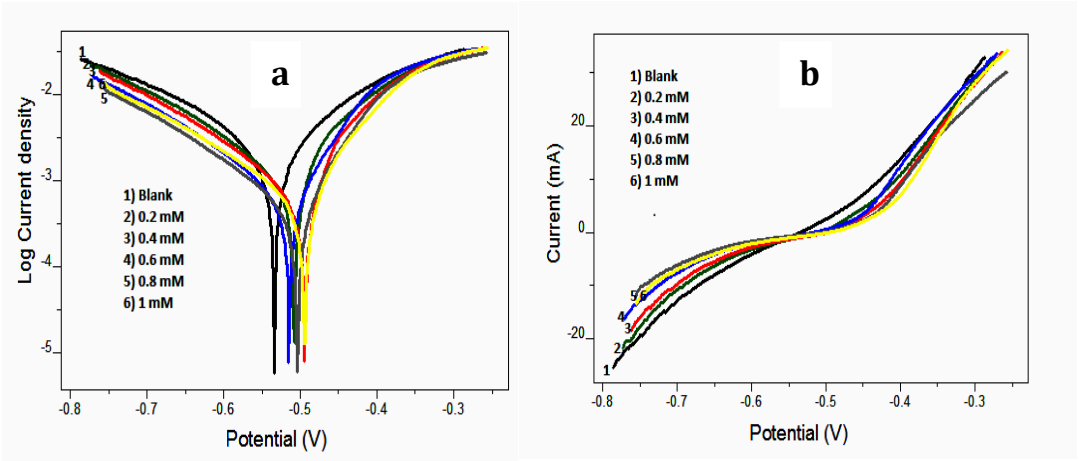

Fig. 3.79: a) Tafel plots and **b)** Linear polarization curves of CS corrosion in the presence and absence of T2CDACH in 0.5M H_2SO_4

Table 3.15: Potentiodynamic polarization parameters of CS corrosion in the presence and absence of 'S' containing heterocyclic Schiff bases in 0.5M H_2SO_4

Inhibitor	Tafel Data						Polarization data	
	C (mM)	$-E_{corr}$ (mV/SCE)	I_{corr} ($\mu A/cm^2$)	$-b_a$ (mV/dec)	b_c (mV/dec)	η_{pol}%	R_p(ohm)	η_{Rp}%
Blank	0	541	2705	205	234	-	15.23	-
A9CNPTDA	0.2	577	602	225	177	77.74	82.17	81.46
	0.4	606	479	232	165	82.29	130	88.28
	0.6	612	402	233	161	85.13	161	90.54
	0.8	608	368	214	158	86.39	204.1	92.53
	1	583	149	154	156	94.49	611.5	97.50
P2CNPTDA	0.2	536	1140	151	190	57.8	30.45	49.98
	0.4	529	893	211	205	66.9	58.35	73.89
	0.6	573	724	232	192	73.23	88.88	82.86
	0.8	562	391	182	167	85.54	142.6	89.32
	1	608	490	233	163	81.88	164.9	90.76
3APNPTDA	0.2	499	1217	211	271	55	36.08	57.78
	0.4	497	1072	212	269	60.36	40.08	62.00
	0.6	528	611	179	220	77.41	76.7	80.14
	0.8	574	610	224	179	77.46	108.8	85.92
	1	564	335	214	199	87.6	172.3	91.16
2APNPTDA	0.2	545	1241	161	186	54.12	29.52	48.40
	0.4	560	927	187	189	65.73	44.83	66.02
	0.6	533	886	150	196	67.25	39.64	61.57
	0.8	583	701	244	170	74.1	69.18	77.98
	1	550	544	172	175	79.88	87.87	82.66
ANNPTDA	0.2	601	456	235	163	83.14	132.7	88.52
	0.4	559	318	180	172	88.24	160.9	90.53
	0.6	558	302	178	161	88.88	184.9	91.76
	0.8	527	189	236	253	93.01	216.6	92.96
	1	474	71.1	163	138	97.37	258.3	94.10
I3A2AT	0.2	580	631	225	179	76.67	71.17	78.60
	0.4	606	483	232	166	82.14	129.9	88.27
	0.6	612	417	233	161	84.58	157.4	90.32
	0.8	608	386	216	160	85.73	199.5	92.36
	1	583	158	155	156	94.15	605.18	97.48
T2CDACH	0.2	543	1674	180	190	37.49	22.75	33.05
	0.4	544	1390	173	181	48.41	33.89	55.06
	0.6	558	1241	165	167	53.65	37.33	59.20
	0.8	555	960	164	174	64.15	46.54	67.27
	1	527	881	139	187	67.10	64.15	76.25

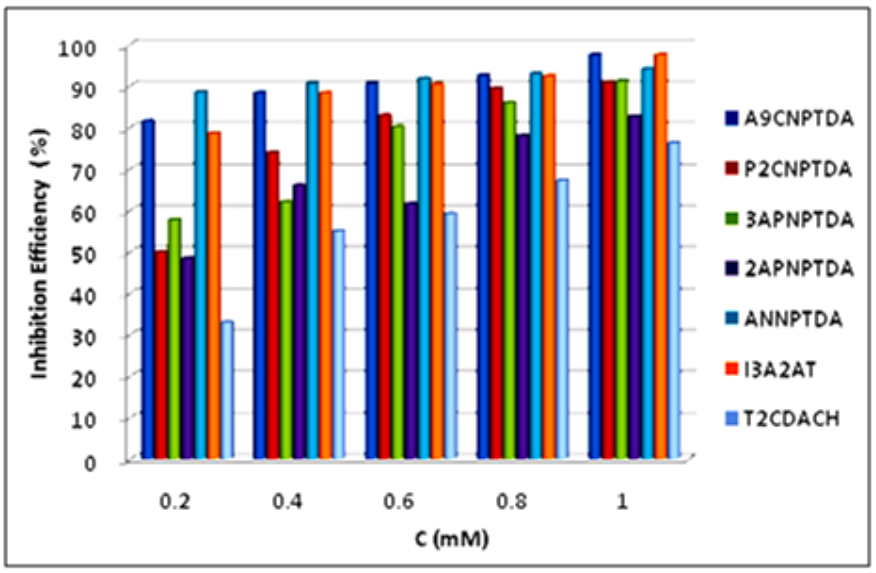

Fig. 3.80: Comparison study of corrosion inhibition potencies (η_{pol}%) of 'S' containing heterocyclic Schiff bases on CS in 0.5M H_2SO_4 at 28^0C

On scrutiny, it was revealed that the corrosion current densities of steel specimens decreased appreciably with the concentration of inhibitors. This is because of these organic molecules obstruct the metal dissolution progression appreciably by either prevailing in the cathodic or anodic process of corrosion or they acted as mixed type inhibitors. On the evaluation of Tafel and Linear polarization curves, it was established that the slope of the Tafel curves of uninhibited solution entirely different from the slope obtained in the presence of inhibitors. The outcome obtained by the potentiodynamic polarization studies were in good harmony with the electrochemical impedance studies.

Among thiadiazole derivatives, the polynuclear heterocyclic Schiff base inhibitor, A9CNPTDA exhibited the maximum inhibition efficiency of 97.50% at 1mM concentration. The heterocyclic Schiff bases, I3A2AT and ANNPTDA, also exhibited excellent inhibition efficiencies (97.48% in the case of I3A2AT and 94.10% in the case of ANNPTDA). But the performance of ANNPTDA in gravimetric studies is very low. Even if the Schiff base inhibitors 3APNPTDA and 2APNPTDA showed poor inhibitive performance as per gravimetric weight loss studies in 0.5M H_2SO_4 at 24h, their corrosion

inhibitory power in accordance with the polarization techniques were very much higher than that of expected. This is because of that, in electrochemical investigations, the contact time between the acid solution and the working electrode is about 30 minutes only whereas in the later the contact time is 24h and more.

Generally, if the shift of E_{corr} is greater than 85 and a significant change is observed in cathodic or anodic slopes, the inhibitor can be considered as cathodic or anodic inhibitors. In the present investigation, the seven heterocyclic Schiff bases namely A9CNPTDA, P2CNPTDA, 3APNPTDA, 2APNPTDA, ANNPTDA, I3A2AT and T2CDACH affects the anodic and cathodic slopes uniformly and E_{corr} values didn't alter considerably with respect to the blank (>85) and therefore these molecules can be regarded as mixed-type inhibitors.

SUMMARY

The corrosion inhibition efficiencies of newly synthesized sulphur containing heterocyclic Schiff base inhibitors namely (E)-(N-anthracene-9-ylmethylene)-5-(4-nitrophenyl)-1,3,4-thiadiazol-2-amine (A9CNPTDA), (E)-5-(4-nitrophenyl)-N-((pyridine -2-yl)methylene)-1,3,4-thiadiazol-2-amine (P2CNPTDA), (E)-5-(4-nitrophenyl)-N-(1 (pyridine-3-yl)ethylidene)-1,3,4-thiadiazol-2-amine (3APNPTDA), (E)-5-(4-nitrophenyl) -N-(1(pyridin-2-yl)ethylidene)-1,3,4-thiadiazol-2-amine (2APNPTDA), N-(anthracen-9(10H)-ylidene)-5-(4-nitrophenyl)-1,3,4-thiadiazol-2-amine (ANNPTDA), N-((1H-indol-3-yl)methylene)thiazol-2amine (I3A2AT) and (13E)-N1,N2-bis((thiophene-2-yl)methylene)cyclohexane-1,2-diamine (T2CDACH) against CS specimens in 1M HCl and 0.5M H_2SO_4 solutions were analysed using weight loss studies and electrochemical investigations like electrochemical impedance spectroscopy (EIS), potentiodynamic polarization studies (PDP) and electrochemical noise measurements. It was found that all these 'S' containing Schiff base ligands exhibited excellent corrosion inhibition efficiency on carbon steel in HCl medium. Generally the corrosion inhibition efficiency was lower in H_2SO_4 medium than in HCl medium. The corrosion inhibition mechanism of the compounds was confirmed by adsorption studies and surface morphological analysis and the effect of temperature and time on the corrosion inhibition efficiency of the compounds was also established. Quantum chemical investigations were performed using Gammess software and optimized geometries were formulated.

According to the weight loss studies in HCl medium, the inhibition efficiencies were increased with the inhibitor concentrations for all the compounds. At a maximum concentration of 1mM, all the studied inhibitors displayed 95.18 - 98.04% inhibition efficiencies by the gravimetric weight loss studies. A9CNPTDA showed pronounced

corrosion inhibition efficiency compared to all other heterocyclic Schiff bases at every concentration and a maximum efficiency of 98.04% was exhibited at 1mM concentration

All the inhibitors were performed very potential anticorrosive activity (92.47-99.6%) towards CS at 1mM concentration during electrochemical studies. The highly delocalized electron clouds of the aromatic rings, interacted with the metal surface deeply and thus prevent the metallic dissolution appreciably. Presence of heteroatoms especially highly polarizable 'S' atom, azomethine moiety, electron-rich aromatic rings and planarity are the root causes by which the molecule showed higher inhibition efficiency. The stability of the inhibitor in aggressive medium is very essential if it is to be recommended for long time use. All synthesized heterocyclic inhibitors except T2CDACH are excellent inhibitors for long time use. This is because of the puckered geometry and the tendency of hydrolysis which prevents the molecule to interact with the metal surface. It was confirmed by UV-Visible study that the molecule undergoes fast hydrolysis into their parent compounds in 1M HCl medium.

Adsorption studies revealed that Langmuir isotherm was the best fit isotherm for all synthesized molecules 1M HCl medium. The values of thermodynamic parameters suggested that adsorption process was spontaneous and the interaction between the metal and inhibitor molecules involves both electrostatic-adsorption and chemisorptions. The role of azomethine group in the inhibitory action was proved when the parent compounds of the Schiff base inhibitors were taken for corrosion studies. The activities were higher for the Schiff bases than the parent compounds. The corrosion inhibition performances of the compounds at elevated temperatures were also studied in HCl medium. Data obviously established that the rate of corrosion is increased at elevated temperatures.

Temperature-dependent gravimetric analysis showed that the activation energy of corrosion was high in 1M HCl solution containing Schiff base molecules. Also it was

observed that activation energy increased with rise in concentration of Schiff bases. Positive value of enthalpy of corrosion reflects the endothermic nature of corrosion. Both Nyquist plot and Bode plot analysis were utilized to get much density on the inhibitory action of these novel Schiff bases by EIS method. During polarization analysis, Tafel extrapolation method and Linear polarization method were performed separately. Surface morphological study established the protective nature of Schiff bases on mild steel surface. Electrochemical noise measurement was also carried out to examine the inhibition capacity. These results are in close agreement with other electrochemical studies. The results obtained from quantum chemical studies are also in close agreement the gravimetric weight loss studies.

In 0.5M sulphuric acid medium, the gravimetric studies gave a different order of corrosion inhibition efficiency for the Schiff base inhibitors, i.e. A9CNPTDA > I3A2AT > P2CNPTDA > T2CNPTDA > ANNPTDA > 3APNPTDA > 2APNPTDA. A maximum of 90.7% was obtained by A9CNPTDA at 1mM concentration. The inhibition efficiencies were lesser than that in HCl medium, which can be explained with the aggressive nature of the sulphuric acid and possibility of hydrolysis in this medium. Weight loss measurements on both Schiff base inhibitors and their corresponding parent compounds were performed and compared. Langmuir isotherm was the best fit one for all the studied molecules. The ΔG^0_{ads} values for all the molecules suggested that the adsorption involved both physisorption and chemisorption. Electrochemical impedance and potentiodynamic investigations in 0.5M H_2SO_4 gave higher corrosion inhibition efficiencies compared to gravimetric studies because it is quick monitoring technique. A9CNPTDA and I3A2AT expressed inhibition efficiency greater than 90% in both experiments. Comparatively least efficiency was reported by T2CDACH. This is because faster hydrolysis nature of this molecule in the early hours stage. One of the polynuclear

derivative ANNPTDA exhibit high inhibition efficiency in EIS analysis (97.02%), but its gravimetric performance is less because its hydrolyzed products (parent compounds) showed less inhibition efficiency in H2SO4 Medium. Polarization studies revealed that the Schiff bases affected cathodic and anodic sites of corrosion (mixed type inhibitor).

REFERENCES

[1] G. Koch, Cost of corrosion, Trends Oil Gas Corros. Res. Technol. 1(2017) 3–30.

[2] E. Sherif, S.-M. Park, Inhibition of copper corrosion in acidic pickling solutions by N-phenyl-1, 4-phenylenediamine, Electrochimica Acta. 51 (2006) 4665–4673.

[3] S. Muralidharan, R. Chandrasekar, S. Iyer, Effect of piperidones on hydrogen permeation and corrosion inhibition of mild steel in acidic solutions, J. Chem. Sci. 112 (2000) 127–136.

[4] M.G. Fontana, N.D. Greene, Corrosion engineering, McGraw-hill, 3 (2018) 1-465.

[5] C. Jomdecha, A. Prateepasen, P. Kaewtrakulpong, Study on source location using an acoustic emission system for various corrosion types, Ndt E Int. 40 (2007) 584–593.

[6] L. Elkadi, B. Mernari, M. Traisnel, F. Bentiss, M. Lagrenee, The inhibition action of 3, 6-bis (2-methoxyphenyl)-1, 2-dihydro-1, 2, 4, 5-tetrazine on the corrosion of mild steel in acidic media, Corros. Sci. 42 (2000) 703–719.

[7] S. Sharma, R. Chaudhary, Inhibitive action of methyl red towards corrosion of mild steel in acids, Bull. Electrochem. 16 (2000) 267–271.

[8] L. Garverick, Corrosion in the petrochemical industry, ASM international, 1994.

[9] A. Yurt, A. Balaban, S.U. Kandemir, G. Bereket, B. Erk, Investigation on some Schiff bases as HCl corrosion inhibitors for carbon steel, Mater. Chem. Phys. 85 (2004) 420–426.

[10] M. Cisse, B. Zerga, F. El Kalai, M.E. Touhami, M. Sfaira, M. Taleb, B. Hammouti, N. Benchat, S. El Kadiri, A.T. Benjelloun, Two dipodal pyridin-pyrazol derivatives as efficient inhibitors of mild steel corrosion in HCl solution—part I: electrochemical study, Surf. Rev. Lett. 18 (2011) 303–313.

[11] Z. Cao, Y. Tang, H. Cang, J. Xu, G. Lu, W. Jing, Novel benzimidazole derivatives as corrosion inhibitors of mild steel in the acidic media. Part II: theoretical studies, Corros. Sci. 83 (2014) 292–298.

[12] J.M. Gaidis, Chemistry of corrosion inhibitors, Cem. Concr. Compos. 26 (2004) 181–189.

[13] H. Shokry, M. Yuasa, I. Sekine, R. Issa, H. El-Baradie, G. Gomma, Corrosion inhibition of mild steel by Schiff base compounds in various aqueous solutions: part 1, Corros. Sci. 40 (1998) 2173–2186.

[14] A. Fekry, M. Ameer, Corrosion inhibition of mild steel in acidic media using newly synthesized heterocyclic organic molecules, Int. J. Hydrog. Energy. 35 (2010) 7641–7651.

[15] C. Verma, D.K. Verma, E.E. Ebenso, M.A. Quraishi, Sulfur and phosphorus heteroatom-containing compounds as corrosion inhibitors: An overview, Heteroat. Chem. 29 (2018) 1-20.

[16] A.A. Al-Amiery, A.A.H. Kadhum, A.H.M. Alobaidy, A.B. Mohamad, P.S. Hoon, Novel corrosion inhibitor for mild steel in HCl, Materials. 7 (2014) 662–672.

[17] A. Asan, S. Soylu, T. Kıyak, F. Yıldırım, S. Öztaş, N. Ancın, M. Kabasakaloğlu, Investigation on some Schiff bases as corrosion inhibitors for mild steel, Corros. Sci. 48 (2006) 3933–3944.

[18] T. Ahamad, S.M. Alshehri, Thermal, microbial, and corrosion resistant metal-containing poly (Schiff) epoxy coatings, J. Coat. Technol. Res. 9 (2012) 515–523.

[19] B. Clubby, Chemical inhibitors for corrosion control, Royal Soc, Chem Camb. 141 (1990).

[20] M. Gojic, L. Kosec, Corrosion inhibition on iron with propargylic alcohol in acid solutions, ISIJ Int. 37 (1997) 685–690.

[21] M. Metikos-Hukovic, R. Babić, Z. Grubać, S. Brinć, Inhibition of the hydrogen evolution reaction on aluminium covered by ‘spontaneous’ oxide, J. Appl. Electrochem. 24 (1994) 325–331.

[22] H. Awad, S.A. Gawad, Mechanism of inhibition of iron corrosion in hydrochloric acid by pyrimidine and series of its derivatives, Anti-Corros. Methods Mater. (2005).

[23] A.Y. Musa, A.A.H. Kadhum, A.B. Mohamad, M.S. Takriff, Experimental and theoretical study on the inhibition performance of triazole compounds for mild steel corrosion, Corros. Sci. 52 (2010) 3331–3340.

[24] B. Joseph, S. John, A. Joseph, B. Narayana, Imidazolidine-2-thione as corrosion inhibitor for mild steel in hydrochloric acid, 14 (2010) 366-374.

[25] P.C. Okafor, Y. Zheng, Synergistic inhibition behaviour of methylbenzyl quaternary imidazoline derivative and iodide ions on mild steel in H2SO4 solutions, Corros. Sci. 51 (2009) 850–859.

[26] M. Abdel Aal, A. Abdel Wahab, A.E. Saied, A study of the inhibiting action of benzene thiols and related compounds on the corrosion of zinc in acidic media, Corrosion. 37 (1981) 557–563.

[27] M. Desai, J. Talati, N. Shah, Schiff bases of ethylenediamine/triethylenetetramine with benzaldehyde/cinnamic aldehyde/salicylaldehyde as corrosion inhibitors of zinc in sulphuric acid, Anti-Corros. Methods Mater. (2008).

[28] A.S. El Din, A. El Hosary, R. Saleh, J.A. El Kader, Peculiarities in the Behaviour of Thiourea as corrosion-inhibitor, Mater. Corros. 28 (1977) 26–31.

[29] M. Benabdellah, A. Tounsi, K. Khaled, B. Hammouti, Thermodynamic, chemical and electrochemical investigations of 2-mercapto benzimidazole as corrosion inhibitor for mild steel in hydrochloric acid solutions, Arab. J. Chem. 4 (2011) 17–24.

[30] M. Hosseini, S.F. Mertens, M. Ghorbani, M.R. Arshadi, Asymmetrical Schiff bases as inhibitors of mild steel corrosion in sulphuric acid media, Mater. Chem. Phys. 78 (2003) 800–808.

[31] M. Muniandy, A.A. Rahim, H. Osman, A.M. Shah, S. Yahya, P.B. Raja, Investigation of some schiff bases as corrosion inhibitors for aluminium alloy in 0.5 M hydrochloric acid solutions, Surf. Rev. Lett. 18 (2011) 127–133.

[32] M. Shah, A. Patel, G. Mudaliar, N. Shah, Schiff bases of triethylenetetramine as corrosion inhibitors of Zinc in Hydrochloric acid, Port. Electrochimica Acta. 29 (2011) 101–113.

[33] M.Q. Mohammed, Synthesis and characterization of new Schiff bases and evaluation as Corrosion inhibitors, J. Basrah Res. 37 (2011) 116–130.

[34] S.P. Fakrudeen, A. Murthyh , V. Raju , Corrosion inhibition of AA6061 and AA6063 alloy in hydrochloric acid media by Schiff base compounds, J. Chil. Chem. Soc. 57 (2012) 1364–1370.

[35] A.K. Singh, M. Quraishi, Study of some bidentate schiff bases of isatin as corrosion inhibitors for mild steel in hydrochloric acid solution, Int J Electrochem Sci. 7 (2012) 3222–3241.

[36] S. Junaedi, A.A. Al-Amiery, A. Kadihum, A.A.H. Kadhum, A.B. Mohamad, Inhibition effects of a synthesized novel 4-aminoantipyrine derivative on the corrosion of mild steel in hydrochloric acid solution together with quantum chemical studies, Int. J. Mol. Sci. 14 (2013) 11915–11928.

[37] K.C. Emregül, A.A. Akay, O. Atakol, The corrosion inhibition of steel with Schiff base compounds in 2M HCl, Mater. Chem. Phys. 93 (2005) 325–329..

[38] M. Vinutha, T. Venkatesha, Review on mechanistic action of inhibitors on steel corrosion in acidic media, Port. Electrochimica Acta. 34 (2016) 157–184.

[39] D.M. Jamil, A.K. Al-Okbi, S.B. Al-Baghdadi, A.A. Al-Amiery, A. Kadhim, T.S. Gaaz, A.A.H. Kadhum, A.B. Mohamad, Experimental and theoretical studies of Schiff bases as corrosion inhibitors, Chem. Cent. J. 12 (2018) 1–9.

[40] P. Shetty, Schiff bases: An overview of their corrosion inhibition activity in acid media against mild steel, Chem. Eng. Commun. 207 (2020) 985–1029.

[41] V.V. Dhayabaran, I.S. Lydia, J.P. Merlin, P. Srirenganayaki, Inhibition of corrosion of commercial mild steel in presence of tetrazole derivatives in acid medium, Ionics. 10 (2004) 123–125.

[42] R. Upadhyay, S. Mathur, Effect of Schiff's bases as corrosion inhibitors on mild steel in sulphuric acid, E-J. Chem. 4 (2007) 408-414.

[43] G. Elewady, Pyrimidine derivatives as corrosion inhibitors for carbon-steel in 2M hydrochloric acid solution, Int J Electrochem Sci. 3 (2008) 1149.

[44] D. Gopi, E.-S.M. Sherif, V. Manivannan, D. Rajeswari, M. Surendiran, L. Kavitha, Corrosion and corrosion inhibition of mild steel in groundwater at different temperatures by newly synthesized benzotriazole and phosphono derivatives, Ind. Eng. Chem. Res. 53 (2014) 4286–4294.

[45] L.O. Olasunkanmi, I.B. Obot, M.M. Kabanda, E.E. Ebenso, Some quinoxalin-6-yl derivatives as corrosion inhibitors for mild steel in hydrochloric acid: experimental and theoretical studies, J. Phys. Chem. C. 119 (2015) 16004–16019.

[46] P. Singh, V. Srivastava, M. Quraishi, Novel quinoline derivatives as green corrosion inhibitors for mild steel in acidic medium: electrochemical, SEM, AFM, and XPS studies, J. Mol. Liq. 216 (2016) 164–173.

[47] Z.Z. Tasic, M.M. Antonijevic, M.B.P. Mihajlovic, M.B. Radovanovic, The influence of synergistic effects of 5-methyl-1H-benzotriazole and potassium sorbate as well as 5-methyl-1H-benzotriazole and gelatin on the copper corrosion in sulphuric acid solution, J. Mol. Liq. 219 (2016) 463–473.

[48] I. Benmahammed, T. Douadi, S. Issaadi, M. Al-Noaimi, S. Chafaa, Heterocyclic Schiff bases as corrosion inhibitors for carbon steel in 1 M HCl solution: hydrodynamic and synergetic effect, J. Dispers. Sci. Technol. (2019) 1–20.

[49] A. Mishra, J. Aslam, C. Verma, M. Quraishi, E.E. Ebenso, Imidazoles as highly effective heterocyclic corrosion inhibitors for metals and alloys in aqueous electrolytes: A review, J. Taiwan Inst. Chem. Eng. 114 (2020) 341-358.

[50] M. Özcan, İ. Dehri, M. Erbil, Organic sulphur-containing compounds as corrosion inhibitors for mild steel in acidic media: correlation between inhibition efficiency and chemical structure, Appl. Surf. Sci. 236 (2004) 155–164.

[51] H.H. Hassan, E. Abdelghani, M.A. Amin, Inhibition of mild steel corrosion in hydrochloric acid solution by triazole derivatives: Part I. Polarization and EIS studies, Electrochimica Acta. 52 (2007) 6359–6366.

[52] F. Bentiss, M. Lagrenée, Heterocyclic compounds as corrosion inhibitors for mild steel in hydrochloric acid medium-correlation between electronic structure and inhibition efficiency, J Mater Env. Sci. 2 (2011) 13–17.

[53] S. Issaadi, T. Douadi, A. Zouaoui, S. Chafaa, M.A. Khan, G. Bouet, Novel thiophene symmetrical Schiff base compounds as corrosion inhibitor for mild steel in acidic media, Corros. Sci. 53 (2011) 1484–1488.

[54] C. Loto, R. Loto, A. Popoola, Corrosion inhibition of thiourea and thiadiazole derivatives: a review, J. Mater. Environ. Sci. 3 (2012) 885–894.

[55] D. Daoud, T. Douadi, S. Issaadi, S. Chafaa, Adsorption and corrosion inhibition of new synthesized thiophene Schiff base on mild steel X52 in HCl and H2SO4 solutions, Corros. Sci. 79 (2014) 50–58.

[56] A. Aouniti, H. Elmsellem, S. Tighadouini, M. Elazzouzi, S. Radi, A. Chetouani, B. Hammouti, A. Zarrouk, Schiff's base derived from 2-acetyl thiophene as corrosion inhibitor of steel in acidic medium, J. Taibah Univ. Sci. 10 (2016) 774–785.

[57] A. Singh, K. Ansari, J. Haque, P. Dohare, H. Lgaz, R. Salghi, M. Quraishi, Effect of electron donating functional groups on corrosion inhibition of mild steel in hydrochloric acid: Experimental and quantum chemical study, J. Taiwan Inst. Chem. Eng. 82 (2018) 233–251.

[58] I. Obot, N. Obi-Egbedi, A. Eseola, Anticorrosion potential of 2-mesityl-1H-imidazo [4, 5-f][1, 10] phenanthroline on mild steel in sulfuric acid solution: experimental and theoretical study, Ind. Eng. Chem. Res. 50 (2011) 2098–2110.

[59] R. Baskar, M. Gopiraman, D. Kesavan, I.S. Kim, K. Subramanian, Synthesis, characterization, and electrochemical studies of novel biphenyl based compounds, Ind. Eng. Chem. Res. 51 (2012) 3966–3974.

[60] K. Shaju, V.P. Raphael, others, Effect of iodide on the corrosion inhibitive behaviour on carbon steel by an azomethine compound derived from anthracene-9 (10 H)-one, Orient. J. Chem. 30 (2014) 807–813.

[61] U. Ekpe, U. Ibok, B. Ita, O. Offiong, E. Ebenso, Inhibitory action of methyl and phenyl thiosemicarbazone derivatives on the corrosion of mild steel in hydrochloric acid, Mater. Chem. Phys. 40 (1995) 87–93.

[62] E. Ebenso, U. Ekpe, B. Ita, O. Offiong, U. Ibok, Effect of molecular structure on the efficiency of amides and thiosemicarbazones used for corrosion inhibition of mild steel in hydrochloric acid, Mater. Chem. Phys. 60 (1999) 79–90.

[63] M. Lashkari, M. Arshadi, DFT studies of pyridine corrosion inhibitors in electrical double layer: solvent, substrate, and electric field effects, Chem. Phys. 299 (2004) 131–137.

[64] S. Abd El-Maksoud, A. Fouda, Some pyridine derivatives as corrosion inhibitors for carbon steel in acidic medium, Mater. Chem. Phys. 93 (2005) 84–90.

[65] F. Kandemirli, S. Sagdinc, Theoretical study of corrosion inhibition of amides and thiosemicarbazones, Corros. Sci. 49 (2007) 2118–2130.

[66] A. Ghazoui, R. Saddik, N. Benchat, M. Guenbour, B. Hammouti, S. Al-Deyab, A. Zarrouk, Comparative study of pyridine and pyrimidine derivatives as corrosion inhibitors of C38 steel in molar HCl, Int J Electrochem Sci. 7 (2012) 7080–7097.

[67] V.P. Raphael, K.J. Thomas, K. Shaju, A. Paul, Corrosion inhibition investigations of 3-acetylpyridine semicarbazone on carbon steel in hydrochloric acid medium, Res. Chem. Intermed. 40 (2014) 2689–2701.

[68] P. Mourya, P. Singh, R. Rastogi, M. Singh, Inhibition of mild steel corrosion by 1, 4, 6-trimethyl-2-oxo-1, 2-dihydropyridine-3-carbonitrile and synergistic effect of halide ion in 0.5 M H2SO4, Appl. Surf. Sci. 380 (2016) 141–150.

[69] W. Zhang, H.-J. Li, Y. Wang, Y. Liu, Y.-C. Wu, Adsorption and corrosion inhibition properties of pyridine-2-aldehyde-2-quinolylhydrazone for Q235 steel in acid medium: Electrochemical, thermodynamic, and surface studies, Mater. Corros. 69 (2018) 1638–1648.

[70] N.N. Hazani, Y. Mohd, S.A.I.S.M. Ghazali, Y. Farina, N.N. Dzulkifli, Electrochemical Studies on Corrosion Inhibition Behaviour of Synthesised 2-acetylpyridine 4-ethyl-3-thiosemicarbazone and Its Tin(IV) Complex for Mild Steel in 1 M HCl Solution, J. Electrochem. Sci. Technol. 10 (2019) 29–36.

[71] G. Avci, Corrosion inhibition of indole-3-acetic acid on mild steel in 0.5 M HCl, Colloids Surf. Physicochem. Eng. Asp. 317 (2008) 730–736.

[72] M. Lebrini, F. Robert, H. Vezin, C. Roos, Electrochemical and quantum chemical studies of some indole derivatives as corrosion inhibitors for C38 steel in molar hydrochloric acid, Corros. Sci. 52 (2010) 3367–3376.

[73] A. Paul, K. Joby Thomas, V.P. Raphael, K. Shaju, Electrochemical and Gravimetric Corrosion Inhibition Investigations of A Heterocyclic Schiff Base Derived From 3-Formylindole., Rct. 100 (2012) 3.

[74] A. Fouda, K. Shalabi, H. Elmogazy, Corrosion inhibition of α-brass in HNO3 by indole and 2-oxyindole, J Mater Env. Sci. 5 (2014) 1691.

[75] X. Ma, X. Jiang, S. Xia, M. Shan, X. Li, L. Yu, Q. Tang, New corrosion inhibitor acrylamide methyl ether for mild steel in 1 M HCl, Appl. Surf. Sci. 371 (2016) 248–257.

[76] C. Li, P. Wang, S. Sun, K. Voisey, D. McCartney, Corrosion behaviour of Al86. 0Co7. 6Ce6. 4 glass forming alloy with different microstructures, Appl. Surf. Sci. 384 (2016) 116–124.

[77] Z. He, F. Mansfeld, Exploring the use of electrochemical impedance spectroscopy (EIS) in microbial fuel cell studies, Energy Environ. Sci. 2 (2009) 215–219.

[78] A. v Homborg, E. Van Westing, T. Tinga, X. Zhang, P. Oonincx, G. d Ferrari, J. De Wit, J. Mol, Novel time–frequency characterization of electrochemical noise data in corrosion studies using Hilbert spectra, Corros. Sci. 66 (2013) 97–110.

[79] T.K. Chaitra, K.N.S. Mohana, H.C. Tandon, Thermodynamic, electrochemical and quantum chemical evaluation of some triazole Schiff bases as mild steel corrosion inhibitors in acid media, J. Mol. Liq. 211 (2015) 1026–1038.

[80] M. Goyal, R. Kumar, O.S. Yadav, R. Sharma, G. Singh, others, Experimental, surface characterization and computational evaluation of the acid corrosion inhibition of mild steel by methoxycarbonylmethyltriphenylphosphonium bromide (MCMTPPB), Indian J. Chem. Technol. IJCT. 24 (2017) 256–268.

[81] Y. Wang, Y. Zuo, X. Zhao, S. Zha, The adsorption and inhibition effect of calcium lignosulfonate on Q235 carbon steel in simulated concrete pore solution, Appl. Surf. Sci. 379 (2016) 98–110.

[82] N. Vlachos, Y. Skopelitis, M. Psaroudaki, V. Konstantinidou, A. Chatzilazarou, E. Tegou, Applications of Fourier transform-infrared spectroscopy to edible oils, Anal. Chim. Acta. 573 (2006) 459–465.

[83] V. Kuz'min, V. Lozitsky, G. Kamalov, R. Lozitskaya, A. Zheltvay, A. Fedtchouk, D. Kryzhanovsky, Analysis of the structure-anticancer activity relationship in a set of Schiff bases of macrocyclic 2, 6-bis (2-and 4-formylaryloxymethyl) pyridines., Acta Biochim. Pol. 47 (2000) 867–875.

[84] H. Hamani, T. Douadi, D. Daoud, M. Al-Noaimi, S. Chafaa, Corrosion inhibition efficiency and adsorption behavior of azomethine compounds at mild steel/hydrochloric acid interface, Measurement. 94 (2016) 837–846.

[85] B. Ateya, B. El-Anadouli, F. El-Nizamy, The adsorption of thiourea on mild steel, Corros. Sci. 24 (1984) 509–515.

[86] T. Zhao, G. Mu, The adsorption and corrosion inhibition of anion surfactants on aluminium surface in hydrochloric acid, Corros. Sci. 41 (1999) 1937–1944.

[87] N. Soltani, H. Salavati, N. Rasouli, M. Paziresh, A. Moghadasi, Adsorption and corrosion inhibition effect of Schiff base ligands on low carbon steel corrosion in hydrochloric acid solution, Chem. Eng. Commun. 203 (2016) 840–854.

[88] M. Bedair, M. El-Sabbah, A. Fouda, H. Elaryian, Synthesis, electrochemical and quantum chemical studies of some prepared surfactants based on azodye and Schiff base as corrosion inhibitors for steel in acid medium, Corros. Sci. 128 (2017) 54–72.

[89] M. Bouklah, N. Benchat, B. Hammouti, A. Aouniti, S. Kertit, Thermodynamic characterisation of steel corrosion and inhibitor adsorption of pyridazine compounds in 0.5 M H2SO4, Mater. Lett. 60 (2006) 1901–1905.

[90] J.R. Macdonald, E. Barsoukov, Impedance spectroscopy: theory, experiment, and applications, History. 1 (2005) 1–13.

[91] A. Xu, X. Wu, H. Xu, F. Jin, G. Wang, Electrochemical impedance spectroscopy (EIS) study of vehicle protective coating performance, in: ICCTP 2011 Sustain. Transp. Syst., 2011: pp. 3827–3834.

[92] B.M. Mistry, N.S. Patel, M.J. Patel, S. Jauhari, Corrosion inhibition performance of 1, 3, 5-triazinyl urea derivatives as a corrosion inhibitor for mild steel in 1 N HCL, Res. Chem. Intermed. 37 (2011) 659–671.

[93] F. Mansfeld, M. Kendig, Evaluation of Protective Coatings with Impedance Measurements, in: F Mansfeld M Kendig Rockwell Int. Sci. Cent. Thousand Oaks CA 91360 Intl Congr. Met. Corr, 1984.

[94] G. Reinhard, U. Rammelt, Discussion and application of impedance testing in corrosion protection investigations, Corrosion. 15 (1984) 175–193.

[95] T. Strivens, C. Taylor, An assessment of A/C impedance as a basic research and routine testing method for studying corrosion of metals under paint films, Mater. Chem. 7 (1982) 199–220.

[96] F. Mansfeld, M. Kendig, Concerning the choice of scan rate in polarization measurements, Corrosion. 37 (1981) 545–546.

[97] A. Mohamed, H. Mostafa, G. El-Ewady, A. Fouda, 10. DD Macdonald, Transient Techniques in Electrochemistry, Plenum Press, New York, Port. Electrochimica Acta. 18 (2000) 99–111.

[98] K.C. Emregül, O. Atakol, Corrosion inhibition of iron in 1 M HCl solution with Schiff base compounds and derivatives, Mater. Chem. Phys. 83 (2004) 373–379.

[99] F. Bentiss, M. Lagrenee, M. Traisnel, J. Hornez, Corrosion inhibition of mild steel in 1 M hydrochloric acid by 2, 5-bis (2-aminophenyl)-1,3,4-oxadiazole, Corrosion. 55 (1999) 968–976.

[100] P.G. Grützmacher, F.J. Profito, A. Rosenkranz, Multi-scale surface texturing in tribology—Current knowledge and future perspectives, Lubricants. 7 (2019) 95-112.

[101] D. Gopi, K. Govindaraju, L. Kavitha, Investigation of triazole derived Schiff bases as corrosion inhibitors for mild steel in hydrochloric acid medium, J. Appl. Electrochem. 40 (2010) 1349–1356.

[102] K.C. Emregül, R. Kurtaran, O. Atakol, An investigation of chloride-substituted Schiff bases as corrosion inhibitors for steel, Corros. Sci. 45 (2003) 2803–2817.

[103] J. Smulko, K. Darowicki, A. Zieliński, Pitting corrosion in steel and electrochemical noise intensity, Electrochem. Commun. 4 (2002) 388–391.

[104] S. Abd El Wanees, M.I. Alahmdi, M. Abd El Azzem, H.E. Ahmed, 4, 6-Dimethyl-2-oxo-1, 2-dihydropyridine-3-carboxylic acid as an inhibitor towards the corrosion of C-steel in acetic acid, Inter J Electrochem Sci. 11 (2016) 3448–3466.

[105] J. Chen, W. Bogaerts, The physical meaning of noise resistance, Corros. Sci. 37 (1995) 1839–1842.

[106] Y. Tan, S. Bailey, B. Kinsella, The monitoring of the formation and destruction of corrosion inhibitor films using electrochemical noise analysis (ENA), Corros. Sci. 38 (1996) 1681–1695.

[107] F. Mansfeld, Z. Sun, C. Hsu, A. Nagiub, Concerning trend removal in electrochemical noise measurements, Corros. Sci. 43 (2001) 341–352.

[108] H. Ashassi-Sorkhabi, D. Seifzadeh, M. Raghibi-Boroujeni, Analysis of electro chemical noise data in both time and frequency domains to evaluate the effect of ZnO nanopowder addition on the corrosion protection performance of epoxy coatings, Arab. J. Chem. 9 (2016)1320–S1327.

[109] A. Homborg, P. Oonincx, J. Mol, Wavelet transform modulus maxima and holder exponents combined with transient detection for the differentiation of pitting corrosion using electrochemical noise, Corrosion. 74 (2018) 1001–1010.

[110] S.F. Burch, S.F. Gull, J. Skilling, Image restoration by a powerful maximum entropy method, Comput. Vis. Graph. Image Process. 23 (1983) 113–128.

[111] D.K. Yadav, M. Quraishi, B. Maiti, Inhibition effect of some benzylidenes on mild steel in 1 M HCl: an experimental and theoretical correlation, Corros. Sci. 55 (2012) 254–266.

[112] S. Benabid, T. Douadi, S. Issaadi, C. Penverne, S. Chafaa, Electrochemical and DFT studies of a new synthesized Schiff base as corrosion inhibitor in 1 M HCl, Measurement. 99 (2017) 53–63.

[113] H. Hamani, T. Douadi, M. Al-Noaimi, S. Issaadi, D. Daoud, S. Chafaa, Electrochemical and quantum chemical studies of some azomethine compounds as corrosion inhibitors for mild steel in 1 M hydrochloric acid, Corros. Sci. 88 (2014) 234–245.

[114] V. Sastri, J. Perumareddi, Molecular orbital theoretical studies of some organic corrosion inhibitors, Corrosion. 53 (1997) 617–622.

[115] M. Shahraki, M. Dehdab, S. Elmi, Theoretical studies on the corrosion inhibition performance of three amine derivatives on carbon steel: Molecular dynamics simulation and density functional theory approaches, J. Taiwan Inst. Chem. Eng. 62 (2016) 313–321.

[116] A. Fouda, M. Ismail, G. EL-ewady, A. Abousalem, Evaluation of 4-amidinophenyl-2, 2′-bithiophene and its aza-analogue as novel corrosion inhibitors for CS in acidic media: experimental and theoretical study, J. Mol. Liq. 240 (2017) 372–388.

[117] P. Senet, Chemical hardnesses of atoms and molecules from frontier orbitals, Chem. Phys. Lett. 275 (1997) 527–532.

[118] A. Béchamp, De l'action des protosels de fer sur la nitronaphtaline et al nitrobenzine;: nouvelle méthode de formation des bases orgnaiques artificielles de zinin, (1854) 1-25.

[119] E. Cano, J. Polo, A. La Iglesia, J. Bastidas, A study on the adsorption of benzotriazole on copper in hydrochloric acid using the inflection point of the isotherm, Adsorption. 10 (2004) 219–225.

[120] D.P. Schweinsberg, G.A. George, A.K. Nanayakkara, D.A. Steinert, The protective action of epoxy resins and curing agents—inhibitive effects on the aqueous acid corrosion of iron and steel, Corrosion Science. 28 (1988) 33–42.

[121] H. Shokry, M. Yuasa, I. Sekine, R. Issa, H. El-Baradie, G. Gomma, Corrosion inhibition of mild steel by Schiff base compounds in various aqueous solutions: part 1, Corrosion Science. 40 (1998) 2173–2186.

[122] A. v Homborg, E. Van Westing, T. Tinga, X. Zhang, P. Oonincx, G. d Ferrari, J. De Wit, J. Mol, Novel time–frequency characterization of electrochemical noise data in corrosion studies using Hilbert spectra, Corrosion Science. 66 (2013) 97–110.

LIST OF PUBLICATIONS

1. **Reeja Johnson,** Joby Thomas Kakkassery K, Vinod Raphael Palayoor, Ragi Kooliyat and Vidhya Thomas Kannanaikkal, "Experimental and Theoretical Investigations on the Corrosion Inhibition Action of Thiadiazole Derivatives on Carbon Steel in 1M HCl medium", *Oriental Journal of Chemistry,* 36(6), 1179-1188, 2020.
   doi: http://dx.doi.org/10.13005/ojc/360624
2. Vidhya Thomas K; Joby Thomas. K; Vinod P Raphael; A S Sabu; K Ragi; **Reeja Johnson,"** *Tinospora cordifolia* Extract as an Environmentally Benign Green Corrosion Inhibitor in Acid Media: Adsorption, Surface Morphological, Quantum Chemical and Statistical Investigations", *Materials Today Sustainability,* 13, 100076, 2021 doi: https://doi.org/10.1016/j.mtsust.2021.100076
3. Vidhya K Thomas, Joby K Thomas, Vinod P Raphael, Ragi K, **Reeja Johnson** and Ramesh Babu "Green Corrosion Inhibition Properties of *Croton Persimilis* Extract on Mild Steel in Acid Media" *Journal of Bio and Tribo corrosion,* 7(121),1-19, 2021 doi: https://doi.org/10.1007/s40735-021-00554-z)
4. Ragi K, Joby Thomas Kakkassery, Vinod P. Raphael, **Reeja Johnson** and Vidhya Thomas K "*In vitro* Antibacterial and *In Silico* Docking Studies of Two Schiff Bases on *Staphylococcus aureus* and its Target Proteins". *Future Journal of Pharmaceutical Sciences*, 7(1), 1-9, 2021 doi: https://doi.org/10.1186/s43094-021-00225-3
5. Ragi K**,** Joby Thomas Kakkassery, Vinod P. Raphael, Binsi M. Paulson and **Reeja Johnson**, "Corrosion Inhibition of Mild steel by N,N'-(5,5-dimethylcyclohexane-1,3-diylidene)dianiline in Acid Media: Gravimetric and Electrochemical Evaluations", *Current Chemistry Letters*, 9, 1-14, 2020 doi: 10.5267/j.ccl.2020.8.001
6. M. Paulson Binsi, Thomas K. Joby, K. Ragi, Varghese C. Sini and **Johnson Reeja**. "Interaction of Two Heterocyclic Schiff Bases Derived from 2-acetyl pyridine on Mild

Steel in Hydrochloric acid: Physicochemical and Corrosion Inhibition Investigations", *Current Chemistry Letters,* 9, 19-30, 2019 doi: 10.5267/j.ccl.2019.6.005

7. Vidhya Thomas K, Joby Thomas K, Vinod P Raphael, Ragi K and **Reeja Johnson,** "*Ixora coccinea* Extract as an Efficient Eco-Friendly Corrosion Inhibitor in Acidic Media: Experimental and Theoretical Approach", *Current Chemistry Letters,* 10(3), 139-50, 2021 doi: http://dx.doi.org/10.5267/j.ccl.2020.12.001
8. Aby Paul, Joby Thomas K, **Reeja Johnson** and Sini Varghese C, "Transition Metal Complexes of (z)-4-((1H-indole-3-yl)methyleneamine)benzoic acid: Synthesis, Structural and Antibacterial studies" *Chemical Science Reviews and Letters*, 4(13), 292-298, 2015
9. Paul. A, Thomas J and **Johnson R,** "Thermal Decomposition Kinetics and mechanism on Mn(II), Ni(II) and Cu(II) complexes of 3-Formyl Indole-2-amino5-Bromo Benzoic acid", *International Journal of Engineering, Science and Mathematics*, 7(2), 25-30, 2018
10. Aby Paul, Joby Thomas K, Sini Varghese C and **Reeja Johnson** "Evaluation on Structural and Thermoanalytical Properties of a Novel Heterocyclic Schiff base Derived from 3-formylindole and Its Metal Chelates" *Chemical Science Reviews and Letters*, 4(13), 278-284, 2015
11. Aby Paul, Joby Thomas K, Sini Varghese C and **Reeja Johnson** "Chelating competency and Antibacterial Properties of (E)-2-((1H-indol-3-yl)metheneamino)-5-bromobenzoic acid and Its Metal Chelates" *International Journal of Research in Chemistry and Environment*, 6(2), 50-54, 2016

LIST OF CONFERENCE PAPERS

1. **Reeja Johnson** and Joby Thomas K, "Electrochemical Corrosion Investigations on

(13E)-N1,N2-bis((thiophen-2-yl)methylene)cyclohexane-1,2-diamine on Mild steel in 1.0M HCl", International Conference on Chemistry and Physics of Materials ICCPM, St.Thomas' College (Autonomous), Thrissur, Dec 19-21, 2018

2. **Reeja Johnson**, Aby Paul, Joby Thomas K, Binsi M. Paulson and Sini Varghese C, "Synthetic, Structure and Antibacterial Analysis of Ni(ll), Cu(ll) and Cd(ll) Complexes of (z)-3-((1H-Indol-3-yl)methyleneamino) benzoic acid", UGC Sponsored National Seminar on Organic Synthesis at St. Joseph's College, Irinjalakuda, Jan 22-23, 2015
3. **Reeja Johnson**, Joby Thomas K and Sangeetha M, "Electrochemical investigations on the "Corrosion Inhibition Properties of N-(Anthracene-9(10H)-Ylidene)-5-(4-nitrophenyl)-1,3,4-Thiadiazole-2-amine on Mild Steel", UGC Sponsered National Seminar on Recent Trends in Chemical Science in Carmel College, Mala, Aug 13-14, 2014
4. Jaicy Joy K, Joby Thomas K., **Reeja Johnson** and Sini Varghese C, "Synthesis and Characterisation of Novel Schiff Base, N-(Anthracen-9(10H)-ylidene)-5-(4-nitrophenyl)-1,3,4-thiadiazol-2-amine and its Transition Metal Complexes", National Seminar on Recent Trends in Chemical Sciences, Carmel College, Mala, Aug 13-14, 2014
5. Shafna Jose, Joby Thomas K, **Reeja Johnson** and Sini Varghese C, "Gravimetric Weight Loss Studies on Imine Derivatives of 5-(4-nitrophenyl)-1,3,4-thiadiazol-2-amine in Acid Medium", UGC sponsored National Seminar on Recent Trends in Chemical Science, Carmel College, Mala, Aug 13-14, 2014
6. Aby Paul, Joby Thomas K, **Reeja Johnson** and Sini Varghese C, "Studies on Physicochemical and Thermal properties of Mn(II) and Cu(II) Chelate of 3-Formyl indole-2-amino-5-nitro benzoic acid", UGC Sponsored National Seminar Advanced Topics in Chemistry, Sree Narayana College, Nattika, Aug 19-20, 2015 (**Best Poster Award**)

7. Aby Paul, Joby Thomas K, Sini Varghese C, **Reeja Johnson** and Binsi M Paulson, "Evaluation of Anticorrosive Properties of 3-Formylindole-2-amino Benzoic Acid and 3-Formylindole-3-amino Benzoic Acid: on Copper in HCl Media," UGC Sponsored National Seminar on Advanced Topics in Chemistry, Sree Narayana College, Nattika, Aug 19-20, 2015
8. Aby Paul, Joby Thomas K, Binsi M Paulson,Sini Varghese C and **Reeja Johnson,** "Vo(ll), Cr(ll) and Fe(lll) Complexes of (Z)-3-((1H-indol-3-yl)methyleneamino) Benzoic Acid," UGC Sponsored National seminar on Green Technologies for Green Environment, S.N.M. College Maliankara, Dec 3-4, 2015
9. Binsi M Paulson, Joby Thomas K, Ragi K, Sini Varghese C and **Reeja Johnson**, "Corrosion Inhibition Efficacy of 2-Acetylpyridine Phenyl Hydrazone on Mild Steel in Acid Media: Physicochemical and Electrochemical investigations", DST Sponsored International Conference on Materials for the Millennium MATCON 2019, Cochin University of Science and Technology, Mar 14-16, 2019
10. Vidhya Thomas K, Joby Thomas K, Ragi. K and **Reeja Johnson**, "Excellent Eco-friendly Corrosion Inhibition Behaviour of *Croton Persimilis* Extract (CPE) for Mild Steel in Acidic Media: Physicochemical, Electrochemical and Surface Morphological Studies", National Seminar on Current Trends in Chemistry (CTriC 2020), Cochin University of Science and Technology, Feb 6-7, 2020
11. Aby Paul, Joby Thomas, Binsi M Paulson, **Reeja Johnson** and Sini Varghese, "Preparation, Chacterisation and Antimicrobial Studies on Transition Metal Complexes of (Z)-2-(1H-indol-3-yl)methyleneamino)-5-nitrobenzoic acid" UGC Sponsered National Seminar on Recent Trends in Chemistry, St. Mary's College, Thrissur, Aug 19-20, 2015

PAPERS COMMUNICATED

1. **Pharmaceutical Chemistry Journal-Springer**

   Reeja Johnson, Joby Thomas Kakkassery, Vinod Raphael Palayoor, Deeya Kuriakose, Vidhya Thomas Kannanaikkal and Binsi M. Paulson, "Inhibitory Competency of Novel Thiadiazole Derivatives on HIV-1 Protease, Human Epidermal Growth Factor Receptor and Acetylcholinesterase: An *In Silico* Analysis" (**Communicated**)

2. **Portugaliae Electrochimica Acta (Elsevier Database / Scopus indexed)**

   J. Reeja, K. Joby Thomas, K. Ragi and M. P. Binsi, "Screening of Corrosion Inhibition Properties of Two Sulphur Containing Schiff Bases on Carbon Steel: Electrochemical and Quantum Chemical Studies" (**Communicated**)